Accelerating the Discovery of Antibacterial Compounds to Validate Drug Targets and Probe Cell Physiology of S. Aureus

Accelerating the discovery of antibacterial compounds to validate drug targets and probe cell physiology of *S. aureus*

A dissertation presented

by

Leigh Morgan Matano

to

The Committee on Higher Degrees in Chemical Biology

in partial fulfilment of the requirements

for the degree of

Doctor of Philosophy

in the subject of

Chemical Biology

Harvard University

Cambridge Massachusetts

July 2017

Dissertation Advisor: Suzanne Walker Leigh Morgan Matano

Accelerating the discovery of antibacterial compounds to validate drug targets and probe cell physiology of *S. aureus*

Abstract

Methicillin-resistant *Staphylococcus aureus* (MRSA) is a Gram-positive pathogen identified by its resistance to beta-lactam antibiotics. In an era where drug-resistant infections are becoming harder and harder to treat, new antibiotics and strategies are needed to combat them. High-throughput screening is one common approach to discover new potential leads for drug development. However, identifying biologically active compounds that inhibit a pathway of interest is difficult and hit prioritization can be challenging. Using pathway-directed whole-cell screening, we rapidly identified biologically active small molecules of two virulence pathways in *S. aureus*: the wall teichoic acid (WTA) and D-alanylation (Dlt) pathways. In this thesis, we discuss: 1) the discovery of a new WTA inhibitor, targocil-II, that showed efficacy in a mouse infection model; 2) a method to rapidly identify inhibitors of nonessential pathways that led to the successful identification of a new inhibitor of the Dlt pathway called DBI-1; and 3) the use of DBI-1 and other Dlt pathway inhibitors as probe compounds to investigate cellular pathways in *S. aureus*. Using these inhibitors, we discovered interesting biology regarding the functions of LtaS, the *S. aureus* lipoteichoic acid synthase. These inhibitors are candidates for combination therapies with existing antibiotics to treat MRSA and are useful tools for probing *S. aureus* physiology.

Table of Contents

Dedication

They say it takes a village to graduate a Ph.D. student… This thesis is dedicated to: my mom and my dad, who encouraged me to continue my education; my sisters Lindsey, Lauren and Lyssa, who helped me get my start and frequently checked in on me; and my friends, who supported and provided me with advice these long five years. To friends from afar – Melanie and Rachel – and to friends near – Liv, Sam, Angela, Charlene and Kelsey – thank you for being the people I depend on every day, for learning and for laughing.

Chapter 1: Pathway directed screening for the discovery of cell wall active antibacterials

A version of this chapter has been published.[1]

1.1 Introduction: the global threat of antibiotic resistance

The incidence of antibiotic-resistant infections is rising worldwide and these infections are increasingly difficult to treat. In the USA alone, antibiotic-resistant bacteria cause at least two million infections and 23,000 deaths annually, and nearly half of those deaths are due to MRSA.[2] The burden of drug resistant infections on healthcare systems is extremely costly and despite the effort of many academic and industrial teams, antibiotic discovery has not kept pace with the rise in antibiotic resistance. The paucity of new antibiotics has been the subject of much debate and scrutiny over the years, with the lack of success in bringing compounds to market attributed to: poor quality compounds in screening libraries; poor financial incentives; unreasonable regulatory barriers; and the changing landscape of resistant microorganisms.[3] Solutions to the antibiotic resistance crisis must come from multiple sources and directions at once. In this thesis, we address one aspect of the problem: improving the efficiency of bioactive compound discovery. Strategic screen design allowed the discovery and rapid target identification of small molecules that inhibit two different virulence pathways in *S. aureus*: the wall teichoic acid pathway (Chapter 2) and the D-alanylation pathway (Chapter 3). Using these compounds as probes, we have begun to elucidate the importance of D-alanines on lipoteichoic acids and explain the functionality of these important polymers (Chapter 4). The methods outlined in this work for high-throughput discovery of bioactive small molecules with desired on-pathway activities are promising contributions to the field of antibacterial discovery. The utility and future directions of this work are summarized in Chapter 5.

1.2 Introduction to high-throughput screening (HTS)

For the past two decades, high throughput screening has served as the most common approach to identify antibacterial compounds for further development, whether for use alone or in combination with other compounds.[4] High throughput screening approaches have generally been classified into two categories: target-based screens, in which an enzyme is screened *in vitro* for direct binding and inhibition, and whole cell screens, in which growth inhibition is the usual readout (Table 1.1). In a much-discussed paper from 2007, Pompliano and coworkers described the results of 67 high throughput screening campaigns carried out over a period of seven years at GlaxoSmithKline against a wide range of antibacterial targets.[5] Only 16 of those screens, each involving approximately 250,000-500,000 compounds, resulted in hits, defined as chemically tractable, low-micromolar inhibitors of a given target, and only five of those hits progressed to leads, defined as compounds with biological activity and some evidence for target engagement. As the paper made abundantly clear, target-based screening is problematic because the likelihood that a hit can be developed into a useful lead is low. While improving the quality of compounds in a library may partially address this problem, the screening process is inherently inefficient. Additionally, target-based screens can only be applied to well-behaved targets, which excludes most membrane proteins and overlooks the possibility that the best-behaved targets for an *in vitro* screen may not be the most druggable targets in a pathway. Whole cell screens have a major advantage over target-based screens because biological activity is guaranteed and bacterial growth/inhibition assays are simple to implement. However, target identification is more difficult and it can also be difficult to prioritize hits for follow-up. Because nuisance compounds with non-specific activities may represent a large fraction of the hits and can be difficult to recognize,

considerable time and effort may be spent sorting through the hits to identify the more promising compounds.

Table 1.1. Pros and cons of different screening approaches. Pathway-directed whole cell screens attempt to merge the advantages of target-based and whole cell screens while circumventing major disadvantages.

	Target-based	Cell-based	Pathway-directed whole cell
Pros	• Predefined target	• Screens performed in relevant organisms • Assay format is simple • Biological activity is guaranteed	• Predefined pathway(s) • Screens performed in relevant organisms • Assay format is simple • Biological activity is guaranteed • On-target activity expected
Cons	• Limited to enzymes that can be expressed • Extensive assay development required • Achieving biological activity for hits can be difficult • Demonstrating on-target biological activity for leads can be challenging	• Many hits; sorting good hits from non-specific toxics is difficult • Target identification can be time consuming	• Assays require appropriate genetic or pharmacological tools

To improve the efficiency of high throughput screening for discovery of biologically active compounds, the field has turned to screening strategies that combine the advantages of target-based and whole cell screens while minimizing the disadvantages. There are different ways to accomplish this. One way is through target depletion. For example, Merck developed an antisense platform to reduce expression of 245 essential genes in *Staphylococcus aureus*.[6] Antisense strains were pooled based on growth rates and then the pools were screened against compound libraries

to identify agents that resulted in depletion of particular antisense strains from the pools. The pathway targeted by a given compound could be deduced from the strains that were most sensitive to it. This strategy not only guarantees the discovery of biologically active compounds, but increases the likelihood that hits will have a desirable mechanism of action.[7] We developed an alternative approach to accomplish the same goal, which involves screening a chemical library against a wildtype and a mutant bacterial strain to identify compounds that differentially affect growth of one of the strains.[8] This approach can be used to discover compounds that inhibit essential targets as well as compounds that inhibit non-essential targets involved in antibiotic resistance or virulence. Below we describe the application of this approach to discover compounds that inhibit cell envelope targets in *Staphylococcus aureus*. Using the same wildtype/mutant strain pair, we have identified multiple biologically active scaffolds for each of two different targets. In a testament to the efficiency of the approach, we report here the discovery of a new class of teichoic acid D-alanylation inhibitors based on following up only two hits from a screen of 230,000 small molecules.

1.3 D-alanylated Teichoic acids in Staphylococcus aureus

Teichoic acids are anionic polymers that are major constituents of the *S. aureus* cell envelope.[9] There are two types: lipoteichoic acids (LTAs), which are embedded in the cell membrane, and wall teichoic acids (WTAs), which are covalently attached to peptidoglycan (Figure 1.1). Both types of teichoic acids play important roles in cell growth and division and are required for survival in a host, making them targets for antibacterials.[10] Lipoteichoic acids are composed of a poly(glycerol phosphate) chain attached to a diglucosyl-diacylglycerol (Glc_2DAG) anchor.[11] The LTA pathway consists of three enzymes: YpfP (also known as UgtP), LtaA, and

LtaS.[9c] YpfP is a glycosyltransferase that transfers two glucose sugars to the diacylglycerol anchor lipid and the flippase LtaA exports the anchor for polymerization.[12] LtaS, a glycerol phosphate synthase, removes glycerol from the membrane lipid phosphatidylglycerol and uses them to make the LTA polymer on the Glc_2DAG anchor.[11a,13] LTAs continue to be produced when synthesis (Δ*ypfP*) or export (Δ*ltaA*) of Glc_2DAG is prevented, but strain growth is compromised and polymer length is altered.[14]

Wall teichoic acids are composed of a disaccharide sugar linked through the reducing end to PG and through the non-reducing end to a poly(ribitol-phosphate) chain.[11b,15] WTA biosynthesis begins with the glycosyltransferase TarO, which transfers N-acetylglucosamine (GlcNac) 1-phosphate from UDP-GlcNac to the undecaprenol lipid carrier.[16] This transfer reaction performed by TarO, unlike the remaining steps of the WTA pathway, is reversible. Then TarA, another glycosyltransferase, adds N-acetylmannosamine (ManNac), completing the disaccharide anchor.[15a,17] From there, a series of enzymes are involved in the polymerization of WTAs: TarB, which adds the first glycerol-phosphate moiety; TarF, which adds the second; and lastly, TarL, which polymerizes the WTA with 40-60 ribitol phosphate repeating units.[9b,15a] Once complete, the two-component ABC transferase TarGH flips WTAs extracellularly and they are covalently attached to peptidoglycan via the Lcp proteins, of which LcpA appears to be the main WTA ligase in *S. aureus*.[18]

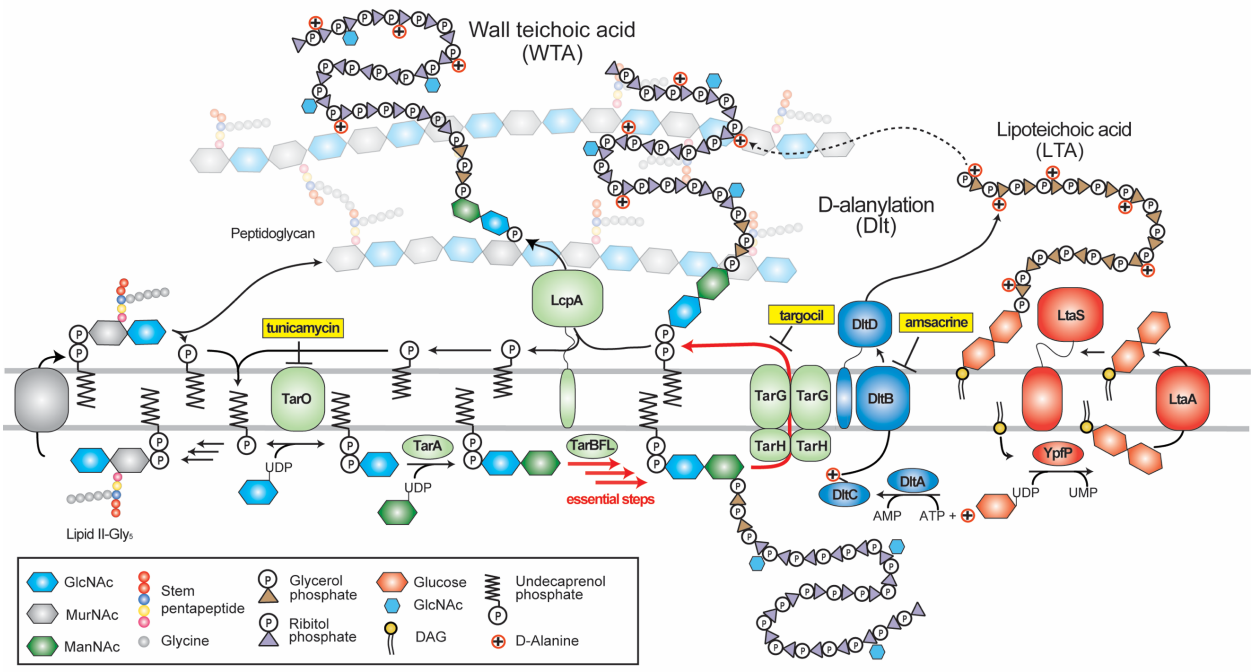

Figure 1.1 Schematic of important cell envelope biosynthetic pathways in *Staphylococcus aureus*. The *S. aureus* cell wall is composed of thick layers of peptidoglycan containing covalently bound wall teichoic acids (WTA). *S. aureus* also contains membrane-bound lipoteichoic acids (LTA). LTA and WTA are modified with D-alanine esters installed by DltABCD. In the schematic, selected WTA enzymes are shown in green, Dlt pathway enzymes are shown in blue, and LTA pathway enzymes are shown in red. The targets of selected inhibitors mentioned in the text are indicated. Figure adapted from Rajagopal and Walker (2016).[19]

Both lipo- and wall teichoic acids are functionalized with D-alanine esters; wall teichoic acids are also heavily glycosylated with N-acetyl-D-glucosamine (TarM, TarS).[9a,20] D-alanine ester levels are regulated by at least one multicomponent sensory system, the GraRS/VraFG system, and increase under various stress conditions.[21] In *S. aureus*, the D-alanylation pathway consists of four proteins: DltA, DltB, DltC and DltD.[9a] The carrier protein ligase DltA charges D-alanines as AMP-esters and transfers them to the carrier protein DltC.[22] The D-alanine esters are

then likely transferred by DltB to either a lipid intermediate or to DltD directly, and DltD then transfers the D-alanine esters onto teichoic acids in a process that remains unknown.[23] Strains in which Dlt pathway genes have been removed are highly susceptible to host immune defenses and are also sensitive to cationic antibiotics such as aminoglycosides.[24] Therefore, compounds that inhibit teichoic acid D-alanylation may be useful as attenuators of *S. aureus in vivo* and as potentiators of aminoglycosides, which have dose-limiting toxicities.

1.4 Exploiting suppression of growth inhibitory activity to target WTA biosynthesis

Although WTAs are not essential for survival *in vitro*, genes that act late in the pathway cannot be deleted unless flux into the pathway is prevented.[25] This behavior is due to the fact that blocking a late step in WTA biosynthesis depletes Lipid II, the peptidoglycan precursor, which is synthesized on the same undecaprenyl phosphate carrier lipid as the WTA precursor.[26] Therefore, it is possible to identify compounds that inhibit a late step in WTA biosynthesis by monitoring growth of a wildtype *S. aureus* strain and a Δ*tarO* mutant in which the first gene in the pathway has been deleted. From a screen of ~55,000 compounds, we identified three compounds that inhibited growth of the wildtype strain but not the mutant (Figure 1.2a, red hits).[8a] We raised resistant mutants and performed targeted sequencing of genes in the WTA pathway based on the expectation that the screen was pathway specific. Only two types of mutations were found: null mutations in *tarO* or *tarA*, the first two genes in the WTA pathway, and missense mutations in *tarG*, which encodes the transmembrane component of the two component ABC transporter that exports WTA precursors from the cytoplasmic surface to the extracellular surface of the membrane.[8a] Replacing wildtype *tarG* with the mutant alleles conferred resistance to the compound, establishing TarG as the target. Compound potency was improved ten-fold through

medicinal chemistry to produce targocil, which has been used as a probe in a number of studies.[27] Other compounds that target TarGH have been identified by Merck using a similar approach and three compounds, including targocil, have shown some efficacy in combination with a beta lactam in a MRSA infection model.[28] Although none of the compounds identified has appropriate pharmacokinetic properties for clinical use, the success of this pathway-directed whole cell screen demonstrated that suppression of compound lethality is a useful screening phenotype. If a genetic suppressor of a lethal block in a pathway can be identified, a similar screening approach can be adapted to identify inhibitors of other essential targets.

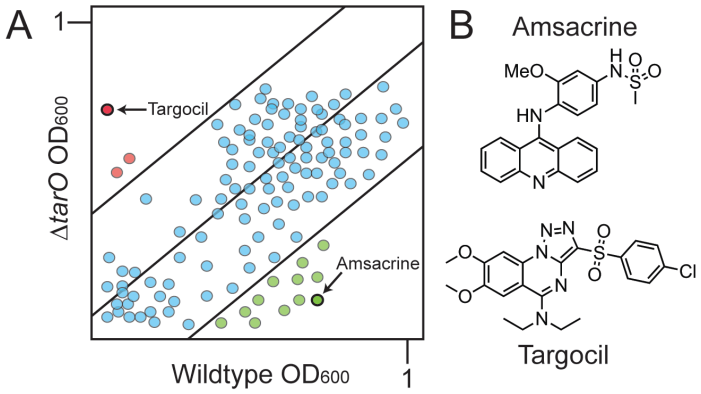

Figure 1.2 Biologically active compounds with activity against preselected pathways can be identified by screening for compounds that differentially inhibit growth of different bacterial strains. (A) Schematic of a plot depicting growth of library compounds against wildtype *S. aureus* and Δ*tarO*. Hit compounds are depicted in green or red depending on whether they are lethal to the the Δ*tarO* or wildtype strain, respectfully. The former are possible late stage WTA inhibitors and the latter inhibit a pathway that becomes essential when WTA biosynthesis is prevented. (B) Structures of two compounds previously identified using the pathway-directed whole cell screening approach depicted in 2A. Amsacrine inhibits DltB, which is required to install D-alanine

Figure 1.2 (Continued)

esters on LTA (see Figure 1.1). Targocil inhibits TarG, which transports WTA precursors to the cell surface for attachment to peptidoglycan.

It is important to note that suppression-based screens are not limited to essential targets. In a recent successful inversion of a pathway-directed screening approach to identify WTA inhibitors, Roemer and coworkers at Merck discovered compounds that suppressed growth inhibition caused by a TarG inhibitor.[29] They identified a promising TarO inhibitor, which is potentially useful for two reasons. First, *S. aureus* that does not produce WTAs cannot survive in a host; second, MRSA strains lacking WTAs are sensitive to beta lactams.[20a,28,30] MRSA strains develop beta lactam resistance through the acquisition of the *mecA* gene, which encodes an intrinsically resistant transpeptidase.[31] It is thought that WTAs act as scaffolds for peptidoglycan biosynthetic machinery required for properly coordinated function of PBP2a.[30a,32] A TarO inhibitor may be useful in combination with existing beta lactams to recover the MRSA market.

1.5 The challenges of targeting nonessential pathways to combat antibiotic resistance

While traditional antibiotics target essential pathways, including nucleic acid synthesis, protein synthesis, and cell wall synthesis, non-essential pathways are receiving increasing attention.[33] Some pathways that are non-essential *in vitro* are thought to be possible antibacterial targets because they are required for infection or survival in a host; others are known to affect virulence properties or pathogen susceptibility to traditional antibiotics.[34] While motivations for pursuing a non-essential target vary, the discovery effort is not any easier. If anything, it is more difficult to identify biologically active inhibitors of non-essential targets because inhibition does

not usually lead to a clear phenotype, at least in a wild type background. One approach that has been used to identify anti-virulence agents and immunomodulatory compounds involves screening in animal models (*e.g., Caenorhabditis elegans*) for compounds that rescue the host from a bacterial infection.[35] This approach has a crucial advantage in that hits are not only biologically active against an organism of interest, they are also biologically active in the context of a host. Key disadvantages include the fact that throughput is only moderate and follow-up can be difficult. It can be challenging to determine whether biological activity is due to inhibition of a bacterial target or a result of immunomodulation. Hence, although the first commercially used class of antibiotics, the sulfa drugs, was fortuitously discovered by screening compounds in mice, *in vivo* screening remains challenging.[36]

1.6 Exploiting synthetic lethality in pathway-directed screening: Identifying a DltB inhibitor

One approach to the discovery of biologically active compounds for non-essential cell envelope targets in *S. aureus* using synthetic lethal screening. The approach was grounded in the discovery that the wall teichoic acid pathway is at the center of a dense network of synthetic lethal relationships.[37] Pathways connected through synthetic lethality to the WTA pathway include the D-alanylation pathway, the LTA pathway, and the GraRS/VraFG stress response pathway that confers protection to several classes of antibiotics (Figure 1.3).[38] We identified these connections by growing a pooled *S. aureus* transposon mutant library in the presence and absence of the natural product tunicamycin, a potent and highly selective TarO inhibitor.[30a,37,39] By sequencing the transposon insertion sites, we were able to identify the genes that became essential when the WTA pathway was inhibited because reads mapping to these genes were depleted in tunicamycin-treated samples. After discovering that some of the pathways synthetically lethal with depletion of WTAs

included other proposed targets, we realized it should be possible to identify biologically active inhibitors of some of these targets using a pathway-directed whole cell screen.

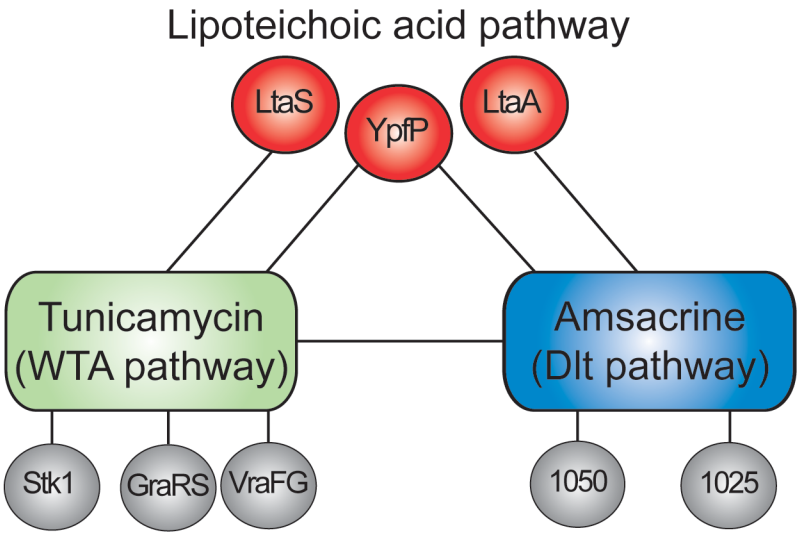

Figure 1.3 Schematic showing selected synthetic lethal interactions between three cell envelope pathways in *Staphylococcus aureus*. Synthetic lethal interactions were identified by probing a high-density transposon mutant library with tunicamycin, which inhibits TarO and prevents WTA synthesis, and amsacrine, which inhibits DltB and prevents D-alanylation of lipoteichoic acids. Inhibiting D-alanylation is lethal to mutants that make abnormal LTA due to deletion of *ypfP* or *ltaA*, but not to mutants that make no LTA (Δ*ltaS* strains). Information on synthetic lethal interactions between the Dlt pathway and other pathways enabled design of a strain panel diagnostic for Dlt pathway inhibitors (see Figure 1.4).

We returned to the same differential growth screen that led to the identification of targocil, but this time with a focus on compounds that killed the Δ*tarO* strain rather than wildtype (Figure 1.2b, green dots). In a pilot screen of ~28,000 compounds, we identified twenty possible hits, of which five were confirmed in a cherry pick. The best of these, amsacrine, inhibited growth of

Δ*tarO* and Δ*tarA* strains at a concentration of five μg/mL.[39a] We grew our previously prepared transposon mutant library in the presence and absence of amsacrine to identify other susceptible mutants on which to select resistant colonies. Reads mapping to only a handful of genes were depleted from the library. These genes included *ypfP* (*ugtP*) and *ltaA*, encoding components of the lipoteichoic acid biosynthetic pathway, and *SAOUHSC_01025* and *SAOUHSC_01050*, encoding polytopic membrane proteins of unknown function (Figure 1.3). These results increased our confidence that the target of amsacrine was in the previously defined WTA synthetic lethal network. To identify the target, we raised resistant mutants in a background containing an inactivating transposon insertion in *SAOUHSC_01050* (hereafter designated as tn::1050) and sequenced seven mutants from independent cultures that contained putative target mutations. The resistance mutations mapped to DltB, the polytopic membrane protein that is a core component of the D-alanylation machinery. Further genetic and biochemical studies confirmed DltB as the target of amsacrine.[39a] This confirmed our ability to use this pathway-directed screening approach to not only find WTA inhibitors but also to find inhibitors of pathways synthetically lethal with WTA biosynthesis.

1.7 Strategy for discovering new inhibitors of the WTA and Dlt pathways

In this introduction, we have discussed two candidate pathways for inhibition, the WTA and Dlt pathways, and our ability to discover inhibitors of both pathways from the same phenotypic screen. The discovery of targocil and amsacrine in early pilot screens demonstrated the utility of this pathway-directed screening approach. For many reasons, discovering inhibitors with the same pathway but from different scaffolds is extremely beneficial: compounds that inhibit different steps are invaluable for probing pathway biology; different scaffolds come with different physical

properties that can provide solutions to issues like solubility; and compounds from different families are unlikely to have the same off-target effects. Scaling up the screen would allow us to identify new inhibitors of the WTA and Dlt pathways while discovering inhibitors of new pathways synthetically lethal with WTA biosynthesis.

This work details the results of a scaled-up pathway-directed high-throughput screen of 230,000 small molecules against the WTA pathway. With previous work done on the pilot screens providing proof-of-principle, the challenge then became how to rapidly identify on-target inhibitors from a much larger screen. Using chemical genetics and the knowledge of synthetic lethal interactions, we designed secondary phenotypic screens to quickly classify compounds into different groups based on what pathways they were expected to target. From there, target identification was quick as the assays to identify inhibitors of these pathways were already developed.[27b,39a] As a result, we rapidly identified and validated a new late-stage WTA inhibitor and two new inhibitors of the Dlt pathway, which we are actively using to continue our biological understanding of these two pathways. The methods devised may be broadly adapted and used to discover compounds that inhibit other pathways of interest that may be out of reach from traditional screening approaches.

1.8 References

1. Matano, L. M., et al., *Bioorg. Med. Chem.* **2016,** *24* (24), 6307-6314.

2. Centers for Disease Control and Prevention. Antibiotic Resistance Threats in the United States, 2013. http://www.cdc.gov/drugresistance/threat-report-2013/pdf/ar-threats-2013-508.pdf (accessed May 21).

3. Walsh, C. T.; Wencewicz, T. A., *J. Antibiot.* **2014,** *67* (1), 7-22.

4. (a) Brown, E. D.; Wright, G. D., *Nature* **2016,** *529* (7586), 336-343; (b) Brooks, B. D.; Brooks, A. E., *Adv. Drug Delivery Rev.* **2014**.

5. Payne, D. J., et al., *Nat. Rev. Drug Discovery* **2007,** *6* (1), 29-40.

6. Donald, R. G. K., et al., *Cell Chem. Biol.* **2009**.

7. Wang, J., et al., *Nat. Lett.* **2006**.

8. (a) Swoboda, J. G., et al., *ACS Chem. Biol.* **2009,** *4* (10), 875-883; (b) Chen, W., et al., *ACS Chem. Biol.* **2009**.

9. (a) Neuhaus, F. C.; Baddiley, J., *Microbiol. Mol. Biol. Rev.* **2003,** *67* (4), 686-723; (b) Brown, S., et al., *Annu. Rev. Microbiol.* **2013,** *67* (1), 313-336; (c) Percy, M. G.; Gründling, A., *Annu. Rev. Microbiol.* **2014**; (d) Schneewind, O.; Missiakas, D., *J. Bacteriol.* **2014,** *196* (6), 1133-42.

10. Pasquina, L. W., et al., *Curr. Opin. Microbiol.* **2013,** *16* (5), 531-537.

11. (a) Gründling, A.; Schneewind, O., *Proc. Natl. Acad. Sci. U. S. A.* **2007,** *104* (20), 8478-8483; (b) Baddiley, J., *Acc. Chem. Res.* **1970,** *3* (3), 98-105.

12. (a) Grundling, A.; Schneewind, O., *J Bacteriol* **2007,** *189* (6), 2521-30; (b) Kiriukhin, M. Y., et al., *J. Bacteriol.* **2001,** *183* (11), 3506-14.

13. Koch, H. U., et al., *Eur. J. Biochem.* **1984,** *138* (2), 357-63.

14. Grundling, A.; Schneewind, O., *J. Bacteriol.* **2007,** *189* (6), 2521-30.

15. (a) Brown, S., et al., *Cell Chem. Biol.* **2008,** *15* (1), 12-21; (b) Meredith, T. C., et al., *J. Bacteriol.* **2008,** *190* (8), 3046-3056.

16. D'Elia, M. A., et al., *J Bacteriol* **2006,** *188* (12), 4183-9.

17. D'Elia, M. A., et al., *Chem Biol* **2009,** *16* (5), 548-56.

18. Schaefer, K., et al., *Nat Chem Biol* **2017,** *13* (4), 396-401.

19. Rajagopal, M.; Walker, S., *Curr. Top. Micriobiol. Immunobiol.* **2016**.

20. (a) Brown, S., et al., *Proc. Natl. Acad. Sci. U. S. A.* **2012,** *109* (46), 18909-18914; (b) Xia, G., et al., *J. Biol. Chem.* **2010**.

21. (a) Herbert, S., et al., *PLoS Pathogens* **2007**; (b) Cui, L., et al., *Antimicrob. Agents Chemother.* **2005**; (c) Meehl, M., et al., *Antimicrob. Agents Chemother.* **2007**.

22. Perego, M., et al., *J Biol Chem* **1995,** *270* (26), 15598-606.

23. Reichmann, N. T., et al., *Micriobiol.* **2013**.

24. (a) Kaito, C.; Sekimizu, K., *J. Bacteriol.* **2007,** *189* (6), 2553-7; (b) Collins, L. V., et al., *J. Infect. Dis.* **2002,** *186* (2), 214-219; (c) Peschel, A., et al., *J. Biol. Chem.* **1999,** *274* (13), 8405-8410; (d) Peschel, A., et al., *Antimicrob. Agents Chemother.* **2000,** *44* (10), 2845-2847.

25. (a) D'Elia, M. A., et al., *J. Bacteriol.* **2006,** *188* (12), 4183-9; (b) D'Elia, M. A., et al., *J. Bacteriol.* **2009**.

26. (a) Qiao, Y., et al., *J. Am. Chem. Soc.* **2014,** *136* (42), 14678-81; (b) Lee, W., et al., *J. Am. Chem. Soc.* **2015**.

27. (a) Lee, K., et al., *Bioorg. Med. Chem. Lett.* **2010,** *20* (5), 1767-70; (b) Campbell, J., et al., *Antimicrob. Agents Chemother.* **2012,** *56* (4), 1810-20; (c) Schirner, K., et al., *ACS Chem. Biol.* **2011,** *6* (5), 407-12; (d) Schirner, K., et al., *Nat. Chem. Biol.* **2015,** *11* (1), 38-45; (e) Farha, M. A., et al., *Proc. Natl. Acad. Sci. U. S. A.* **2015**.

28. Wang, H., et al., *Cell Chem. Biol.* **2013,** *20* (2), 272-84.

29. Lee, S. H., et al., *Sci. Transl. Med.* **2016,** *8* (329).

30. (a) Campbell, J., et al., *ACS Chem. Biol.* **2011,** *6* (1), 106-116; (b) Atilano, M. L., et al., *Proc. Natl. Acad. Sci. U. S. A.* **2010,** *107* (44), 18991-18996.

31. (a) Zapun, A., et al., *FEMS Microbiol. Rev.* **2008,** *32* (2), 361-385; (b) Matsuhashi, M., et al., *J. Bacteriol.* **1986**; (c) Pinho, M. G., et al., *Proc. Natl. Acad. Sci. U. S. A.* **2001,** *98* (19), 10886-10891.

32. Farha, M. A., et al., *ACS Chem. Biol.* **2013,** *8* (1), 226-33.

33. (a) Clatworthy, A. E., et al., *Nat. Chem. Biol.* **2007,** *3* (9), 541-8; (b) Smith, P. A.; Romesberg, F. E., *Nat. Chem. Biol.* **2007**.

34. Rasko, D. A.; Sperandio, V., *Nat. Rev. Drug Discovery* **2010**.

35. (a) Casadei, G., et al., *Proc. Natl. Acad. Sci. U. S. A.* **2006**; (b) Irazoqui, J. E., et al., *Nat. Rev. Immunol.* **2010**.

36. Rubin, R. P., *Pharmacological Reviews* **2007,** *59* (4), 289-359.

37. Santa Maria, J. P., et al., *Proc. Natl. Acad. Sci. U. S. A.* **2014,** *111* (34), 12510-12515.

38. (a) Falord, M., et al., *PLoS One* **2011**; (b) Falord, M., et al., *Antimicrob. Agents Chemother.* **2012**.

39. (a) Pasquina, L., et al., *Nat. Chem. Biol.* **2015**; (b) Hancock, I. C., et al., *FEBS Lett.* **1976**.

40. Santa Maria, J. P., Jr., et al., *Proc Natl Acad Sci U S A* **2014,** *111* (34), 12510-5.

Chapter 2: An antibiotic that inhibits the ATPase activity of an ABC transporter by binding to a remote extracellular site

A version of this chapter has been submitted for publication.

Authors:

Leigh M. Matano[1], Heidi G. Morris[1], Anthony R. Hesser[1], Sara E. S. Martin[1], Wonsik Lee[1], Tristan W. Owens[2], Emaline Laney[1], Hidemasa Nakaminami[3], David Hooper[3], Timothy C. Meredith[4]* and Suzanne Walker[1*]

Affiliations:

[1]Department of Microbiology and Immunobiology, 77 Ave Louis Pasteur, Boston, MA 02115, [2]Department of Chemistry and Chemical Biology, 12 Oxford St., Cambridge, MA 02138, [3]Division of Infectious Diseases, Massachusetts General Hospital, 55 Fruit St., Boston, MA 02114, [4]Department of Biochemistry and Molecular Biology, 206 South Frear Laboratory, University Park, PA 16802

Contributions:

LMM conducted the HTS, analyzed the data, performed the MIC testing, raised mutants, sequenced mutations, and wrote first draft

HGM conducted the HTS, performed the *B. subtilis* MIC and disk diffusion assay

ARH expressed and purified TarGH, developed the *in vitro* assay for ATPase activity, performed all biochemistry experiments and calculations, TWO provided plasmids for TarGH expression

SESM synthesized the panel of analogs, WL measured lipid II levels of inhibitor treated samples

EL with mentoring from LMM and WL determined F.O.R. for targocil-II

HN and DH conducted skin abscess model infection, *TM and SW are corresponding authors

Chapter 2: An antibiotic that inhibits the ATPase activity of an ABC transporter by binding to a remote extracellular site

S. aureus has proven to be a highly adaptable pathogen, developing resistance almost as quickly as new antibiotics come to market.[1] Maintaining a pipeline of antibiotics with activity against *S. aureus* is necessary to stay ahead of emerging resistance.[2] We describe here the discovery of a small molecule with promising anti-staphylococcal activity both *in vitro* and *in vivo*. The compound inhibits an ABC transporter in the wall teichoic acid (WTA) biosynthetic pathway, and we show that it blocks the ATPase activity of the nucleotide binding domain (NBD) by binding to a remote site. These studies show that the coupled conformational changes of the two domains in ABC transporters can be exploited to develop specific inhibitors that block activity of the highly-conserved ATPase, thus providing a new paradigm for ABC transporter inhibition.

2.1 The wall teichoic acid pathway is a good antibiotic target

The WTA pathway is a promising antibacterial target because WTAs, which are covalently attached to peptidoglycan, play crucial roles in cell division, antibiotic resistance, and pathogenesis.[3] WTA precursors are synthesized on a lipid carrier on the inner leaflet of the plasma membrane and then exported to the cell surface by the two component ABC transporter TarGH (Figure 2.1).[3b] ABC transporters are found in all domains of life and use ATP binding and hydrolysis to power conformational changes to translocate molecules across the cell membrane.[4] Although WTAs are required for infection,[3a] the first and second steps in the biosynthetic pathway, catalyzed by TarO and TarA, respectively, can be blocked genetically or pharmacologically without loss of viability; however, inhibiting subsequent steps is lethal.[5] The lethal phenotype resulting from a late block in the pathway, which is due to depletion of peptidoglycan precursors (see below),[2e,6] inspired us to develop a pathway-specific, whole cell assay for WTA-targeted

antibiotics that involved screening a wildtype strain for growth inhibition while counterscreening a WTA null (Δ*tarO*) strain for suppression of bioactivity.[3b,7] Using this screening approach, several WTA inhibitors were previously discovered, but limited solubility precluded further development and also hampered efforts to elucidate the mode of inhibition.

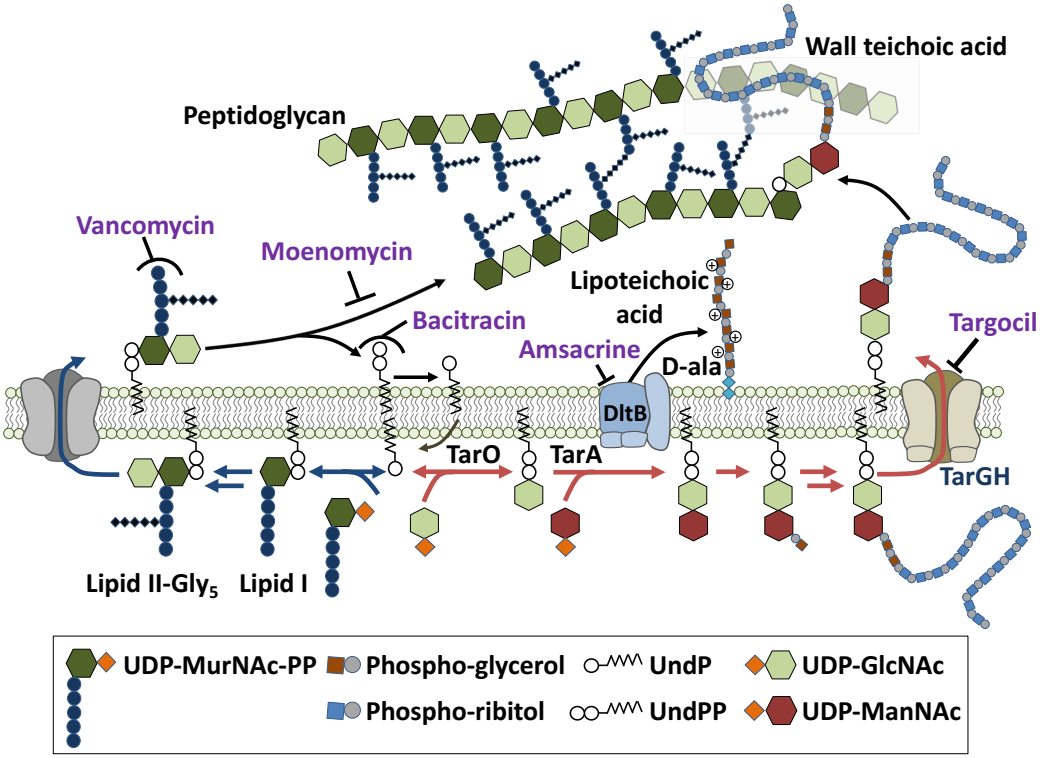

Figure 2.1 Schematic of cell wall biosynthetic pathways. Blue arrows denote the peptidoglycan pathway and red arrows denote the WTA pathway; these pathways use the same undecaprenyl (UndP) carrier lipid. Antibiotic structures and legend abbreviations explained in Figure 2.2.

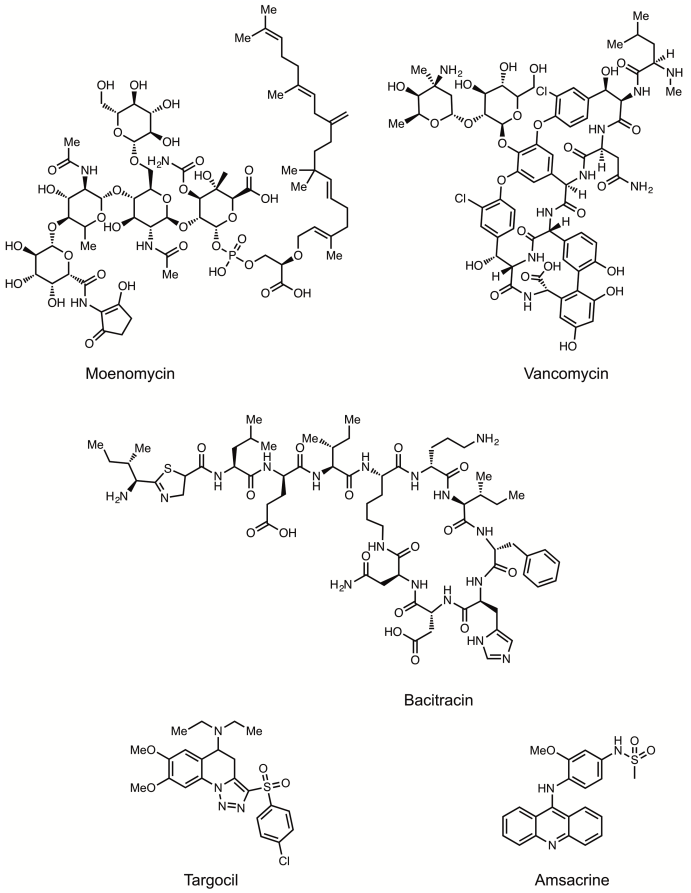

Figure 2.2: Structures of antibiotics and compounds used in this work. Legend abbreviations from Figure 2.1, main text are as follows: undecaprenol phosphate (UndP), undecaprenol pyrophosphate (UndPP), phosphotidyl-glycerol (Phospho-glycerol), phosphotidyl-ribitol (Phospho-ribitol), uridine diphosphate N-acetylmuramyl-pentapeptide (UDP-MurNAc-PP), uridine diphosphate N-acetylglucosamine (UDP-GlcNAc), uridine diphosphate N-acetylmannosamine (UDP-ManNAc).

2.2 Discovery of a late-stage WTA inhibitor from a high-throughput pathway-directed screen

With the goal of identifying better WTA inhibitors, we screened 230,000 small molecules at a final concentration of ~15 μM against wildtype *S. aureus* and the Δ*tarO* knockout strain. The screen produced a single strong hit (**1**), which proved to be a furanocoumarin derivative (Figure 2.3A). Compound **1** was found to have a minimum inhibitory concentration (MIC) of 1 μg/mL against *S. aureus*, including β-lactam resistant strains (MRSA), which is comparable to targocil, a well-characterized WTA-active antibiotic we discovered previously.[7a] A literature search revealed that compound **1** had been identified as a growth inhibitor in a 2,000,000-compound screen for *S. aureus* antibiotics, but its target was not identified.[8] Based on structurally related compounds also reported as hits in that large screen, we synthesized a panel of analogs. Two L-proline derivatives (**2** and **4**) were found to be especially potent inhibitors of wildtype *S. aureus* growth (0.125 μg/mL), but showed no activity against the Δ*tarO* strain (Figure 2.3B and Table 2.1). The kinetic solubility of these compounds was two to three logs greater than targocil's and the half-lives were 20-40 times longer in mouse liver microsomes (Table 2.2). The compounds were not cytotoxic, and treatment with compound **2** substantially reduced *S. aureus* CFUs recovered from a subcutaneous abscess infection (Table 2.2, Table 2.3). Moreover, compounds **2** and **4**, delivered in a dose of 1.25 mg/kg, rescued 17 of 20 mice from a lethal intraperitoneal inoculum of *S. aureus* (Figure 2.4). Based on the promising antibiotic properties of the compound, we elucidated its mechanism of action.

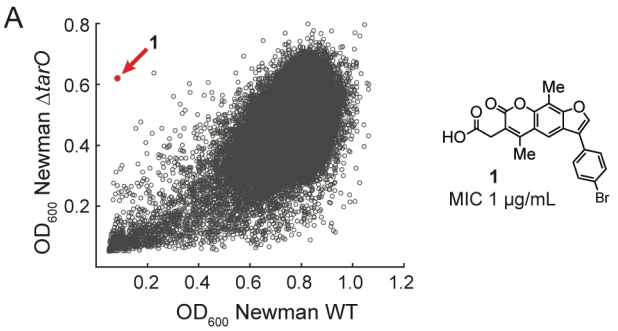

B

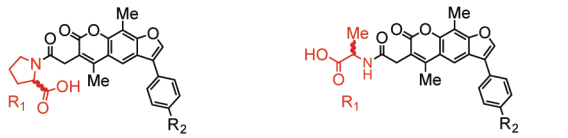

Compound	R_1	R_2	MIC μg/mL	Compound	R_1	R_2	MIC μg/mL
2	L-Pro	Cl	0.125	**6**	L-Ala	Cl	0.25
3	D-Pro	Cl	2	**7**	D-Ala	Cl	2
4	L-Pro	Br	0.125	**8**	L-Ala	Br	0.25
5	D-Pro	Br	1	**9**	D-Ala	Br	2

Figure 2.3 A HTS screening hit led to potent anti-MRSA compounds. (A) Plot of high-throughput screening results. Each circle represents the average OD_{600} of the strains in the presence of a library compound tested in duplicate. One compound (compound **1**, red circle) inhibited growth of the WT strain but not Δ*tarO*. (B) Synthesized analogs of **1** and their activities against *S. aureus* Newman. MICs against MRSA strains are identical (Table 2.1). For a complete list of analogs tested, see appendix 3.

Table 2.1: Minimum inhibitory concentrations (MICs) of select synthesized analogs against *S. aureus* strains. Analogs were tested for activity against four methicillin-resistant (MRSA) strains: community-acquired strains USA100, MW2 (USA400) and USA300 and hospital-acquired strain 1784A. Strains were grown in 96-well plates in TSB with concentrations of compound from 64 to 0.0625 μg/mL and monitored for 16-18 hours. No activity was observed against Newman Δ*tarO* and activity against wildtype Newman was retained even in the presence of 50% fetal bovine serum (FBS). The frequency of resistance was determined for **2** and targocil. Two-thirds of the resistant mutants for **2** contain inactivating mutations in TarO or TarA that would impair pathogenesis.

Compound	USA100	USA300	1784A	MW2	Newman Δ*tarO*	Newman, 50% FBS	Frequency of resistance
1	1	1	1	1	>64	32	n.d.
2	0.125	0.125	0.125	0.125	>64	1	2.7×10^{-8}
4	0.125	0.125	0.125	0.125	>64	2	n.d.
6	0.25	0.25	0.25	0.25	>64	4	n.d.
8	0.25	0.25	0.25	0.25	>64	4	n.d.
Targocil	1	1	1	1	>64	32	1.2×10^{-7}

Table 2.2: Furanocoumarin analogs show improved solubility and stability in comparison to targocil. Percent viability assay was performed by Christine Anderson with the Harvard CETR core. Kinetic solubility and mouse liver microsomal stability was outsourced to The Drug Metabolism and Pharmacokinetics Core at The Scripps Research Institute. See methods for full description of assay procedures.

Compound	Kinetic Solubility (μM)	Microsomal Stability (half-life, min)	Eukaryotic Cell Viability (10 μM)
1	9	35.6	100%
2	54	58.3	100%
4	21	>120	100%
6	18	>120	100%
8	11	>120	100%
Targocil	0.1	2.8	100%

Table 2.3: Colony forming units (CFUs) of mouse subcutaneous abscesses treated with 2 or targocil. Exponential-phase cells of *S. aureus* MW2 were washed and diluted twenty-fold in phosphate buffered saline (PBS). The cell suspension was then mixed with an equal volume of autoclaved Cytodex-1 beads that had been hydrated with either PBS, drug diluent alone, or a series of drug concentrations. **2** was diluted in PBS, and targocil was diluted in 5% or 25% DMSO. Beads were allowed to settle, and the supernatant was removed before mixing with bacteria. 0.2 ml of the bacteria-bead suspension was injected subcutaneously into the shaved flank of a mouse. The inoculum for each abscess typically contained 1-3 x 10^6 CFUs. After 48 hours the mice were euthanized, and the subcutaneous abscesses were removed, homogenized in TSB, and placed on ice. Dilutions of the homogenate in TSB were then promptly plated on trypticase soy agar and the number of colonies counted after 24 hr incubation at 37°C. Numbers reported are the average of four abscesses.

Amount delivered (μg)	**2** (CFUs)	Targocil (CFUs)
Control	1.66E+08	3.66E+08
2	1.23E+08	1.88E+08
4	3.80E+07	2.69E+08
10	1.61E+06	6.25E+08
40	3.10E+05	4.90E+08
100	1.13E+02	4.85E+08

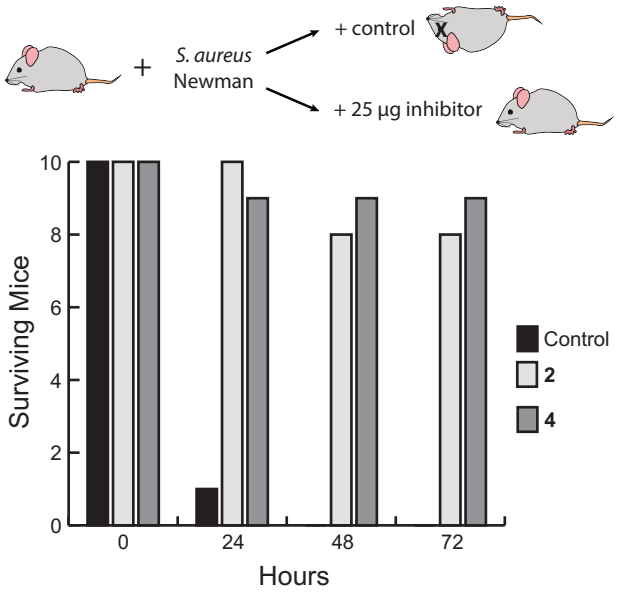

Figure 2.4: >80% of mice treated with compound 2 or 4 were rescued from S. aureus infection in a simple bacteremia model. Three groups of female Balb/C mice (ten animals per group) were challenged with 6 X 10^8 CFUs of the Newman strain of *S. aureus* administered by intraperitoneal (IP) injection, followed immediately by IP injection of 25 µg **2** (prepared by dissolving compound in DMSO at 2.5 mg/mL and diluting 1:20 in PBS), 25 µg **4**, or vehicle alone. Animals were monitored twice daily for survival.

2.3 Compound 2 depletes cell wall precursors, as expected for a WTA inhibitor

We first assessed the effect of the compound on pool levels of the peptidoglycan precursor, Lipid II, using a previously developed assay.[2e,6] Compounds that inhibit a late step in the wall teichoic acid pathway deplete Lipid II because this peptidoglycan precursor is biosynthesized on the same carrier lipid, undecaprenyl phosphate (UndP, Figure 2.1).[2e,5-6] If the UndP carrier lipid is sequestered in WTA precursors, it is not available for peptidoglycan precursor synthesis. Cultures of *S. aureus* were treated for ten minutes with targocil, **2**, or three peptidoglycan synthesis

inhibitors with mechanisms of action that lead either to Lipid II depletion (bacitracin, which inhibits carrier lipid recycling) or Lipid II accumulation (moenomycin and vancomycin, which inhibit peptidoglycan assembly; Figure 2.1, Figure 2.5A). Cellular lipids were extracted and the Lipid II present therein was labeled with biotin to enable detection by streptavidin-HRP.[2e,6] Like targocil and bacitracin, compound **2** depleted Lipid II. Combined with the suppression of bioactivity in the Δ*tarO* strain, this result confirmed inhibition of a late step in the WTA pathway.

2.4 Resistant colonies have mutations in *tarG*, the gene for the transmembrane domain of the TarGH flippase

To identify the molecular target within the WTA pathway, we selected resistant mutants on compound **2**. Twenty-seven colonies from three independent cultures were selected for evaluation. We expected two classes of mutants: those with mutations in the molecular target and those with mutations that disrupted function of TarO or TarA.[3b,5] To sort these mutants, we made use of the teichoic acid D-alanylation inhibitor, amsacrine, which prevents growth of WTA null strains.[9] Seventeen mutants were unable to grow on the inhibitor (Figure 2.5B), and all of these were found to contain null mutations in *tarO* or *tarA*; all other mutants contained point mutations that resulted in amino acid substitutions in TarG, the transmembrane component of the ABC transporter that exports WTA precursors to the cell surface (Figure 2.5C; Table 2.4). These results validated the procedure used to classify mutants and suggested that TarG is the target of **2**.

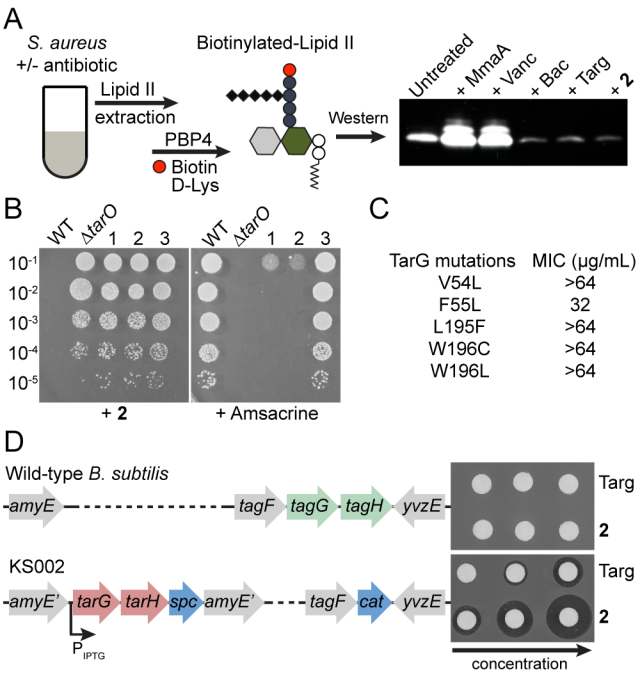

Figure 2.5 TarG is the target of 2. (A) Schematic of assay to detect Lipid II abundance after antibiotic treatment, with results for control antibiotics and **2** shown. Extracted Lipid II is labeled with biotin-D-Lys using *S. aureus* PBP4 to enable detection with HRP-streptavidin. (B) Mutants resistant to **2** (lanes 1-3) were sorted into two groups by plating on amsacrine. Amsacrine-susceptible mutants 1 and 2 had mutations in *tarA* while amsacrine-resistant mutant 3 had a mutation in *tarG* (see Table 2.4 for full mutant list). (C) Amino acid substitutions in TarG that conferred high level resistance to **2**. (D) Disk diffusion assay shows that strain KS002, in which *B. subtilis* TagGH was replaced with *S. aureus* TarGH, is sensitive to **2**.

Table 2.4: Table of isolated mutants resistant to compound 2 and their sensitivities to amsacrine. Three different *S. aureus* Newman starter cultures designated by group A, B, or C were diluted from overnights, grown until an OD_{600} of 1 and plated on TSB agar plates containing 10 μg/mL compound **2**. Resistant colonies were passaged twice on TSB agar plates containing no compound. Mutants were then inoculated overnight in TSB, diluted 1:100 in fresh TSB and grown to an OD_{600} of 1. Serial dilutions of samples were made and then plated on TSB agar plates containing either 10 μg/mL amsacrine or 10 μg/mL **2**. Those sensitive to amsacrine and resistant to compound **2** contain mutations in *tarO* and *tarA* while those that showed no sensitivity had mutations in *tarG*.

Mutant #	Phenotype	Gene	Mutation
1 (A)	$Amsa^S$	tarA	G96S
2 (A)	$Amsa^S$	tarA	521_525del
3 (A)	$Amsa^R$	tarG	V54L
4 (A)	$Amsa^S$	tarO	506delG
5 (A)	$Amsa^S$	tarO	506delG
6 (A)	$Amsa^R$	tarG	W196C
7 (A)	$Amsa^R$	tarO	T167K
8 (B)	$Amsa^R$	tarG	Y190S
9 (B)	$Amsa^S$	tarO	S289*
10 (B)	$Amsa^S$	tarO	880_891del
11 (B)	$Amsa^S$	tarA	506delG
12 (B)	$Amsa^R$	tarG	F55L
13 (B)	$Amsa^S$	tarA	G118R
14 (B)	$Amsa^S$	tarA	R222I
15 (B)	$Amsa^S$	tarA	R222I
16 (B)	$Amsa^S$	tarA	Q132*
17 (C)	$Amsa^R$	tarG	W196C
18 (C)	$Amsa^R$	tarG	W196L
19 (C)	$Amsa^S$	tarO	331delT
20 (C)	$Amsa^R$	tarG	F55L
21 (C)	$Amsa^S$	tarO	777delG
22 (C)	$Amsa^S$	tarO	777delG

Table 2.4 (Continued)

23 (C)	Amsa^S	tarO	502_517del
24 (C)	Amsa^S	tarG	L195F
25 (C)	Amsa^R	tarG	F189V
26 (C)	Amsa^S	tarO	S14R
27 (C)	Amsa^R	tarG	L195F

2.5 TarGH is confirmed as the target of compound 2

We used two different approaches to confirm TarG as the target. First, we expressed one of the resistant *tarG* alleles in a clean *S. aureus* background and found that expression conferred dominant resistance (Figure 2.6A). Second, after verifying that **2** did not inhibit growth of *B. subtilis* (Figure 2.6B), we made use of a previously engineered *B. subtilis* strain in which the endogenous WTA transporter genes (*tagGH*) were replaced with the *S. aureus* transporter genes at an ectopic locus.[10] Compound **2** did not show a zone of inhibition in a disk diffusion assay against wildtype *B. subtilis*, but it showed a dose-dependent inhibition zone when tested against the strain expressing the *S. aureus* transporter (Figure 2.5D). This gain of sensitivity to compound **2** upon heterologous expression of *S. aureus tarGH* in *B. subtilis* confirmed the *S. aureus* wall teichoic acid transporter as its target.

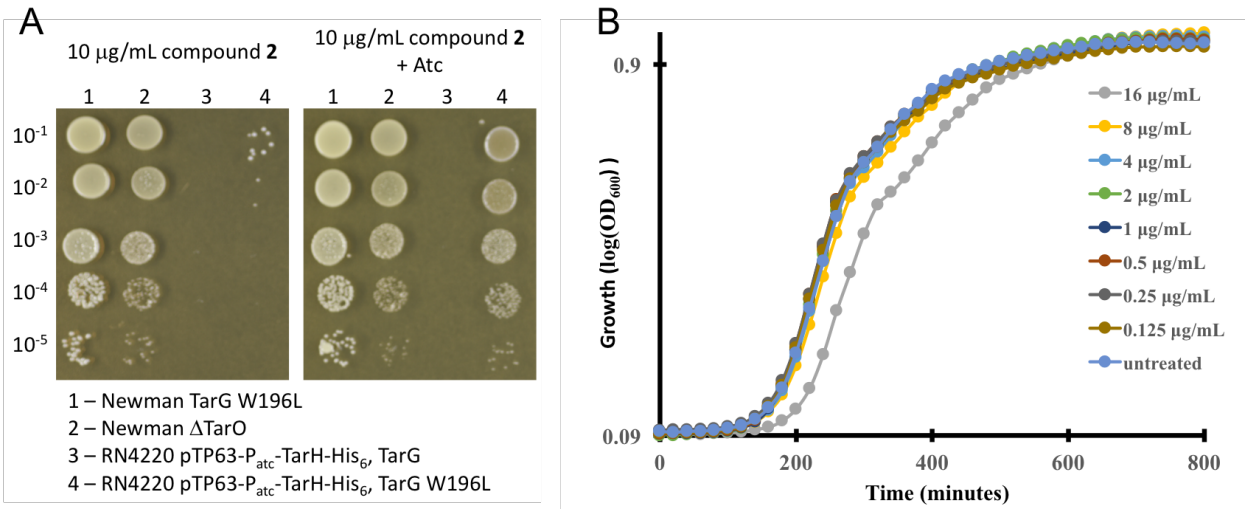

Figure 2.6: Mutations in tarG confer complete resistance to compound 2 and has no activity against B. subtilis. (A). (B) A series of 10-fold dilutions were plated on 10 µg/mL **2** without and with inducer (400 nM anhydrotetracycline). Expression of *tarG* W196L confers resistance to compound **2**, but expression of a second copy of wildtype *tarG* does not confer resistance. (B) Growth of wildtype *B. subtilis* PY79 in the presence of increasing concentrations of **2**. Wildtype PY79 was grown in LB at 37°C with the indicated concentration of **2** in 96 well plates. Growth of PY79 was unaffected by **2** in concentrations exceeding 100X the MIC against WT *S. aureus* Newman (0.125 µg/mL). The data is averaged from three biological replicates.

2.6 Compound 2 inhibits ABC transporter activity in vitro

Several classes of compounds that inhibit WTA export have now been identified and some of the TarG mutations resistant to **2** were previously selected with structurally distinct WTA inhibitors (Table 2.5).[3b,7b] Thus, there appears to be a common inhibitor binding site; however, it was unclear how any of these inhibitors blocked TarGH transport. Elucidating how these compounds act may not only provide insight into how to improve WTA inhibitors, but could guide efforts to develop inhibitors of other ABC transporters. The ABC transporter family is very large

and includes many possible therapeutic targets in both prokaryotes and eukaryotes, but few mechanistic studies on inhibitors have been reported.[11] P-glycoprotein inhibitors have received the most attention due to the importance of this ABC transporter in multidrug resistance in cancer.[12] Inhibitors that compete with ATP for binding to the nucleotide binding domain (NBD) or with exported substrates have been studied, but were abandoned due to lack of specificity and toxicity.[13] The most promising P-glycoprotein inhibitors identified to date bind to the transmembrane (TM) domain in a manner that prevents substrate transport, but nevertheless allows robust ATP hydrolysis.[11c,14]

Table 2.5: List of mutations in tarG and overlap between different inhibitor classes. Some mutations in *tarG* identified with compound **2** were previously found to confer resistance to a different class of inhibitors, suggesting a common inhibitor binding site.

TarG Mutation	Targocil[3b]	L275/L638[7b]	Compound **2**
V54L		L638	Yes
V54F		L638	
F55L			Yes
P64L		L275, L638	
W73C	Yes		
G77A		L638	
F82L	Yes	L275, L638	
C156Y		L638	
F189V			Yes
Y190C		L638	
Y190S			Yes
L195F			Yes
W196L		L638	Yes
W196C		L638	Yes
P198S		L638	
H208Y		L275	
Y217C		L638	

To obtain information on how **2** inhibits TarGH, we co-expressed wildtype TarG with either TarH-His_6 or an ATPase-inactive TarH-His_6 mutant (E169Q), solubilized the complexes in dodecylmaltoside, purified them over a Co^{2+} affinity column followed by size exclusion chromatography, and reconstituted them into proteoliposomes.[15] The ATPase activity of the reconstituted transporter, measured using a continuous chromogenic assay, was similar to the activity reported for other ABC transporters.[16] The addition of 1.0 μM compound **2** strongly inhibited ATPase activity even though the ATP concentration was 1000-fold higher (Figure 2.7A). Additional experiments showed that the ATPase activity of the WT transporter inhibited with 1.0 μM **2** was comparable to that of a TarGH mutant containing a mutation that impairs ATP hydrolysis (TarH E169Q) (Figure 2.8A; Figure 2.8B).

To locate the binding site of **2** relative to the ATPase, we generated a homology model for TarGH using the human ABCG5/ABCG8 sterol transporter as the template and mapped the resistance mutations to the modeled structure (Figure 2.7B,C).[17] In agreement with the topology of many other ABC exporters, each TarGH dimer has 12 TM helices,[16b,18] which are grouped such that TM helices one and two from one monomer are in close proximity to TM helix five of the other monomer. The high-level resistance mutations selected with compound **2** map near the extracellular ends of TM helices one and five, suggesting that the binding site spans the dimer interface; given the symmetry, it is likely that two molecules of **2** bind to the dimer. Because **2** inhibits ATP hydrolysis, but binds to a site on the opposite side of the membrane, the compound must lock the TM domain in a conformation that prevents the coupled inter-domain structural changes required for ongoing ATP hydrolysis by the NBDs.

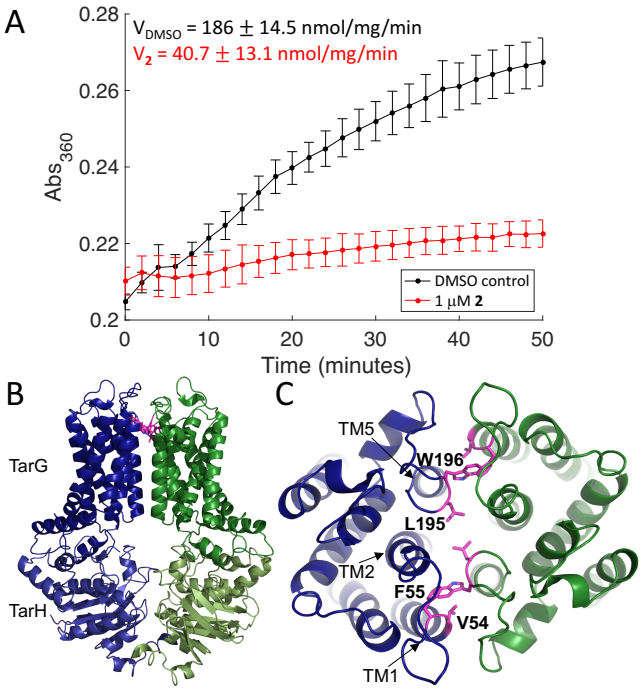

Figure 2.7 Compound 2 inhibits the ATPase activity of TarGH in proteoliposomes even though it binds in a remote location. (A) Averaged ATPase activity (n=3; error bars=SD) of reconstituted TarGH (200 nM) in the absence (black curve) and presence (red curve) of compound **2** (1 μM). Saturating levels of ATP (1 mM) were used. (B) Homology model of TarGH. TarH is cytoplasmic and much of TarG is embedded in the membrane. C) Top view of the TarG dimer. Mutations in residues shown in pink give high level resistance to **2**.

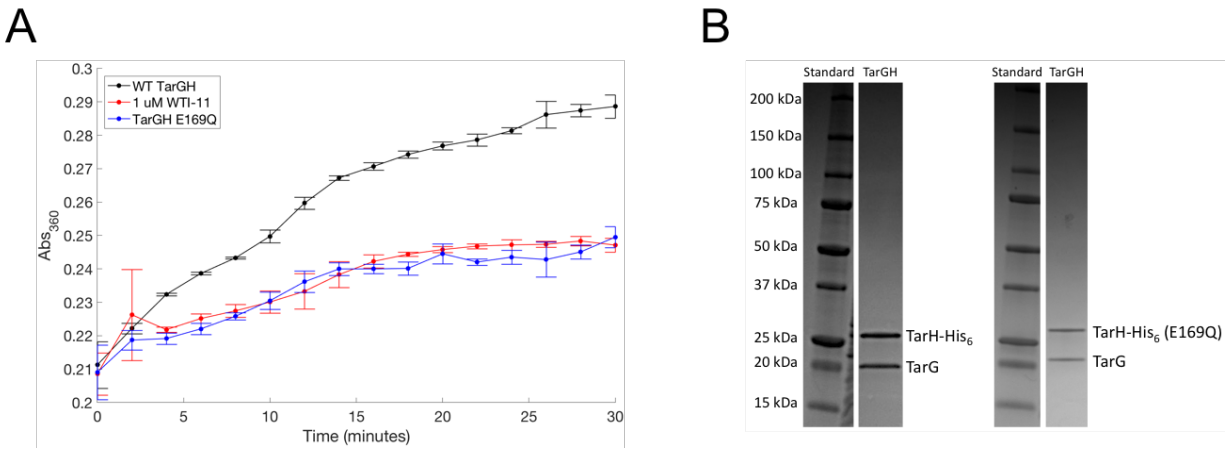

Figure 2.8: ATPase activity of the WT transporter inhibited with 1.0 µM 2 was comparable to that of a TarGH mutant containing a mutation that impairs ATP hydrolysis. (A) Compound **2** reduces the ATPase activity of WT TarGH in proteoliposomes to a low level that matches the low activity of the ATPase inactive TarH E169Q transporter. Assays were conducted in an identical manner to the experiment in Figure 2.7A with 1 mM ATP and 200 nM TarGH. The average and standard deviation of 3 technical replicates are shown. The background absorbance at 360 nm is higher in these proteoliposome preparations compared to that in Figure 2.6A, suggesting an uncharacterized contaminating activity. (B) Coomassie-stained gels showing TarGH bands following purification. The samples loaded correspond to the eluted fraction from Co^{2+} affinity chromatography prior to further purification on a size-exclusion chromatography column. Bands were assigned by comparison to Western Blots of FLAG-TarG and TarH-His_6 samples run under identical conditions.

2.7 Conclusions

In this chapter, we discuss the discovery and target identification of a new late-stage WTA inhibitor. Using a pathway-directed screening approach, we rapidly identified hit compound **1** as a WTA inhibitor simply based on the screening phenotype. Having narrowed the region of

biological space that was being targeted, we quickly identified the target of this class of compounds as the WTA flippase TarGH based off the following findings: 1) mutations in *tarG* cause dominant high-level resistance in a single step; 2) *S. aureus* treated with compound **2** show depleted amounts of cell wall precursors; 3) replacing the *B. subtilis* TaGH with *S. aureus* TarGH confers sensitivity to this class of compounds; and 4) in an *in vitro* biochemical reaction, compound **2** was found to prevent ATPase activity of TarGH. Compound **2**, hereafter to be called targocil-II, is the first known example of an ABC transporter inhibitor that prevents ATP hydrolysis by binding to an allosteric site in the TM domain. Given the sequence diversity of TM domains, this mode of binding has clear advantages with respect to specificity over ATP-competitive inhibitors that bind to a conserved binding pocket. Now that conditions have been developed to obtain the purified ABC transporter in active form, it may be possible to obtain structural information with inhibitor bound to facilitate development of transport inhibitors for therapeutic use. Furthermore, the preliminary *in vivo* activity of targocil-II suggests that this class of compounds have promising therapeutic potential, which will be followed up with subsequent experiments in more robust mouse models.

2.8 Methods

Reagents and Methods

S. aureus Newman was grown in tryptic soy broth (TSB) for liquid cultures or on TSB with 1.5% agar for spot dilutions at 30°C. High-throughput screening was done at the ICCB-Longwood Screening Facility. Analog **1** was purchased from ChemDiv (D143-0317). Analog **1b** was purchased from ChemDiv (D143-0316). Analogs **2**-**8** were synthesized. Amsacrine was purchased from Abcam (ab142742).

High Throughput screening (HTS)

HTS was performed at the ICCB Longwood facility at Harvard Medical School. Cultures of *S. aureus* Newman and *S. aureus* Newman Δ*tarO* were inoculated in TSB and grown overnight at 30°C and diluted the next day to an OD_{600} of 1. 384-well plates (Corning 3702) were prepared for screening by predispensing 30 μL of TSB using a Matrix Wellmate plate filler. 100 nL of compounds were pinned into lanes 1-22 of the prefilled 384-well plates for a final volume of ~15 μM. Immediately following, 50 μL of cells (OD_{600} =1 cells diluted 1:625 in TSB) was added to each well using the Matrix Wellmate for a final volume of 80 μL and final OD_{600} of .001. Lane 23 served as a no compound control. 10 μg/mL erythromycin (final concentration) was added to lane 24 as a positive control. Plates were incubated at 30°C for 16-18 hr. Plates were read using a PerkinElmer EnVision plate reader. Screening was performed in duplicate for each strain.

Raising resistant mutants

S. aureus Newman was inoculated in TSB and grown overnight. Cultures were diluted 1:100 and grown until to OD_{600} ~1. Cultures and ten-fold dilutions thereof were plated in 100 μL aliquots onto TSA plates containing 10 μg/mL compound **2** (approximately ~10^8 and 10^7 CFUs were plated). 100 μL of 10^{-6} and 10^{-7}-fold dilutions of the culture were plated onto no-compound control plates and used to back-calculate starting culture concentrations for calculating frequency of resistance. Plates were incubated overnight at 30°C. Resistant colonies isolated from plating 3 different starter cultures and were restreaked twice on TSA plates before testing. Genomic DNA was isolated from confirmed resistant colonies and targeted sequencing of WTA pathway genes was performed.

Spot dilutions

Resistant mutants were grown overnight, diluted 1:100, and grown over several hours until an OD_{600} of ~1. All strains were normalized to an OD_{600} of 1, and then serially diluted tenfold (from 10^{-1} to 10^{-5}). 5 μL of diluted culture was spotted onto TSA plates with 10 μg/mL compound **2**, 10 μg/mL amsacrine, or no compound. Plates were incubated at 30°C overnight.

Minimum inhibitory concentration (MIC) determination

S. aureus strains were inoculated and grown in TSB overnight. In the morning, strains were diluted 1:100 and grown for several hours until OD_{600} of ~1. All cultures were normalized to an OD_{600} of 1, then diluted 1:1000. 147 μL of diluted culture was added to each well of a 96-well plate. Compound dilution series were made in DMSO and 3 μL aliquots were transferred into 147 μL for final concentrations of 0-64 μg/mL in a final volume of 150 μL. Plates were then incubated 16-18 hours at 30°C and OD_{600} read by SpectraMax Plus 384 microplate reader (Molecular Devices). For assessing serum shift, TSB was spiked with 50% fetal bovine serum (ATCC cat#30-2020) and MIC was performed as described above. For the *B. subtilis* growth curves, PY79 and KS002 (+IPTG) were grown overnight in LB media at 37°C while shaking. After 16 hours, cultures were diluted 1:100, grown for 6-8 hours at 37°C and normalized to an OD_{600} of 1. Cultures were then diluted 1:1000 and 150 μL was plated in 96-well format. **2** was added in decreasing two-fold dilutions from 64 μg/mL to 0.03125 μg/mL. Growth was monitored over a 14-hour period (37°C, shaking), with reads every 20 minutes using a SpectraMax Plus 384 microplate reader.

Disk diffusion assay

Overnight cultures of WT *B. subtilis* and KS002[10] (1 mM IPTG) were diluted into fresh LB media to an OD_{600} of 0.1, grown to OD_{600} of approximately 0.8, then diluted to a final OD_{600} of 0.1 in 20 mL LB agar containing 1 μM IPTG. Filter disks were soaked with compound (**2** or targocil) and

placed on top. The plates were incubated overnight at 37°C and the zones of inhibition around the filter disk was interpreted as relative sensitivity against the compound.

Lipid extraction and Lipid II detection by western blot

The bacterial lipids were extracted as described.[6] Briefly, *S. aureus* RN4220 was grown to exponential phase (OD_{600} = 0.4) at 37°C. 2 mL of culture were then treated with the following antibiotics for 10 minutes at 37°C: 0.6 μg/mL **2**, 2.5 μg/mL **1**, 0.5 μg/mL moenomycin, 10 μg/mL vancomycin, 2.5 μg/mL targocil, 10 μg/mL bacitracin. Following biomass normalization based on OD_{600}, bacterial cells were harvested by centrifugation and resuspended in 0.3 mL pH 7.5 phosphate-buffered saline (PBS) then mixed with 1.5 mL of 2:1 methanol:chloroform immediately. The mixture was vortexed for 10 minutes at room temperature and centrifuged at 10 minutes at 4000 x *g* at room temperature. The supernatant was then transferred in a new glass tube and mixed with 1.0 mL of 1:1 chloroform:PBS (pH 7.5) followed by 10 minutes vortexing at room temperature. The mixture was then centrifuged for 10 minutes at 4000 x g to separate the organic and aqueous layers. The separated organic layer (bottom) was collected, dried, and resuspended in 20 μL DMSO.

The *S. aureus* Lipid II in the total lipid extract was labeled with biotin-D-Lys (BDL) using the *S. aureus* PBP4 as described.[6] Briefly, 2 μL of the Lipid extract was incubated with 10 μM of PBP4 and 3 mM BDL in a reaction buffer containing 12.5 mM HEPES pH 7.5, 20 mM $MnCl_2$, and 2.5 mM Tween-80 in 10 μL reaction volume for 1 hour at room temperature. The reactions were quenched by adding an equal amount of 2x SDS loading buffer and resolved on an SDS polyacrylamide gel (4-20% gradient), then transferred to a PVDF membrane (BioRad) and blotted with streptavidin-HRP (1:10000 dilution, Pierce). Finally, the Lipid II labeled with BDL was

visualized using ECL Prime Western Blotting Detection Reagent (GE Ambersham) and CL-XPosure Film (ThermoFisher Scientific).

Protein expression and purification

The genes encoding *S. aureus* NCTC8325 TarG and TarH with a C-terminal His_6 affinity tag were cloned into separate multiple cloning sites in the pCDFDuet-1 vector (Novagen). TarGH was co-expressed with the pRARE plasmid (Novagen) in *E. coli* KRX cells (Promega) grown at 37°C in LB Miller broth supplemented with 10% glycerol. Expression was induced by adding 0.02% L-rhamnose at an OD_{600} of 0.6 for 4 hours. All subsequent steps were performed at 4°C. Cells were harvested by centrifugation and resuspended in buffer A (20 mM Tris pH 8.0, 10% glycerol) plus 1 mM PMSF and 1 mM $MgCl_2$. DNase and lysozyme were added at 100 µg/mL and cells were disrupted in an EmulsiFlex-C5 homogenizer at 15,000 psi external pressure. Cell debris was pelleted, and membranes in the supernatant were subsequently pelleted by ultracentrifugation at 100,000*g*. Membranes were solubilized in buffer A plus 400 mM NaCl, 1 mM ATP or AMP-PNP, and 1% (w/v) *n*-dodecyl-D-maltopyranoside (DDM, Anatrace). Solubilized proteins were loaded on TALON resin (Clontech) equilibrated with buffer B (10 mM Tris pH 8.0, 100 mM NaCl, 10% glycerol, 0.03% DDM), washed with buffer B plus 200 mM NaCl and 10 mM imidazole, and eluted in buffer B plus 120 mM imidazole. The elution was further purified by size exclusion chromatography on a Superdex 200 Increase 10/300 GL (GE Healthcare) with buffer C (10 mM Tris pH 8.0, 100 mM NaCl, 0.03% DDM). Peak fractions were combined, concentrated to 20 µM in an Amicon Ultra-15 100 kDa cut-off concentrator (Millipore). Aliquots were flash frozen with liquid nitrogen and stored at -80°C. TarG and TarH(E169Q)-His_6 were co-expressed and purified in the same manner.

Reconstitution in proteoliposomes

E. coli polar lipid extract (Avanti Polar Lipids) was hydrated in buffer D (20 mM Tris pH 8.0, 100 mM NaCl) to 20 mg/mL at room temperature. After three freeze/thaw cycles, liposomes were extruded through a 100 nm polycarbonate membrane for 15 passes using an Avanti Mini Extruder (Avanti Polar Lipids), diluted with two volumes of buffer D + 0.4% DDM, and incubated at 4°C for 10 minutes. Liposomes were mixed with a freshly thawed aliquot of protein (1:10,000 mol protein:lipids) for 1 hour at 4°C, and detergent was removed with Bio-Beads SM-2 resin (Bio-Rad). Proteoliposomes were stored at 4°C and used within 1 day.

ATPase assays

ATPase activity in proteoliposomes was measured with the EnzChek® Phosphate Assay Kit (Molecular Probes) at 26°C in a 96-well format. The reaction mixture containing 20 mM Tris pH 8.0, 100 mM NaCl, 5 mM $MgCl_2$, 1 mM ATP or AMP-PNP, and **2** or DMSO control (a final concentration of 0.2% DMSO) was incubated with the MESG and purine nucleoside phosphorylase reagents for 10 minutes at room temperature to consume contaminating P_i. Reactions were initiated by addition of proteoliposome solution at a final protein concentration of 200 nM and absorbance at 360 nm was monitored using a SpectraMax Plus 384 microplate reader. Initial rates were measured as the slope of the linear region of product formation and based on a phosphate standard series.

Generation of TarGH homology model

TarG and TarH homology models were generated using the Phyre2 server.[17a] Models were aligned in PyMOL to corresponding subunits of the structure of the human ABCG5/8 sterol exporter (PDB 5DO7), as this is the only published ABC transporter structure from which a TarG homology model could be generated.[17b] TarH residues 244-264 are not shown due to low model confidence.

Hepatic microsomal stability

Microsome stability was evaluated by incubating 1 μM compound with 1 mg/ml mouse hepatic microsomes in 100 mM potassium phosphate buffer, pH 7.4. The reactions were held at 37° C with continuous shaking and initiated by adding NADPH, 1mM final concentration. The final incubation volume was 300 μl and 40 μl aliquots were removed at 0, 5, 10, 20, 40, and 60 minutes. The removed aliquot was added to 160 μl acetonitrile to stop the reaction and precipitate the protein. NADPH dependence of the reaction is evaluated in parallel incubations without NADPH. At the end of the assay, the samples are centrifuged through a 0.45 micron filter plate (Millipore Solventer low binding hydrophilic plates, cat# MSRLN0450) and analyzed by LC-MS/MS. The data was log transformed and results are reported as half-life. Assays were performed by Michael Cameron at The Drug Metabolism and Pharmacokinetics Core at the Scripps Research Institute.

Kinetic solubility

Compounds, prepared as 10 mM DMSO stock solutions, were introduced to pre-warmed pH 7.4 phosphate buffered saline in a 96–well plate. The final DMSO concentration was 1% and the plate was maintained with orbital shaking at 37°C for 24 hours. The samples were centrifuged through a Millipore Multiscreen Solvinter 0.45 micron low binding PTFE hydrophilic filter plate and analyzed by HPLC with peak area compared to standards of known concentration. Assays were performed by Michael Cameron at The Drug Metabolism and Pharmacokinetics Core at the Scripps Research Institute.

Eukaryotic Toxicity

Toxicity testing was done with Vero cells prepared in DMEM with 10% FBS. 200 μL of 0.5 x 10^5/mL were plated in a 96-well clear bottom plates (NUNC #165305). Plates were gently shaken

and incubated at room temperature for one hour and then set overnight at 37°C, 5% CO_2. Compound was thawed and diluted into D-10 media with 1% DMSO (D-10-1). After 24 hours, media was removed from cells and replaced with 200 μL of diluted compound at various concentrations. Samples treated with DMSO were used as controls. Plates were incubated overnight at 37°C, 5% CO_2. Cell viability was assessed after 24 hours using Promega CellTiter-Glo® Luminescent Cell Viability Assay (#G7571). Percent viability was calculated using (Mean Value – Mean Blank) / (Mean Control - Mean Blank) * 100%. The assay was performed by Christine Anderson with the Harvard CETR core.

Subcutaneous abscess model

Swiss Webster male mice that were 4 to 6 weeks old were used for the subcutaneous abscess model. Exponential-phase cells of *S. aureus* MW2 were prepared by 100-fold dilution of overnight cultures into brain heart infusion media and incubation at 37°C until the OD_{600} was 0.8. Cells were washed and diluted twentyfold in phosphate buffered saline (PBS). The cell suspension was then mixed with an equal volume of autoclaved Cytodex-1 beads (131 to 220 μm, Sigma) that had been hydrated with either PBS, drug diluent alone, or a series of drug concentrations. **2** was diluted in PBS, and targocil was diluted in 5% or 25% DMSO. Beads were allowed to settle, and the supernatant was removed before mixing with bacteria. 0.2 ml of the bacteria-bead suspension was injected subcutaneously into the shaved flank of a mouse anesthetized with ketamine and xylazine. The inoculum for each abscess typically contained 1-3 x 10^6 CFUs. After 48 hours the mice were euthanized, and the subcutaneous abscesses were removed aseptically, homogenized in 5 mL trypticase soy broth (TSB), and placed on ice. Dilutions of the homogenate in TSB were then promptly plated on trypticase soy agar and the number of colonies counted after 24 h incubation at 37°C. The amount of drug delivered in the subcutaneous inoculum (in μg) was calculated as

the drug concentration in the bead hydrating solution (in μg/mL) divided by 2 and multiplied by 0.2 mL. Values were expressed as mean and standard deviation from 2 to 4 abscesses.

Mouse model

Three groups of female Balb/C mice (ten animals per group) were challenged with 6 X 10^8 CFUs of *S. aureus* Newman administered by intraperitoneal (IP) injection, followed immediately by IP injection of 25 μg **2** (prepared by dissolving **2** in DMSO at 2.5 mg/mL and diluting 1:20 in PBS), 25 μg **4**, or vehicle alone. Animals were monitored twice daily for survival. Assays were performed by Christine Anderson of the CETR core (HMS).

2.9 Furanocoumarin analog synthesis

General Information

D- and L-alanine methyl ester hydrochloride were prepared from the corresponding amino acids following a published literature procedure,[19] and the products were in good agreement with characterization data reported in the literature.[20] Diisopropylethylamine (DIPEA) was dried on alumina according to published procedures. All other chemicals were purchased from commercial sources as noted below and used as received. Brine refers to a saturated solution of NaCl. NMR spectra were recorded on a Varian Mercury 400 or Varian Inova 500 (400 and 500 MHz for ^{1}H, respectively) instrument in $CDCl_3$ and were recorded at ambient temperatures. Chemical shifts are reported in units of parts per million (ppm). ^{1}H NMR were calibrated using the residual protio-solvent as a standard. Low-resolution mass spectra (LRMS) were obtained on an Agilent Technologies 1100 series LC-MSD instrument using electrospray ionization (ESI). High-resolution mass spectra (HRMS) were obtained on a Bruker micrOTOFQ-II mass spectrometer. Optical rotations ([α]) were measured on a Jasco DIP 370 digital polarimeter at 589 nm (sodium

D line) at ambient temperature using a 1 mL cell with a 0.5 dm path length. Column chromatography was performed with 40-63 μm silica gel purchased from Sorbent Technologies, with the eluent reported in parentheses. Analytical thin-layer chromatography (TLC) was performed on precoated glass plates and visualized by UV or by staining with $KMnO_4$.

Representative Procedure for Synthesis of Analogs:

A 4 mL vial was charged with the appropriate amino acid methyl ester hydrochloride (1 equiv), the appropriate psoralen (ChemDiv, 1 equiv), and a stir bar. The vial was sealed with a PTFE lined septum cap and was purged with nitrogen for approximately 5 minutes. Dimethylformamide (EMD DriSolv) was added via syringe. The cap was opened briefly, and **1-[Bis(dimethylamino)methylene]-1*H*-1,2,3-triazolo[4,5-*b*]pyridinium 3-oxid hexafluorophosphate** (HATU, aapptec, 1.1 equiv) was added. The cap was again placed on the vial, and DIPEA (1.1 equiv) was added via syringe. The reaction was stirred at rt for 3 h. Upon completion, the reactions were diluted with 200 μL each of water and EtOAc. The EtOAc layer was removed, and the water layer was extracted with EtOAc (2 x 200 μL). The combined organic layers were washed with brine, dried with $MgSO_4$, filtered, and concentrated *in vacuo*. The products were purified via flash column chromatography (30-40% EtOAc in Hexane with 0.1% Et_3N), and presence of product was confirmed with LRMS. The resulting esters were transferred to 4 mL vials and saponified using LiOH (approximately 10 equiv, 1 M in H_2O) in tetrahydrofuran (THF, EMD, ACS Grade, 1:1 v/v with H_2O) with stirring at 4ºC overnight. Reactions were quenched at 4ºC with stirring using HCl (3 M, 2 equiv). Brine (300 μL) was added, and the mixture was extracted with EtOAc (4 x 150 μL). The combined organic layers were dried with $MgSO_4$, filtered, and concentrated *in vacuo* to afford the final product.

2: Following the general protocol: L-proline methyl ester hydrochloride (Fluka, 4.3 mg, 0.026 mmol), **1b** (10 mg, 0.026 mmol), HATU (10.9 mg, 0.029 mmol), and DIPEA (9.5 μL, 0.055 mmol) were reacted in dimethylformamide (140 uL) at rt for 3 h. 4.5 mg (35%) of the ester product was obtained after purification. The ester was further reacted with LiOH (90 μL, 0.09 mmol) in THF (90 μL) to afford 3.2 mg (75%) of **2** as a white solid. ^{1}H NMR (400 MHz, $CDCl_3$) δ 7.83 (app s, 2H), 7.56 (d, 2H), 7.49 (d, 2H), 4.67 – 4.56 (m, 1H), 3.90 (d, *J* = 16.0 Hz, 1H), 3.82 (app t, *J* = 6.6 Hz, 2H), 3.74 (d, *J* = 16.0 Hz, 1H), 2.64 (s, 3H), 2.54 (s, 3H), 2.52 – 2.44 (m, 1H), 2.15 – 2.06 (m, 2H), 2.06 – 1.96 (m, 1H). HRMS (EI) m/z, calcd for [$C_{26}H_{22}ClNO_6$]: 502.1033; found: 502.1007. $[\alpha]_D^{24}$ -53.5º (c = 0.32, $CHCl_3$).

3: Following the general protocol: D-proline methyl ester hydrochloride (Fluka, 4.3 mg, 0.026 mmol), **1b** (10 mg, 0.026 mmol), HATU (10.9 mg, 0.029 mmol), and DIPEA (9.5 μL, 0.055 mmol) were reacted in dimethylformamide (140 uL) at rt for 3 h. 4.0 mg (31%) of the ester product was obtained after purification. The ester was further reacted with LiOH (90 μL, 0.09 mmol) in THF (90 μL) to afford 3.5 mg (>99%) of **3** as a white solid. ^{1}H NMR (400 MHz, $CDCl_3$) δ 7.83 (app s, 2H), 7.56 (d, *J* = 8.6 Hz, 2H), 7.49 (d, *J* = 8.5 Hz, 2H), 4.63 (dd, *J* = 7.9, 2.8 Hz, 1H), 3.90 (d, *J* = 16.0 Hz, 1H), 3.82 (dd, *J* = 7.3, 5.9 Hz, 2H), 3.74 (d, *J* = 16.0 Hz, 1H), 2.64 (s, 3H), 2.55 (s, 3H), 2.51 – 2.46 (m, 1H), 2.17 – 2.06 (m, 2H), 2.06 – 2.03 (m, 1H). HRMS (EI) m/z, calcd for [$C_{26}H_{22}ClNO_6$]: 480.1208; found: 480.1203. $[\alpha]_D^{24}$ 47.8º (c = 0.35, $CHCl_3$).

4: Following the general protocol: L-proline methyl ester hydrochloride (Aldrich, 3.8 mg, 0.023 mmol), **1** (10 mg, 0.023 mmol), HATU (9.5 mg, 0.025 mmol), and DIPEA (8.3 μL, 0.048 mmol) were reacted in dimethylformamide (120 uL) at rt for 3 h. 3.9 mg (31%) of the ester product was obtained after purification. The ester was further reacted with LiOH (90 μL, 0.09 mmol) in THF

(90 μL) to afford 3.3 mg (89%) of **4** as a white solid. ^{1}H NMR (500 MHz, $CDCl_3$) δ 7.84 (s, 1H), 7.82 (s, 1H), 7.65 (d, *J* = 8.5 Hz, 2H), 7.49 (d, *J* = 8.4 Hz, 2H), 4.63 (dd, *J* = 8.0, 2.6 Hz, 1H), 3.89 (d, *J* = 16.1 Hz, 1H), 3.85 – 3.79 (m, 2H), 3.74 (d, *J* = 16.1 Hz, 1H), 2.64 (d, *J* = 0.7 Hz, 3H), 2.54 (s, 3H), 2.52 – 2.45 (m, 1H), 2.16 – 2.06 (m, 2H), 2.06 – 1.99 (m, 1H). HRMS (EI) m/z, calcd for [$C_{26}H_{22}BrNO_6$]: 546.0523; found: 546.0512. $[\alpha]_D^{24}$ -48.1º (c = 0.33, $CHCl_3$).

5: Following the general protocol: D-proline methyl ester hydrochloride (Fluka, 3.8 mg, 0.023 mmol), **1** (10 mg, 0.023 mmol), HATU (9.5 mg, 0.025 mmol), and DIPEA (8.3 μL, 0.048 mmol) were reacted in dimethylformamide (120 uL) at rt for 3 h. 5.5 mg (44%) of the ester product was obtained after purification. The ester was further reacted with LiOH (90 μL, 0.09 mmol) in THF (90 μL) to afford 3.9 mg (76%) of **5** as a white solid. ^{1}H NMR (500 MHz, $CDCl_3$) δ 7.83 (s, 1H), 7.82 (s, 1H), 7.65 (d, *J* = 8.5 Hz, 2H), 7.49 (d, *J* = 8.5 Hz, 2H), 4.62 (dd, *J* = 7.9, 2.7 Hz, 1H), 3.89 (d, *J* = 16.1 Hz, 1H), 3.82 (dd, *J* = 7.2, 5.3 Hz, 2H), 3.73 (d, *J* = 16.0 Hz, 1H), 2.63 (s, 3H), 2.54 (s, 3H), 2.53 – 2.46 (m, 1H), 2.15 – 2.06 (m, 3H). HRMS (EI) m/z, calcd for [$C_{26}H_{22}BrNO_6$]: 546.0523; found: 546.0511. $[\alpha]_D^{24}$ 40.2º (c = 0.39, $CHCl_3$).

6: Following the general protocol: L-alanine methyl ester hydrochloride (3.6 mg, 0.023 mmol), **1b** (10 mg, 0.026 mmol), HATU (10.9 mg, 0.029 mmol), and DIPEA (9.5 μL, 0.055 mmol) were reacted in dimethylformamide (140 uL) at rt for 3 h. 6.6 mg (54%) of the ester product was obtained after purification. The ester was further reacted with LiOH (90 μL, 0.09 mmol) in THF (90 μL) to afford 5.4 mg (86%) of **6** as a white solid. ^{1}H NMR (400 MHz, $cdcl_3$) δ 7.83 (app s, 2H), 7.55 (d, *J* = 8.6 Hz, 2H), 7.49 (d, *J* = 8.7 Hz, 2H), 6.94 (d, *J* = 6.9 Hz, 1H), 4.49 (p, *J* = 7.2 Hz, 1H), 3.68 (d, *J* = 2.9 Hz, 2H), 2.63 (s, 3H), 2.62 (s, 3H), 1.44 (d, *J* = 7.2 Hz, 3H). HRMS (EI) m/z, calcd for [$C_{24}H_{20}ClNO_6$]: 454.1052; found: 454.1053. $[\alpha]_D^{24}$ -17.7º (c = 0.54, $CHCl_3$).

7: Following the general protocol: D-alanine methyl ester hydrochloride (3.6 mg, 0.023 mmol), **1b** (10 mg, 0.026 mmol), HATU (10.9 mg, 0.029 mmol), and DIPEA (9.5 μL, 0.055 mmol) were reacted in dimethylformamide (140 uL) at rt for 3 h. 2.1 mg (17%) of the ester product was obtained after purification. The ester was further reacted with LiOH (90 μL, 0.09 mmol) in THF (90 μL) to afford 1.8 mg (90%) of **7** as a white solid. ^{1}H NMR (500 MHz, $CDCl_3$) δ 7.84 (app s, 2H), 7.55 (d, *J* = 8.3 Hz, 2H), 7.50 (d, *J* = 8.3 Hz, 2H), 6.93 (d, *J* = 6.8 Hz, 1H), 4.48 (p, *J* = 6.8 Hz, 1H), 3.69 (d, *J* = 4.8 Hz, 2H), 2.65 (s, 3H), 2.64 (s, 3H), 1.45 (d, *J* = 7.2 Hz, 3H). HRMS (EI) m/z, calcd for [$C_{24}H_{20}ClNO_6$]: 454.1052; found: 454.1044. $[\alpha]_D^{24}$ 20.4º (c = 0.18, $CHCl_3$).

8: Following the general protocol: L-alanine methyl ester hydrochloride (3.2 mg, 0.023 mmol), **1** (10 mg, 0.023 mmol), HATU (9.5 mg, 0.025 mmol), and DIPEA (8.3 μL, 0.048 mmol) were reacted in dimethylformamide (120 uL) at rt for 3 h. 4.0 mg (34%) of the ester product was obtained after purification. The ester was further reacted with LiOH (90 μL, 0.09 mmol) in THF (90 μL) to afford 2.8 mg (72%) of **8** as a white solid. ^{1}H NMR (500 MHz, $CDCl_3$) δ 7.84 (d, *J* = 3.0 Hz, 2H), 7.65 (dd, *J* = 8.5, 1.2 Hz, 2H), 7.49 (dd, *J* = 8.4, 1.2 Hz, 2H), 6.93 (d, *J* = 6.9 Hz, 1H), 4.56 – 4.42 (m, 1H), 3.69 (d, *J* = 4.7 Hz, 2H), 2.64 (s, 3H), 2.63 (d, *J* = 1.0 Hz, 3H), 1.45 (dd, *J* = 7.2, 1.1 Hz, 3H). HRMS (EI) m/z, calcd for [$C_{24}H_{20}BrNO_6$]: 520.0371; found: 520.0375. $[\alpha]_D^{24}$ -20.2º (c = 0.28, $CHCl_3$).

9: Following the general protocol: D-alanine methyl ester hydrochloride (3.2 mg, 0.023 mmol), **1** (10 mg, 0.023 mmol), HATU (9.5 mg, 0.025 mmol), and DIPEA (8.3 μL, 0.048 mmol) were reacted in dimethylformamide (120 uL) at rt for 3 h. 2.6 mg (22%) of the ester product was obtained after purification. The ester was further reacted with LiOH (90 μL, 0.09 mmol) in THF (90 μL) to afford 2.1 mg (84%) of **9** as a white solid. ^{1}H NMR (500 MHz, $CDCl_3$) δ 7.84 (d, *J* =

3.2 Hz, 2H), 7.65 (d, J = 8.4 Hz, 2H), 7.49 (d, J = 8.3 Hz, 2H), 6.93 (d, J = 6.8 Hz, 1H), 4.49 (p, J = 8.0, 7.5 Hz, 1H), 3.75 – 3.62 (m, 2H), 2.65 (s, 3H), 2.63 (s, 3H), 1.45 (d, J = 7.2 Hz, 3H). HRMS (EI) m/z, calcd for [$C_{24}H_{20}BrNO_6$]: 520.0366; found: 520.0344. $[\alpha]_D^{24}$ 18.1º (c = 0.21, $CHCl_3$).

2.10 References

1. (a) Wright, G. D. *ACS Infect Dis.* **2015,** *1*, 80-84; (b) Chambers, H. F.; Deleo, F. R. *Nat Rev Microbiol.* **2009,** *7*, 629-641.

2. (a) http://www.who.int/mediacentre/news/releases/2017/bacteria-antibiotics-needed/en/ (accessed March 6, 2017); (b) Okano, A.; Nakayama, A.; Schammel, A. W.; Boger, D. L. *J. Am. Chem. Soc.* **2014,** *136*, 13522-13525; (c) Bouley, R.; Kumarasiri, M.; Peng, Z.; Otero, L. H.; Song, W.; Suckow, M. A.; Schroeder, V. A.; Wolter, W. R.; Lastochkin, E.; Antunes, N. T.; Pi, H.; Vakulenko, S.; Hermoso, J. A.; Chang, M.; Mobashery, S. *J. Am. Chem. Soc.* **2015,** *137*, 1738-1741; (d) O'Daniel, P. I.; Peng, Z.; Pi, H.; Testero, S. A.; Ding, D.; Spink, E.; Leemans, E.; Boudreau, M. A.; Yamaguchi, T.; Schroeder, V. A.; Wolter, W. R.; Llarrull, L. I.; Song, W.; Lastochkin, E.; Kumarasiri, M.; Antunes, N. T.; Espahbodi, M.; Lichtenwalter, K.; Suckow, M. A.; Vakulenko, S.; Mobashery, S.; Chang, M. *J. Am. Chem. Soc.* **2014,** *136*, 3664-3672; (e) Lee, W.; Schaefer, K.; Qiao, Y.; Srisuknimit, V.; Steinmetz, H.; Müller, R.; Kahne, D.; Walker, S. *J. Am. Chem. Soc.* **2016,** *138*, 100-103.

3. (a) Weidenmaier, C.; Kokai-Kun, J. F.; Kristian, S. A.; Chanturiya, T.; Kalbacher, H.; Gross, M.; Nicholson, G.; Neumeister, B.; Mond, J. J.; Peschel, A. *Nat Med.* **2004,** *10*, 243-245; (b) Swoboda, J. G.; Meredith, T. C.; Campbell, J.; Brown, S.; Suzuki, T.; Bollenbach, T.; Malhowski, A. J.; Kishony, R.; Gilmore, M. S.; Walker, S. *ACS Chem Biol.* **2009,** *4*, 875-883; (c) Campbell, J.; Singh, A. K.; Santa Maria, J. P.; Kim, Y.; Brown, S.; Swoboda, J. G.; Mylonakis, E.; Wilkinson, B. J.; Walker, S. *ACS Chem Biol.* **2011,** *6*, 106-116.

4. Wilkens, S. *F1000Prime Rep.* **2015,** *7*, 14.

5. (a) D'Elia, M. A.; Pereira, M. P.; Chung, Y. S.; Zhao, W.; Chau, A.; Kenney, T. J.; Sulavik, M. C.; Black, T. A.; Brown, E. D. *J Bacteriol.* **2006,** *188*, 4183-4189; (b) D'Elia, M. A.; Millar, K. E.; Beveridge, T. J.; Brown, E. D. *J. Bacteriol.* **2006,** *188*, 8313-8316; (c) D'Elia, M. A.; Henderson, J. A.; Beveridge, T. J.; Heinrichs, D. E.; Brown, E. D. *J. Bacteriol.* **2009,** *191*, 4030-4034.

6. Qiao, Y.; Lebar, M. D.; Schirner, K.; Schaefer, K.; Tsukamoto, H.; Kahne, D.; Walker, S. *J Am Chem Soc.* **2014,** *136*, 14678-14681.

7. (a) Lee, K.; Campbell, J.; Swoboda, J. G.; Cuny, G. D.; Walker, S. *Bioorg Med Chem Lett.* **2010,** *20*, 1767-1770; (b) Wang, H.; Gill, C. J.; Lee, S. H.; Mann, P.; Zuck, P.; Meredith, T. C.; Murgolo, N.; She, X.; Kales, S.; Liang, L.; Liu, J.; Wu, J.; Santa Maria, J.; Su, J.; Pan, J.; Hailey, J.; Mcguinness, D.; Tan, C. M.; Flattery, A.; Walker, S.; Black, T.; Roemer, T. *Chem Biol.* **2013,** *20*, 272-284.

8. Cheng, T. J.; Wu, Y. T.; Yang, S. T.; Lo, K. H.; Chen, S. K.; Chen, Y. H.; Huang, W. I.; Yuan, C. H.; Guo, C. W.; Huang, L. Y.; Chen, K. T.; Shih, H. W.; Cheng, Y. S.; Cheng, W. C.; Wong, C. H. *Bioorg. Med. Chem.* **2010,** *18*, 8512-8529.

9. (a) Pasquina, L.; Santa Maria, J. P.; McKay Wood, B.; Moussa, S. H.; Matano, L. M.; Santiago, M.; Martin, S. E.; Lee, W.; Meredith, T. C.; Walker, S. *Nat Chem Biol.* **2016,** *12*, 40-45; (b) Schaefer, K.; Matano, L. M.; Qiao, Y.; Kahne, D.; Walker, S. *Nat Chem Biol.* **2017,** *13*, 396-401; (c) Matano, L. M.; Morris, H. G.; Wood, B. M.; Meredith, T. C.; Walker, S. *Bioorg. Med. Chem.* **2016,** *24*, 6307-6314.

10. Schirner, K.; Stone, L. K.; Walker, S. *ACS Chem Biol.* **2011,** *6*, 407-412.

11. (a) Aller, S. G.; Yu, J.; Ward, A.; Weng, Y.; Chittaboina, S.; Zhuo, R.; Harrell, P. M.; Trinh, Y. T.; Zhang, Q.; Urbatsch, I. L.; Chang, G. *Science.* **2009,** *323*, 1718-1722; (b) Jin, M. S.; Oldham,

M. L.; Zhang, Q.; Chen, J. *Nature.* **2012,** *490*, 566-569; (c) Loo, T. W.; Clarke, D. M. *Biochem. Pharmacol.* **2014,** *92*, 558-566; (d) Loo, T. W.; Clarke, D. M. *J. Biol. Chem.* **2015,** *290*, 29389-29401; (e) Sherman, D. J.; Okuda, S.; Denny, W. A.; Kahne, D. *Bioorg. Med. Chem.* **2013,** *21*, 4846-4851.

12. Szakacs, G.; Paterson, J. K.; Ludwig, J. A.; Booth-Genthe, C.; Gottesman, M. M. *Nat Rev Drug Discov.* **2006,** *5*, 219-234.

13. Crowley, E.; McDevitt, C. A.; Callaghan, R. *Methods Mol Biol.* **2010,** *596*, 405-432.

14. Falasca, M.; Linton, K. J. *Expert Opin Investig Drugs.* **2012,** *21*, 657-666.

15. Moody, J. E.; Millen, L.; Binns, D.; Hunt, J. F.; Thomas, P. J. *J. Biol. Chem.* **2002,** *277*, 21111-21114.

16. (a) Borths, E. L.; Poolman, B.; Hvorup, R. N.; Locher, K. P.; Rees, D. C. *Biochemistry.* **2005,** *44*, 16301-16309; (b) Perez, C.; Gerber, S.; Boilevin, J.; Bucher, M.; Darbre, T.; Aebi, M.; Reymond, J. L.; Locher, K. P. *Nature.* **2015,** *524*, 433-438.

17. (a) Kelley, L. A.; Mezulis, S.; Yates, C. M.; Wass, M. N.; Sternberg, M. J. *Nat Protoc.* **2015,** *10*, 845-858; (b) Lee, J. Y.; Kinch, L. N.; Borek, D. M.; Wang, J.; Urbatsch, I. L.; Xie, X. S.; Grishin, N. V.; Cohen, J. C.; Otwinowski, Z.; Hobbs, H. H.; Rosenbaum, D. M. *Nature.* **2016,** *533*, 561-564.

18. (a) Dawson, R. J.; Locher, K. P. *Nature.* **2006,** *443*, 180-185; (b) Ward, A.; Reyes, C. L.; Yu, J.; Roth, C. B.; Chang, G. *Proc Natl Acad Sci U S A.* **2007,** *104*, 19005-19010.

19. Imramovsky, A.; Jorda, R.; Pauk, K.; Reznickova, E.; Dusek, J.; Hanusek, J.; Krystof, V. *Eur. J. Med. Chem.* **2013,** *68*, 253-259.

20. Anantharaj, S.; Jayakannan, M. *Biomacromolecules.* **2012,** *13*, 2446-2455.

Chapter 3: Exploiting synthetic lethality in pathway-directed screening: identification of a new D-alanylation inhibitor scaffold

A version of this chapter has been published.[1]

Authors:

Leigh M. Matano[1], Heidi G. Morris[1], B. McKay Wood[1], Timothy C. Meredith[2,*], Suzanne Walker[2,*]

Affiliations

[1]Department of Microbiology and Immunobiology, 4 Blackfan Circle, Boston, MA, 02115, USA

[2]Department of Biochemistry and Molecular Biology, 206 South Frear Laboratory, University Park, PA, 16802, USA

Contributions:

LMM conducted the screen, analyzed the data, submitted the cherry-pick, followed up on characterizing the inhibitors, performed *in vitro* biochemistry assay, wrote first draft

HGM conducted the screen and categorized the cherry-picks

BMW designed and provided materials for the *in vitro* D-alanylation assay

*TCM and SW are corresponding authors

Chapter 3: Exploiting synthetic lethality in pathway-directed screening: identification of a new D-alanylation inhibitor scaffold

3.1 Targeting the D-alanylatin pathway in *S. aureus*

As mentioned in Chapter 1, the D-alanylation pathway in *S. aureus* consists of four enzymes, DltA-D, that are required for the attachment of positively charged D-alanine esters to LTAs and WTA polymers (Figure 3.1).[2] The addition of D-alanines begins with DltA, which resembles adenylation domains of nonribosomal peptide synthetases.[3] DltA charges D-alanine as an AMP ester and then transfers the moiety to DltC, which is modified by a phosphopantetheine cofactor and shares homology to acyl carrier proteins.[4] DltC then transfers the D-alanine ester to DltB, an uncharacterized polytopic membrane protein predicted to have ten membrane-spanning helices with homology to M-BOAT acyl transferases. It's role in the process of D-alanylation is unknown, but it is predicted to either transfer D-alanine to a lipid intermediate or to DltD for attachment to LTA polymers.[2a,5]

D-alanylated LTAs have many physiological functions, of which the D-alanine ester modification is of great importance.[2a] The pathway was originally discovered in a transposon mutagenesis screen for factors sensitizing *S. aureus* to positively charged antimicrobial peptides, but had been studied for years in other Gram positive bacteria.[2b,2c,6] Removing D-alanines sensitizes *S. aureus* to positively charged antimicrobials, antibiotics, impairs biofilm formation, and attenuates *S. aureus* virulence *in vivo*.[7] For these attributes, the Dlt pathway has been recognized as a promising candidate for therapeutic inhibition.[2a,4a]

To find inhibitors of the Dlt pathway, previous graduate students Lincoln Pasquina and John Santa Maria performed a pilot screen for small molecules lethal to a WTA biosynthesis null strain and discovered amsacrine as a DltB inhibitor.[8] The Dlt pathway was previously known to

be in the synthetic lethal network of WTA biosynthesis. Thus, the discovery of amsacrine provided proof-of-concept for our strategy to identify biologically active inhibitors of non-essential targets by exploiting synthetic lethality. However, while amsacrine has already proven useful as a probe to map synthetic interactions with the Dlt pathway, it cannot be used to validate the Dlt pathway as a pharmacological target in animals because it acts as a eukaryotic topoisomerase poison.[9] Poor pharmacological properties and/or unacceptable safety profiles are commonly encountered barriers to development. For this reason, it is desirable, if not imperative, to have multiple scaffolds against a particular target in order to move forward if animal studies are a goal. The ability to identify new scaffolds rapidly is crucial. Because the pilot screen of 28,000 compounds had been successful and the screening approach offered the possibility of identifying inhibitors to several different targets, we screened an additional 230,000 compounds in duplicate at a final concentration of ~15 micromolar and identified 200 synthetic lethal 'hits' (Figure 3.2). The next challenge was to sort the compounds into different groups, among which were possible Dlt pathway inhibitors.

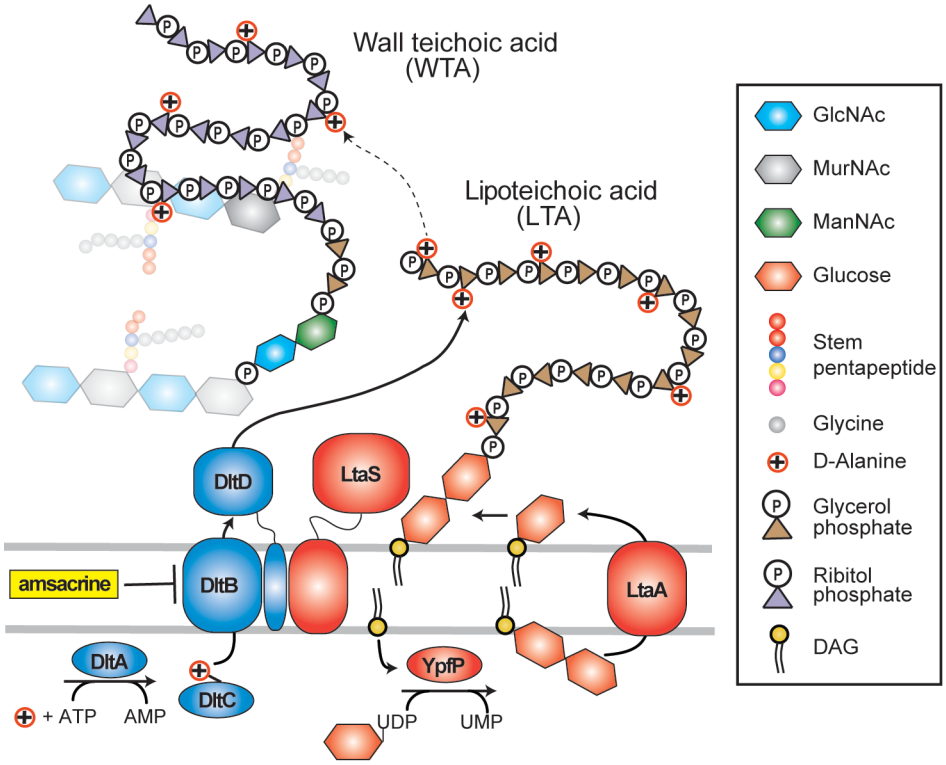

Figure 3.1 Schematic of Dlt pathway and attachment to LTA and WTA polymers in *Staphylococcus aureus*. DltA charges D-alanines as AMP esters and then transfers them to DltC. From there, DltB and DltD are involved in the transfer to LTAs, which are membrane-bound teichoic acids consisting of glycerol-phosphate repeating units. D-alanines are then transferred from LTAs to WTAs by an unknown mechanism. Amsacrine was previously discovered from a pilot screen as a DltB inhibitor.[8a]

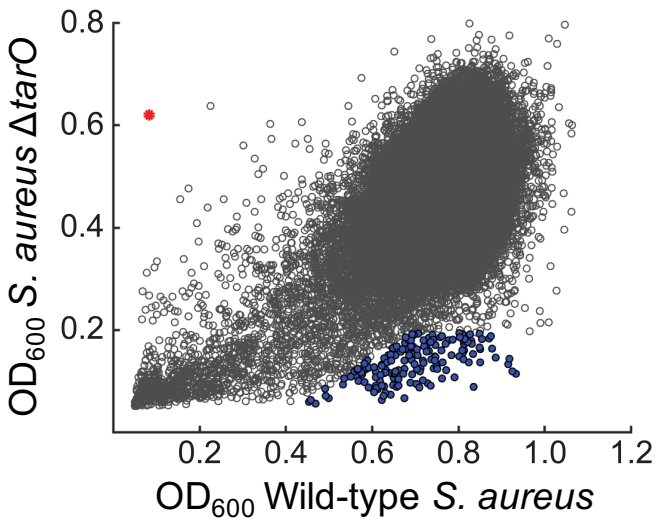

Figure 3.2 A HTS of 230,000 compounds led to the identification of 200 hit compounds synthetically lethal with WTA biosynthesis. Each circle represents the average OD_{600} of the strains in the presence of a library compound tested in duplicate. 200 compounds (dark blue circles) prevented the growth of the Δ*tarO* strain but not WT, and are candidate inhibitors for pathways lethal with inhibition of WTA biosynthesis, such as the Dlt pathway. One compound (red circle) was identified as a late-stage WTA inhibitor (see Chapter 2).

3.2 Using the Dlt synthetic lethal network to screen for pathway inhibitors

To find phenotypes unique to Dlt pathway inhibition, we took a chemical genetics approach. Pathways in the *S. aureus* cell wall are highly connected, and determining these networks provides valuable insight about their importance. Transposon libraries adapted for high-throughput sequencing is a powerful methodology for discovering important relationships between pathways in bacteria.[10] Transposons are mobile genetic elements that insert into chromosomes with the help of a transposase. When a transposon inserts into and disrupts a gene, it is assumed to be inactivating, acting as a proxy for a genetic knockout. For next-generation high-throughput

sequencing, transposons have been adapted to include barcodes for insertion site sequencing. This process has been streamlined in *S. aureus* to make high-density libraries of transposon mutants all pooled together in one sample.[11] The sample can then be exposed to an experimental condition, such as treatment with an inhibitor, and sequenced for transposon insertion sites (Figure 3.3). Genes that have little or no transposon insertions compared to the untreated control are considered essential under that condition.

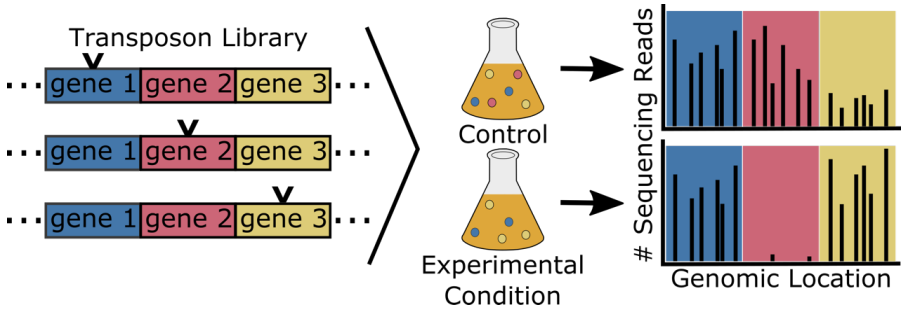

Figure 3.3 Schematic of next-generation transposon library construction, treatment, and sequencing (tn-seq). High-saturation transposon libraries are constructed with mutants containing transposons inserted chromosomally in different genes of *S. aureus*. The pooled library is then exposed to a selective pressure. Genomic DNA is isolated from treated and untreated samples and sent for high-throughput sequencing. Reads of transposon insertion sites are mapped and statistical analyses performed to find genes with reads that are depleted (e.g. red gene). These genes are essential in context of the experimental condition.

Previously, high-saturation transposon libraries were exposed to tunicamycin treatment, revealing a list of pathways that were synthetically lethal with WTA biosynthesis inhibition.[12] These are pathways that are nonessential when inhibited individually, but are essential in the absence of WTA. As discussed earlier, the knowledge of the synthetic lethal network led to the

discovery and identification of amsacrine as a Dlt pathway inhibitor.[8a] What we needed was the knowledge of what pathways were essential in the absence of the Dlt pathway so we could use those phenotypes to classify new inhibitors. To identify the network of synthetic lethal interactions with Dlt pathway inhibition, we treated our pooled high-density transposon library with amsacrine and validated a subset of hits (Figure 3.4). The results included an interesting set of genes: genes in the WTA pathway, two genes of unknown function *SAOUHSC_01025* and *SAOUHSC_01050*, and two out of three genes in the LTA pathway. We found it interesting that only the first two steps of the LTA pathway, YpfP and LtaA, were lethal with D-alanylation inhibition but not the last enzyme LtaS that polymerized the polymer (see Chapter 4 for more details). To rapidly classify of our 200 hit compounds, we planned on using these phenotypes as unique identifiers for Dlt pathway inhibitors.

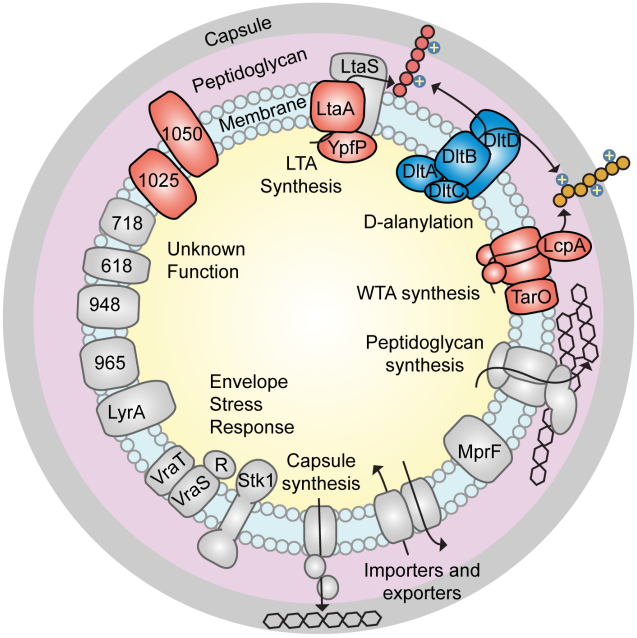

Figure 3.4: Summary of synthetic lethal network of the Dlt pathway. Proteins, shown in red, are synthetically lethal with the Dlt pathway, shown in blue. Proteins that are not synthetically lethal with Dlt pathway inhibition are shown in grey. Of note are the protein of unknown function

Figure 3.4 (Continued)

SAOUHSC_01050 and the diglucosyldiacylglycerol synthase YpfP, responsible for synthesis of the lipid anchor for LTAs, for the sensitivity of their knockouts to amsacrine. Knockout out LtaS, the lipoteichoic acid polymerase and the final step of the LTA pathway, is not sensitive to amsacrine treatment. This unique phenotype was exploited to design the secondary screen to identify new Dlt pathway inhibitors. See Chapter 4 for more details regarding the biology behind the LTA and Dlt pathways.

3.3 Rapid identification of three new Dlt pathway inhibitors

Based on the results obtained through analyzing tn-seq data treated with amsacrine, we organized our cherry pick stage of hit validation to identify putative Dlt pathway inhibitors. Screening at Harvard Medical School is typically carried out at a single concentration, with cherry pick validation performed using only the screening strain(s) in a dose-response format. By testing three additional strains, tn::1050, Δ*ypfP*, and Δ*ltaS*, along with the wildtype and Δ*tarO* strains, we expected to be able to recognize Dlt pathway inhibitors based on the fact that they would not affect growth of the wildtype of Δl*taS* strains, but would inhibit growth of the other three strains (Figure 3.5A).[12-13] We screened the 200 'hits' identified in the primary screen against our five test strains and three compounds representing two different scaffolds emerged as possible Dlt pathway inhibitors (Figure 3.5B). Two compounds, one from each scaffold, were purchased for follow-up. We tested DBI-1 and DltI-1 in a cell-based assay for inhibition of D-alanylation and found that both blocked incorporation of radiolabeled D-ala into lipoteichoic acid (Figure 3.5C). The concentration at which inhibition is observed is similar to the concentration that inhibits growth of susceptible strains. DBI-1 was more potent against Δ*tarO* and other susceptible strains whereas

DltI-1 had the same MIC as amsacrine (1 µg/mL versus 5 µg/mL). Furthermore, DltI-1 proved toxic to wildtype *S. aureus* at higher concentrations, suggesting a secondary, lethal target. Therefore, we focused on the other scaffold, DBI-1, which displayed the same susceptibility profile as amsacrine (Figure 3.6).

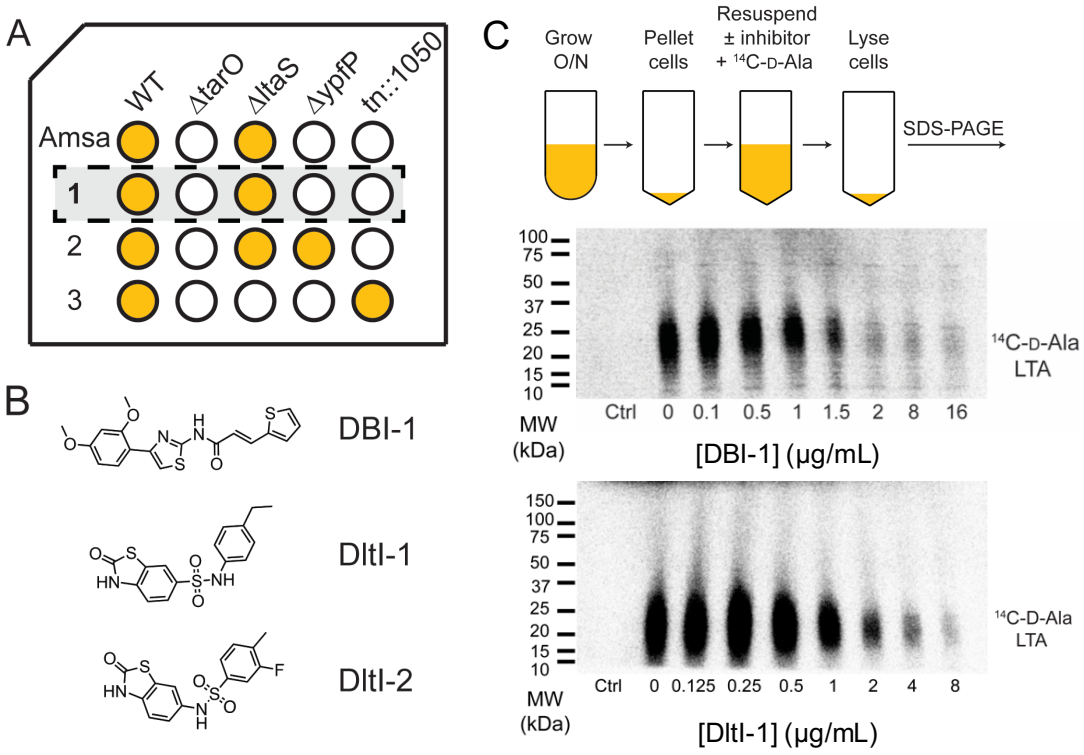

Figure 3.5 New Dlt pathway inhibitors were rapidly identified by testing synthetic lethal hits from a high throughput screen against a strain panel diagnostic for Dlt pathway inhibition. (A) Schematic of a plate showing possible outcomes of treatment of five different strains against test compounds. Amsacrine, a validated DltB inhibitor, was used as a positive control. It inhibits growth of the Δ*tarO*, Δ*ypfP* and tn::1050 strains, but not of the wildtype or Δ*ltaS* strains. (B) Three possible Dlt pathway inhibitors from two different scaffolds were identified from the 200 synthetic lethal hits that were cherry-picked from the 230,000-compound screen and tested against these five strains. (D) PAGE autoradiograph showing ^{14}C-D-Ala LTA after treatment of cells with increasing concentrations of DBI-1 or DltI-1.

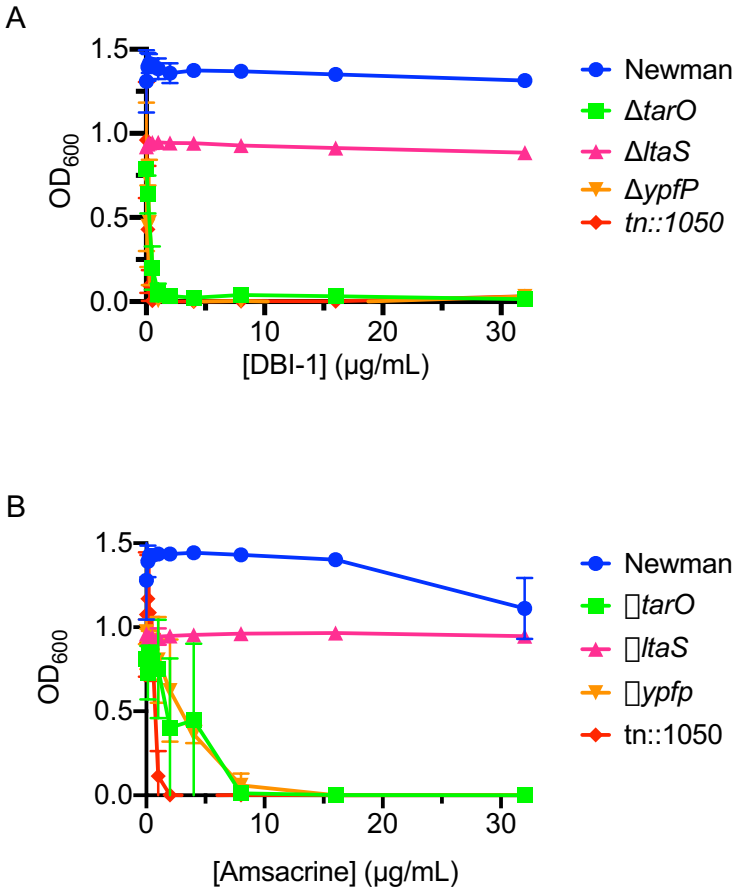

Figure 3.6. DBI-1 has the same growth profile as amsacrine. Growth inhibition of five *S. aureus* strains in the presence of increasing concentrations of DBI-1 (top panel—A) and amsacrine (bottom panel—B). Wildtype Newman and four mutant strains lacking functional copies of *tarO*, *ltaS*, *ypfP*, or *SAOUHSC_01050* (tn::1050) were grown in 96 well plates in TSB containing the indicated concentrations of either DBI-1 or the previously validated DltB inhibitor amsacrine. Preventing D-alanylation is lethal to Δ*tarO*, Δ*ypfP*, and tn::1050 but not Δ*ltaS* or wildtype *S. aureus*. The data is from three biological replicates. Error bars are typically large near the MIC of a compound because MIC measurements are only accurate to within two-fold of the inhibitory concentration.

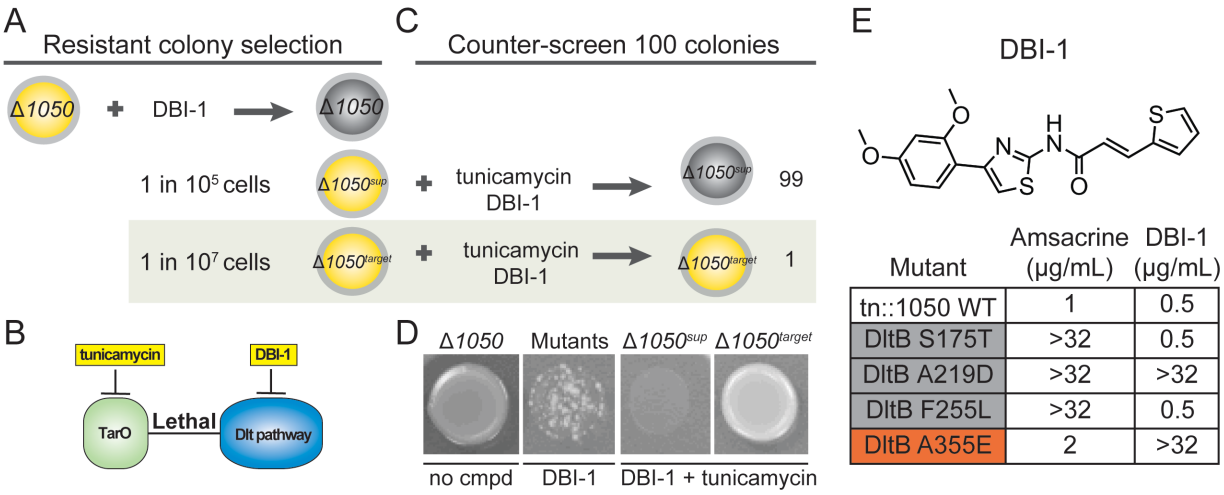

Mutant	Amsacrine (μg/mL)	DBI-1 (μg/mL)
tn::1050 WT	1	0.5
DltB S175T	>32	0.5
DltB A219D	>32	>32
DltB F255L	>32	0.5
DltB A355E	2	>32

Figure 3.7 Colonies resistant to tunicamycin and DBI-1 have mutations in DltB. (A) Using the tn::1050 background, resistant colonies are raised to DBI-1. These colonies either have suppressor mutations (~1 in 10^5 cells) or target mutations (~1 in 10^7 cells). (B) To screen for resistant colonies, we used the synthetic lethality of tunicamycin and DBI-1. Tunicamycin, which inhibits TarO and thereby WTA biosynthesis, in combination with DBI-1 treatment is lethal to *S. aureus*. (C) Colonies are counter screened by checking for growth in tunicamycin and DBI-1. Only those containing resistant mutations in the target should survive, and the frequency should be around 1 in every 100 colonies. (D) The illustration of this concept with examples from resistant colonies raised to DBI-1. Tn::1050 mutants with suppressors that compensate for the lack of *SAOUHSC_1050* do not survive DBI-1 and tunicamycin treatment, but colonies with mutants in the target do. (E) Structure of DBI-1 and minimum inhibitory concentrations against a panel of mutants selected by plating amsacrine (gray boxes) or DBI-1 (red boxes). Resistant colonies have mutations in DltB.

3.4 Identification of the target of DBI-1

To identify the target of DBI-1, we raised spontaneous mutants in the susceptible tn::1050 background (Figure 3.7A). The frequency of resistance to DBI-1 in this background is ~1 in 10^5, which is very high. We expected two different types of mutations to occur: suppressor mutations that compensate for the lack of *SAOUHSC_01050* and mutations in the target of DltB. To identify colonies with target mutations, we made use of the synthetic lethal relationship between the WTA and Dlt pathways (Figure 3.7B). Treatment with tunicamycin, a WTA inhibitor, and DBI-1, a suspected Dlt pathway inhibitor, is lethal to *S. aureus*. Treating a mutant raised in the tn::1050 background with these two compounds will continue to be lethal unless the colony has a mutation in the target of DBI-1, which occurs at a frequency of 1 out of a hundred resistant colonies (Figure 3.7C). This method was previously worked out by graduate student Lincoln Pasquina and used to identify the target of amsacrine as DltB.[8a] Two of four colonies selected in independent experiments and identified as possible target mutants displayed a stable resistance phenotype (Figure 3.7D); both were found to contain the same mutation in *dltB*, a C→A transversion that resulted in substitution of glutamate for alanine at amino acid 355 (Figure 3.7E). We also tested the compound against amsacrine-resistant mutants containing other amino acid substitutions at three different sites in DltB. One of these mutants (A219D) was cross-resistant to DBI-1.

Using pathway-directed screening followed by a phenotype-based counter-screen, we rapidly classified three small molecules as Dlt pathway inhibitors. We identified DBI-1 as a DltB inhibitor based on the following lines of evidence: 1) it has the expected growth inhibition profile against the diagnostic panel of strains; 2) we identified two mutants from independent cultures that contained putative target mutations and both were found to have the same mutation in *dltB*; 3) the compound was cross-resistant to an allele of *dltB* that was previously found in a selection with the

validated DltB inhibitor, amsacrine; and 4) the compound was shown to inhibit D-alanylation of lipoteichoic acids in a cell-based biochemical assay. Target identification is difficult and time consuming, but using this method we prioritized our hits and quickly identified the target of DBI-1. This is a promising strategy to rapidly identify inhibitors of other nonessential pathways.

3.5 The DBI-1 scaffold and activity of select analogs

The DBI-1 inhibitor scaffold contains a cinnamide substituent, placing it in a large family of compounds containing cinnamic acid derivatives. Cinnamic acid derivatives are produced by many different plants, and various natural products as well as synthetic analogs containing this feature have anticancer,[15] antifungal,[16] antimalarial,[17] and antimicrobial activities.[18] DBI-1, however, had no effect on viability of Vero cells (Table 3.2) and did not have antimicrobial activity against wildtype *S. aureus*. Furthermore, limited SAR studies we have carried out show that the cinnamide moiety is not essential for activity against the tn::1050 strain, which is susceptible to D-alanylation inhibitors and also suggests that DBI-1 is not a covalent inhibitor (Table 3.1, see appendix 4 for full panel of compounds tested). In contrast, the methoxy-substituted benzene ring and the thiazole are critical for activity. This knowledge will be used for the rational design of analogs with increased potency or for photocrosslinking experiments for further studies on the binding site of DBI-1.

Table 3.1 Activity of DBI analogs against *S. aureus* USA300 tn::1050. Data is from two biological replicates. Removal of methoxy groups (DBI-5) or replacement of the thiazole with a triazole (DBI-6) results in loss of activity against the tn::1050 strain, showing that both groups are important for activity. However, activity is retained even with the loss of the cinnamide substituent (DBI-3). See Appendix 4 for all analogs tested.

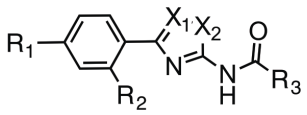

Analog	R_1	R_2	R_3	X_1	X_2	MIC
DBI-1	-OMe	-OMe	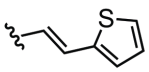	-CH	-S	0.5
DBI-2	-OMe	-OMe	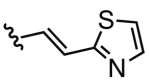	-CH	-S	0.5
DBI-3	-OMe	-OMe	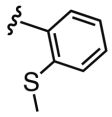	-CH	-S	2
DBI-4	-OMe	-H	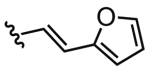	-CH	-S	4
DBI-5	-H	-H	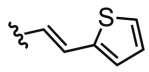	-CH	-S	>32
DBI-6	-OMe	-H	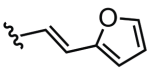	-NH	-N	>32

Table 3.2 Table of luminescent data and calculated percent viability for four replicates at varying concentrations of DBI-1. Toxicity testing was done with Vero cells prepared in DMEM with 10% FBS. 200 µL of 0.5 x 10^5/mL were plated in a 96-well clear bottom plates (NUNC #165305). Plates were gently shaken and incubated at room temperature for one hour and then set overnight at 37°C, 5% CO_2. Compound was thawed and diluted into D-10 media with 1% DMSO (D-10-1). After 24 hours, media was removed from cells and replaced with 200 µL of diluted compound at various concentrations. Samples treated with DMSO were used as controls. Plates were incubated overnight at 37°C, 5% CO_2. Cell viability was assessed after 24 hours using Promega CellTiter-Glo® Luminescent Cell Viability Assay (#G7571). Percent viability was calculated using (Mean Value – Mean Blank) / (Mean Control - Mean Blank) * 100%. Assay was done by Christine Anderson with the CETR core.

DBI-1 Concentration	10 µM	5 µM	2.5 µM	1.3 µM	0 µM
Replicate 1	175614	175702	175736	174664	145837
Replicate 2	175588	175817	175819	175741	169845
Replicate 3	174898	175636	175797	175876	173255
Replicate 4	174511	174924	175367	173522	173465
Mean	175153	175520	175680	174951	165600
% Viability	106	106	106	106	

3.6 Conclusions

In this chapter, we discuss the rapid discovery of new Dlt pathway inhibitors using pathway-directed whole-cell screening. From 230,000 compounds, we identified 200 hits that were lethal to *S. aureus* Newman Δ*tarO* but not wild-type. The challenge then became how to find inhibitors of the Dlt pathway from these 200 hits. Using a phenotypic secondary screen based on the synthetic lethal network of the Dlt pathway, we identified three candidate Dlt pathway inhibitors. We characterized and identified the target of DBI-1 as DltB. We now have two small

molecules that inhibit DltB, which we proved to be highly-druggable. DBI-1 is more potent than amsacrine and is not toxic to eukaryotic cells. Having more than one scaffold that inhibit the same target is extremely useful; the differences in properties ensures the phenotypes observed are not due to off target effects. Since DBI-1 is not lethal to wild-type *S. aureus*, it can also be used as a second way to validate the synthetic lethal network of the Dlt pathway. In Chapter 4 we demonstrate this use in the treatment of a high-density *S. aureus* transposon library with all the Dlt pathway inhibitors we have discovered to date, proving they have the same tn-seq profile. Furthermore, DBI-1 is also a promising candidate for *in vivo* evaluation of Dlt pathway inhibition. The second scaffold discovered, DltI-1, was not initially pursued due to a possible second target, but this does not necessarily exclude promise of activity *in vivo* if DltI-1 is not toxic to eukaryotic cells. Further work is underway to determine the mechanism of action of DBI-1 and the target of DltI-1. It is not yet clear whether these classes of compounds can be developed for administration in animals, but our ability to correctly identify a new Dlt pathway inhibitor during the cherry-pick stage of hit validation demonstrates how efficient pathway-directed whole cell screening can be for discovering new scaffolds rapidly.

3.7 Methods

Reagents and general methods

S. aureus was grown in tryptic soy broth (TSB) or on TSB with 1.5% agar at 30°C. High-throughput screening was done at the ICCB-Longwood Screening Facility. DBI-1 was purchased from Life Chemicals (F0715-0438). Amsacrine was purchased from Abcam (ab142742).

High-throughput screening

Overnight cultures of *S. aureus* Newman WT and Δ*tarO* were grown in tryptic soy broth (TSB) at 30°C. Before dispensing into 384 well plates, cultures were diluted to an OD600 of one. 30 μL of TSB was predispensed into 384 well plates (Corning 3702) using a Matrix Wellmate plate filler. 100 nL of compound was then pin transferred into lanes 1-22 of the prefilled 384 well plates (final concentration ~15 μM). 50 μL of diluted overnight cultures (diluted 1:625) were added to the wells for a final volume of 80 μL and a final dilution of 1:1000. 10 μg/mL erythromycin final concentration was added to lane 24 as a positive control. Screening was done in duplicate for each strain. Plates were incubated at 30ºC for 16-18 hrs and OD_{600} was measured on a PerkinElmer Envision plate reader.

Principle component analysis

PCA was done as previously described.[8a] An X-Y scatter plot of compound data with optical density of each of the strains on each axis. The line of best fit was yielded through the positive and negative controls as the first component and the distance of each point from that line was the second component. The Z score was calculated for each compound by dividing the distance over the standard deviation.

Cherry-pick strains and procedures

Overnight cultures of *S. aureus* Newman WT, Newman Δ*tarO*, SEJ1 Δ*ltaS*, RN4220 Δ*ypfP* and USA300 JE2 tn::1050 were grown in TSB at 30ºC. Before dispensing into 384 well plates, cultures were diluted to an OD_{600} of 1 and then further diluted 1:1000. Compounds provided by the ICCB-L for the cherry pick were administered to 384 well plates dry at screening concentration (100 nL of 5 mg/mL stock) using the Hewlett Packard D300 Digital Dispenser. Amsacrine was used as a positive control. Then 80 μL of diluted cultures were added to the wells using a Matrix Wellmate

plate filler. Compounds were tested in duplicate for each strain. Plates were incubated at 30ºC for 16-18 hours and OD_{600} was measured on a PerkinElmer Envision plate reader.

Minimum inhibitory concentration determination

Overnight cultures of wildype and mutant strains were diluted 1:100 and grown until OD_{600} ~1. Strains were normalized to OD_{600} of 1, diluted 1:1000 and 147 µL was dispensed into a 96 well plate. All compound dilution series were made in DMSO. 3 µL aliquots were made and transferred into 147 µL for final concentration 0-32 µg/mL in 150 µL. Plates were incubated overnight at 30ºC for 16-18 hours and OD_{600} was read on a 384SpectramaxPlus plate reader.

Raising resistant mutants

Raising and screening resistant mutants to DBI-1 was performed as previously described.[8a]

^{14}C-D-Ala-LTA detection assay

^{14}C-D-Ala incorporation into LTA was performed as described previously.[8a] Briefly, an overnight of *S. aureus* Newman was diluted 1:100 and grown at 30ºC in TSB until an OD_{600} of 0.6. Eight 1 mL aliquots were spun down and resuspended in buffer (0.25X TSB, pH 6.0, 200 µg/mL D-cycloserine) plus eight DBI-1 concentrations (0,0.1,0.5,1,1.5,2,8,16 µg/mL DBI-1) for 30 minutes at 30ºC shaking at 300 rpm. Samples were then spun down, resuspended in the same buffer containing appropriate DBI-1 concentration plus the addition of ^{14}C-D-Ala and were incubated for another 30 minutes at 30ºC shaking at 300 rpm. Samples were then spun down, resuspended in SDS loading buffer, boiled for 5 minutes at 95ºC, spun down again and 20 µL of supernatant were added to a 4-20% Tris-glycine gel (Bio-Rad). ^{14}C-D-Ala was added to the first lane as a control. The gel was dried and exposed to a phosphor storage screen for 72 hours before imaging.

^{14}C-D-Ala-DltC detection assay

DltA and DltC have been expressed by other groups previously and were purified by Dr. McKay Wood for this experiment.[3,4b] Reaction mixture was set up in a volume of 18.5 µL in dionized H_2O and final concentrations of the following:100 µM DltC, 200 nM ATP, 5 mM TCEP, 5 nCi/µL ^{14}C-D-Ala, 10 µM $MgCl_2$, 30 mM bisTris pH 6.55, and 50 mM NaCl. Inhibitor in DMSO was added to each sample in a volume of 1 µL for final concentrations of either no compound (+/- DMSO controls), 1 µg/mL DBI-1, and 10 µg/mL DBI-1. After adding inhibitor, 0.5 µL of DltA was added to each sample for a final concentration of 5 µM. Final volume for each reaction was 20 µL. Samples were incubated at 30ºC for 3 minutes before placed on ice and SDS loading buffer was added. Entire aliquot was run on a 4-20% Tris-glycine gel (Bio-Rad). The gel was dried and exposed to a phosphor storage screen for 24 hours before imaging.

NMR of DBI-1

^{1}H NMR was taken on a Varian 400 MHz instrument and recorded at ambient temperature. DBI-1 sample was prepared in deuterated-DMSO at a concentration of 10 mg/mL. NMR was calibrated to deutero-solvent as a standard. See appendix 5 for NMR.

3.8 References

1. Matano, L. M.; Morris, H. G.; Wood, B. M.; Meredith, T. C.; Walker, S. *Bioorg. Med. Chem.* **2016,** *24*, 6307-6314.

2. (a) Neuhaus, F. C.; Baddiley, J. *Microbiol. Mol. Biol. Rev.* **2003,** *67*, 686-723; (b) Peschel, A.; Otto, M.; Jack, R. W.; Kalbacher, H.; Jung, G.; Gotz, F. *J. Biol. Chem.* **1999,** *274*, 8405-8410; (c) Perego, M.; Glaser, P.; Minutello, A.; Strauch, M. A.; Leopold, K.; Fischer, W. *J Biol Chem.* **1995,** *270*, 15598-15606.

3. Du, L.; He, Y.; Luo, Y. *Biochemistry.* **2008,** *47*, 11473-11480.

4. (a) May, J. J.; Finking, R.; Wiegeshoff, F.; Weber, T. T.; Bandur, N.; Koert, U.; Marahiel, M. A. *The FEBS journal.* **2005,** *272*, 2993-3003; (b) Zimmermann, S.; Pfennig, S.; Neumann, P.; Yonus, H.; Weininger, U.; Kovermann, M.; Balbach, J.; Stubbs, M. T. *FEBS Lett.* **2015,** *589*, 2283-2289; (c) Debabov, D. V.; Heaton, M. P.; Zhang, Q.; Stewart, K. D.; Lambalot, R. H.; Neuhaus, F. C. *J. Bacteriol.* **1996,** *178*, 3869-3876.

5. Reichmann, N. T.; Cassona, C. P.; Grundling, A. *Micriobiol.* **2013**.

6. Heaton, M. P.; Neuhaus, F. C. *J. Bacteriol.* **1992,** *174*, 4707-4717.

7. (a) Collins, L. V.; Kristian, S. A.; Weidenmaier, C.; Faigle, M.; Van Kessel, K. P.; Van Strijp, J. A.; Götz, F.; Neumeister, B.; Peschel, A. *J. Infect. Dis.* **2002,** *186*, 214-219; (b) Kristian, S. A.; Lauth, X.; Nizet, V.; Goetz, F.; Neumeister, B.; Peschel, A.; Landmann, R. *J Infect Dis.* **2003,** *188*, 414-423; (c) Weidenmaier, C.; Kokai-Kun, J. F.; Kristian, S. A.; Chanturiya, T.; Kalbacher, H.; Gross, M.; Nicholson, G.; Neumeister, B.; Mond, J. J.; Peschel, A. *Nat Med.* **2004,** *10*, 243-245; (d) Weidenmaier, C.; Peschel, A.; Xiong, Y.-Q. Q.; Kristian, S. A.; Dietz, K.; Yeaman, M. R.; Bayer, A. S. *The Journal of infectious diseases.* **2005,** *191*, 1771-1777; (e) Peschel, A.; Vuong, C.; Otto, M.; Gotz, F. *Antimicrob. Agents Chemother.* **2000,** *44*, 2845-2847.

8. (a) Pasquina, L.; Santa Maria, J. P., Jr.; McKay Wood, B.; Moussa, S. H.; Matano, L. M.; Santiago, M.; Martin, S. E.; Lee, W.; Meredith, T. C.; Walker, S. *Nat Chem Biol.* **2016,** *12*, 40-45; (b) Santa Maria, J. P., Jr.; Sadaka, A.; Moussa, S. H.; Brown, S.; Zhang, Y. J.; Rubin, E. J.; Gilmore, M. S.; Walker, S. *Proc Natl Acad Sci U S A.* **2014,** *111*, 12510-12515.

9. Cain, B. F.; Atwell, G. J. *European Journal of Cancer.* **1974**.

10. van Opijnen, T.; Camilli, A. *Nat Rev Microbiol.* **2013,** *11*, 435-442.

11. Santiago, M.; Matano, L. M.; Moussa, S. H.; Gilmore, M. S.; Walker, S.; Meredith, T. C. *BMC Genomics.* **2015,** *16*, 252.

12. Santa Maria, J. P.; Sadaka, A.; Moussa, S. H.; Brown, S.; Zhang, Y. J.; Rubin, E. J.; Gilmore, M. S.; Walker, S. *Proc. Natl. Acad. Sci. U. S. A.* **2014,** *111*, 12510-12515.

13. (a) Corrigan, R. M.; Abbott, J. C.; Burhenne, H.; Kaever, V.; Grundling, A. *PLoS Pathogens.* **2011,** *7*, e1002217; (b) Pasquina, L.; Jr, J. P.; Wood, M. B.; Moussa, S. H.; Matano, L. M.; Santiago, M.; Martin, S. E. S.; Lee, W.; Meredith, T. C.; Walker, S. *Nat. Chem. Biol.* **2015**.

14. Kelley, L. A.; Mezulis, S.; Yates, C. M.; Wass, M. N.; Sternberg, M. J. *Nat Protoc.* **2015,** *10*, 845-858.

15. De, P. B., M.; Bedos-Beval, F. *Curr. Med. Chem.* **2011,** *18*, 1672-1703.

16. Tawata, S.; Taira, S.; Kobamoto, N.; Zhu, J. *Bioscience.* **1996**.

17. Wiesner, J.; Mitsch, A.; Wißner, P.; Jomaa, H.; Schlitzer, M. *Bioorg. Med. Chem. Lett.* **2001,** *11*, 423-424.

18. Guzman, J. D. *Molecules.* **2014,** *19*, 19292-19349.

Chapter 4: D-alanyation inhibitors are useful probes for studying *S. aureus* physiology

The previous chapter identified three small molecules as inhibitors of the D-alanylation pathway in *S. aureus*. In this chapter, we discuss: 1) the treatment of a transposon library with three different D-alanylation inhibitors; 2) the establishment of a list of genes in synthetic lethal network of the Dlt pathway; 3) the essentiality of D-alanines on abnormal lipoteichoic acids; and 4) the distinction between two important functions of LtaS. This chapter demonstrates the utility of small molecules as powerful tools to discover new biology.

4.1 What is synthetic lethality and what can we learn from it?

Synthetic lethality is defined as when two simultaneous perturbations are lethal, but any of those perturbations individually is not. This relationship can be observed with two loss-of-function genes (gene-gene interactions),[1] with compound treatment and a loss-of-function gene (drug-gene interactions),[2] or treatment with two compounds (drug-drug interactions).[3] The ability of organisms to tolerate almost all single and most double perturbations, whether environmental or genetic, suggests nature designed protective buffers through redundancy or compensatory pathways.[4] Therefore, two genes that are synthetically lethal are implicated to be part of pathways that are functionally connected. Decades of work in many fields from microbiology[5] to cancer[6] have used this relationship to assign protein function or determine compound mechanism of action. The synthetic lethal phenotype has enabled powerful inferences critical to the discovery of new biology.

4.2 Treating transposon libraries with small molecules to discover synthetic lethal networks

With the advent of high-throughput next-generation sequencing (NGS) techniques, one powerful way to find synthetic lethal relationships is with NGS-compatible transposon sequencing.[7] Transposons are mobile genetic elements that can hop in and out of the genome with the aid of an enzyme called a transposase. If a transposon gets inserted into a gene, it is assumed to be inactivating, and thereby acts as a proxy for a genetic knockout. Transposon libraries consist of pooled strains of bacteria, each strain containing a different random transposon insertion.[8] The pool is then exposed to a selective pressure, like antibiotics. Mutants that were sensitive to treatment were isolated, their transposons insertion sites sequenced, and further experiments were done to explain the biology.[9] This method was a low-throughput way to find synthetic lethal relationships by identifying loss-of-function mutants. In the current age, transposon libraries that have been adapted for high-throughput sequencing are easily able to identify what mutants survive selection as well as those that drop out of the pool.[10] Transposon sequencing has become very useful for large-scale discovery of gene-gene or compound-gene relationships.[11]

Several groups have made high-throughput transposon libraries in *S. aureus* to look at gene essentiality.[12] However, *S. aureus* is notorious for being genetically intractable; even in heavily mutagenized strains, the transformation efficiency, commonly the way transposon-containing plasmids are put into *S. aureus* for making transposon libraries, is low.[13] Combined with low transposon integration efficiency,[14] this makes it difficult to get high-saturation libraries in *S. aureus*. Furthermore, these plasmids require a high-temperature curing step that, as a result, precludes the insertion of the transposon into genes that are temperature sensitive.[15] Many cell wall pathways, including those we are interested in, are temperature sensitive, making this a less-than-ideal method for library construction. For these reasons, we engineered a new method for building

high-efficiency NGS compatible transposon libraries in *S. aureus* that used a phage transposition method, completely bypassing the need for a high-temperature curing step (Figure 4.1).[16] Our libraries were multiplexed from six different transposon constructs containing different promoters allowing for insertional inactivation, upregulation or downregulation of genes. For establishing synthetic lethal networks, all types of transposon constructs were pooled and analyzed for genetic inactivation.

There are two general approaches for discovering synthetic lethal interactions of a specific gene by high-throughput transposon sequencing (tn-seq): building a transposon library in the gene-inactivated background[17] or treating a transposon library with an inhibitor of the gene-encoded protein.[2b] Small molecules are especially valuable in this space due to their ability to perturb a pathway without further genetic manipulation of the organism. This enables us to use the same tn-seq library and compare results across treatments with different inhibitors. Genes with transposon insertions that are present in the control but depleted or absent in the inhibited library are synthetically lethal with inhibitor treatment.

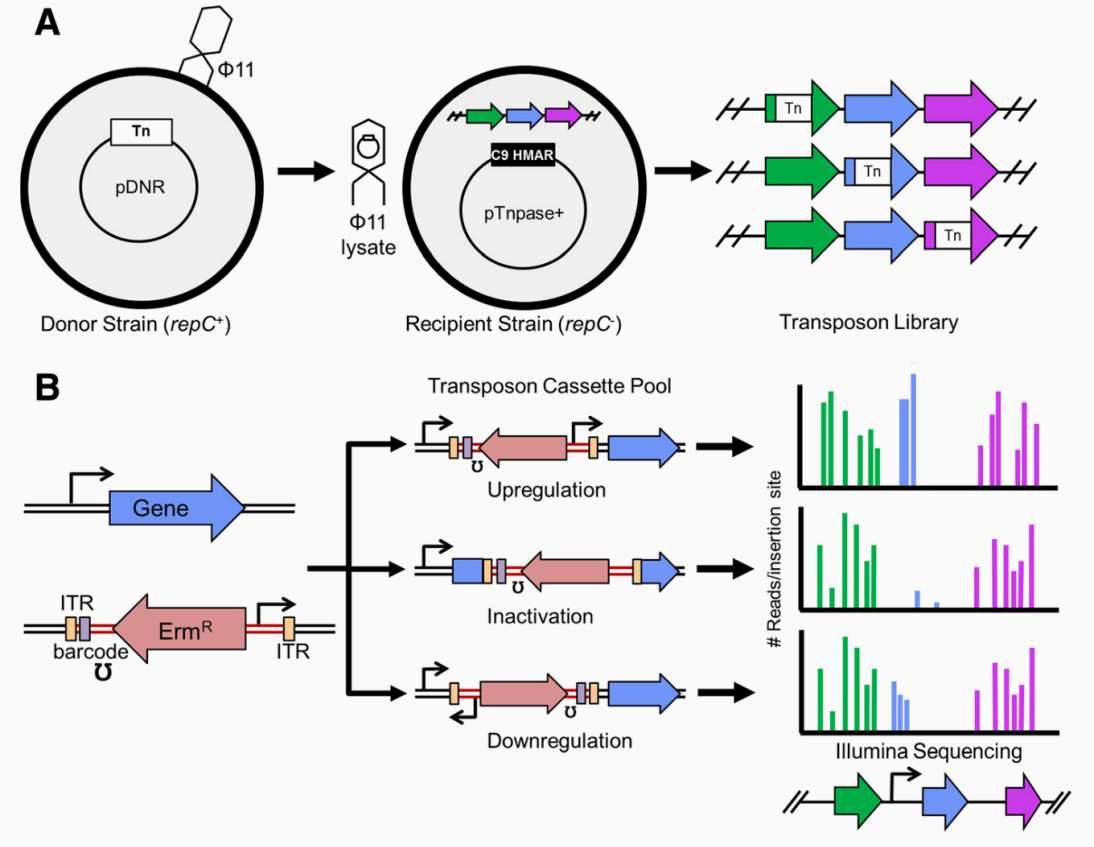

Figure 4.1 Method of constructing high-density transposon libraries in S. aureus using phage-based transposition. (A) A transducing lysate of the transposon cassette marked with erythromycin is made and used to infect a recipient strain where it is unable to replicate (*repC*$^-$) unless integrated chromosomally by the Himar1 transposase. Stable integrates are selected for using erythromycin and mutants are pooled together into one library. (B) The transposons were designed with outward facing promoters of varying strengths that allow for upregulation and downregulation in addition to simple inactivation. For the purpose of this work, insertions will be analyzed as inactivating. Figure taken from Santiago et. al.[16]

4.3 Treatment of the HG003 tn-seq library with several D-alanylation inhibitors identifies the synthetic lethal network of the Dlt pathway

After constructing the high-saturation NGS-compatible transposon library in methicillin-sensitive *S. aureus* strain HG003, treatment with antibiotics was an obvious application.[18] As mentioned in the first chapter, a small molecule inhibitor of the Dlt pathway, amsacrine, was discovered by a previous group member, Lincoln Pasquina.[2b] We grew the HG003 library in the presence of varying concentrations of amsacrine (10, 20 and 30 μg/mL) to identify genes sensitive to D-alanylation inhibition. After samples were grown for many generations, genomic DNA was harvested and sent for sequencing. Reads were mapped to a reference genome and data was analyzed using the Mann-Whitney U test. Genes showing greater than a five-fold depletion in reads with a P-value less than 0.05 were classified as hits (Table 4.1, Appendix 6). From this analysis, five genes were established as synthetically lethal with Dlt pathway inhibition: genes of unknown function *SAOUHSC_01050* and *SAOUHSC_01025*; *lcpA*, encoding one of three WTA ligases; and two genes encoding enzymes in the LTA biosynthesis pathway, *ugtP* and *ltaA*.

In the previous chapter, we discovered two new Dlt pathway inhibitors, DBI-1 and DltI-1. To determine if they have similar tn-seq profiles to amsacrine, we treated the HG003 tn-seq library with DBI-1 and DltI-1 at concentrations of 2.5 and 5 μg/mL (Appendix 6). Treatments with all three compounds produced a remarkably similar gene profile, some even containing identical depletion ratios (Table 4.1). Using the small molecule inhibitors of D-alanylation, we have confirmed our ability to use tn-seq to identify antibacterials that inhibit the same target or pathway. Furthermore, because each inhibitor had a different scaffold, we knew hits were not a result of off-target affects.

Table 4.1 Tn-seq identifies five genes that are synthetically lethal with Dlt pathway inhibition. The same set of genes are depleted in tn-seq libraries treated with amsacrine (10 μg/mL), DBI-1 (2.5 μg/mL) and DltI-1 (2.5 μg/mL), proving the ability of tn-seq to identify small molecules inhibiting the same pathway. Table includes genes with depleted tn-seq reads (fold change < 0.25) across treatments with different Dlt pathway inhibitors with a P value < 0.05. The ratio of genes depleted for amsacrine and DltI-1 are remarkably similar, perhaps due to the similarity of their MIC (5 μg/mL). Full tables are available in appendix six.

			Fold-change		
Locus Tag	Gene	Pathway	Amsacrine	DBI-1	DltI-1
SAOUHSC_01050	Hypothetical protein	Unknown	0.22	0.13	0.22
SAOUHSC_01025	Hypothetical protein	Unknown	0.08	0.05	0.08
SAOUHSC_01361	*lcpA*	WTA biosynthesis	0.12	0.11	0.15
SAOUHSC_00953	*ugtP*	LTA biosynthesis	0.11	0.04	0.10
SAOUHSC_00952	*ltaA*	LTA biosynthesis	0.07	0.03	0.05

4.4 The genes in the Dlt pathway synthetic lethal network

Treatment of the tn-seq library with three different scaffolds of Dlt pathway inhibitors resulted in a short list of genes that are in the synthetic lethal network with the D-alanylation pathway. Of these five genes, two were of unknown function (*SAOUHSC_01050* and *SAOUHSC_01025*), one was in the WTA biosynthesis pathway (*lcpA*), and the last two were in the LTA biosynthesis pathway (*ypfP* and *ltaA*). Studying this network, we have used the synthetic lethal relationships to learn about these pathways and the importance of the D-alanine modification on teichoic acids.

4.4.1 D-alanylation inhibitors reveal important information about proteins of unknown function SAOUHSC_01050 and SAOUHSC_01025

SAOUHSC_01050 (1050) and *SAOUHSC_01025* (1025) are genes of unknown function conserved in *Staphylococcal* species predicted to encode membrane proteins. Both have been implicated as important in cell envelope stress, and knockouts of these two genes sensitize *S. aureus* to cell wall targeting antibiotics.[18] However, strains lacking 1050 and 1025 are not sensitive to tunicamycin, and they are not present in the synthetic lethal network with WTA biosynthesis.[19] What the function of these two genes are or what pathways they are a part of is unknown, but their unique association with the Dlt pathway was exploited to identify the target of amsacrine.[2b] Using a mutant strain with a transposon in 1050 (tn::1050), resistant colonies were raised to amsacrine treatment at a frequency of ~1 in 10^5 cells. In this group of resistant colonies, we expected to find very few with mutations in the target of amsacrine (frequency of ~1 in 10^7) and the rest to contain suppressor mutations that bypass the essentiality of 1050 in the absence of D-alanylation (Figure 4.2).

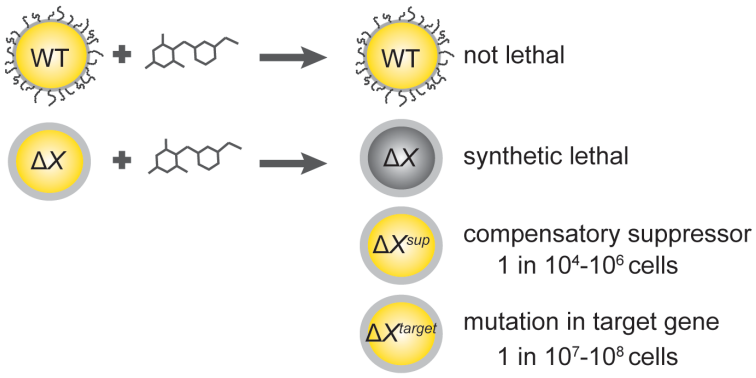

Figure 4.2 Schematic for the types of resistant mutants to inhibitors of nonessential pathways. A small molecule that inhibits a nonessential pathway will not be lethal to wild-type *S. aureus* but will be lethal to a susceptible mutant strain Δ*X*. Resistance mutants in this background will either contain suppressors that compensate for the lack of gene *X* (~1 in 10^{4-6} cells) or mutations in the target gene, which occur at a much lower frequency (~1 in 10^{7-8}). These values are approximate, and can vary greatly depending on the inhibitor and the target.

To learn what these suppressor mutations were, we plated the tn::1050 strain and selected for mutants that were resistant to amsacrine but did not have mutations in *dltB*. The genomic DNA of 11 mutants with suppressors were isolated from three independent cultures and sent for whole-genome sequencing at the Tufts genomic facility in Boston. The sequence reads were mapped to the USA300 JE2 reference strain. Out of 11 mutants, nine had mutations in a gene called *vraS* and one had a mutation in *vraT* (Table 4.3). VraRST (*vraR/vraS* are homologous to *B. subtilis yvqC/yvqE*) is a multi-component system that responds to cell wall stress.[20] VraR and VraS upregulation was originally identified as a mechanism for causing intermediate resistance of *S. aureus* to vancomycin.[20] VraS is the transmembrane sensor protein, which responds to cell wall damage and undergoes autophosphorylation.[21] The phosphoryl group quickly gets transferred to VraR, the response regulator that turns on gene expression.[21] VraT is another membrane protein

that regulates VraRS, although it is un known if this regulation occurs through scaffolding or some other mechanism.[22] Many genes are regulated by VraRST, including those involved in cell wall biosynthesis.[20b] How these mutations affect VraRST activity and which downstream gene(s) are the culprit(s) for the protection of tn::1050 from amsacrine is not clear. More work must be done to validate the sequencing and determine what genes are responsible for this phenotype.

Table 4.3 Amsacrine resistant tn::1050 mutants contain suppressor mutations in vraS and vraT. Whole-genome sequencing results of eleven USA300 JE2 tn::1050 colonies resistant to amsacrine. Nine contained mutations in *vraS* and one had a mutation in *vraT*, members of a two-component stress singling pathway.

USA300 tn::1050 Mutant	Gene	Locus tag (HG003)	Mutation
1	*vraT*	SAOUHSC_02100	P174S
2	*vraS*	SAOUHSC_02099	D26Y
3	*vraS*	SAOUHSC_02099	G64V
4	*vraS*	SAOUHSC_02099	R6*
5	*vraS*	SAOUHSC_02099	T125N
6	*vraS*	SAOUHSC_02099	Q288K
7	*vraS*	SAOUHSC_02099	W77C
8	*vraS*	SAOUHSC_02099	W77C
9	*vraS*	SAOUHSC_02099	L50*
10	*vraS*	SAOUHSC_02099	T129N

4.4.2 Small molecule inhibitors of the Dlt pathway identify LcpA as the main WTA ligase

Some of these data have been published.[23]

The WTA biosynthesis pathway was already confirmed as a synthetic lethal partner with the Dlt pathway.[2] We expected to see genes in the WTA pathway with depleted transposon insertions in Dlt inhibitor-treated transposon libraries. However, due to the essentiality of the later

steps in the biosynthesis and the severe fitness defect in knocking out the pathway, we typically observe poor coverage of most WTA genes in tn-seq libraries. Perhaps because of some redundancy between them, this does not hold true for the genes encoding the WTA ligases, which are responsible for attaching WTA polymers covalently to peptidoglycan. There are three purported ligases with this function: LcpA, LcpB and LcpC.[24] Transposon insertions in the gene *lcpA*, which encodes the WTA ligase LcpA, were depleted in libraries treated with Dlt pathway inhibitors, but insertions in *lcpB* or *lcpC* were not (Figure 4.3A, Figure 4.3B). This immediately suggested that these ligases may not have completely redundant functions in *S. aureus*.[25] The synthetic lethal profile was confirmed by looking at the susceptibility of genetic knockouts to amsacrine (Figure 4.3C). Strains lacking LcpA were sensitive to amsacrine, but strains lacking LcpB or LcpC only were not. Further analysis revealed that LcpA knockout strains also had similar sensitivities to beta-lactam antibiotics oxacillin and cefaclor as Δ*tarO* mutants, suggesting that LcpA is the main WTA ligase in *S. aureus*.[23] Biochemical experiments were done by Kaitlin Schaefer to confirm the Lcp proteins as WTA ligases, which had never been done before. The reconstitution of the WTA ligase activity of LCP proteins in *S. aureus* has been reported[23] and will be further described in Kaitlin Schaefer's thesis.

The Lcp proteins had been proposed to have redundant functions in *S. aureus* and the field lacked the context to establish the physiological relevance of each ligase. Using chemical genetics, the Dlt pathway inhibitors, and the synthetic lethal relationship with the WTA pathway, we identified LcpA as the main WTA ligase.[23] What was less clear was the reason for the synthetic lethality between these pathways and why, in the absence of WTAs, D-alanines on LTAs become essential. One way to gain more information about a cellular pathway is to raise resistant mutants to a selecting condition. However, our efforts to raise spontaneous mutants in the Δ*tarO*

background to amsacrine were hampered by a haze that formed on the agar plates. This haze, which may be due to cell lysis after several cellular divisions, prevented the isolation of spontaneous resistant colonies. To examine why D-alanylation is important on teichoic acids we decided to look at the synthetic lethal relationship between the Dlt and LTA pathways.

A

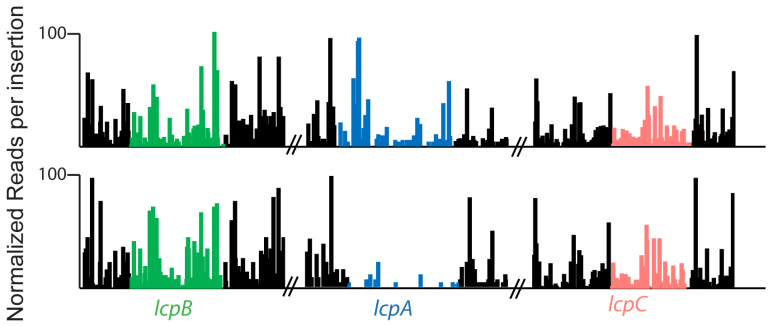

B

Gene	Locus tag	Reads Control	Reads Treatment	Corrected P-value	Fold-change
Replicate 1					
lcpA	SAOUHSC_01361	662	60	6.09E-05	0.092
lcpB	SAOUHSC_00997	918	807	0.349	0.879
lcpC	SAOUHSC_02583	1087	895	0.290	0.824
Replicate 2					
lcpA	SAOUHSC_01361	662	24	2.55E-06	0.038
lcpB	SAOUHSC_00997	918	621	0.179	0.677
lcpC	SAOUHSC_02583	1087	704	0.145	0.648

C

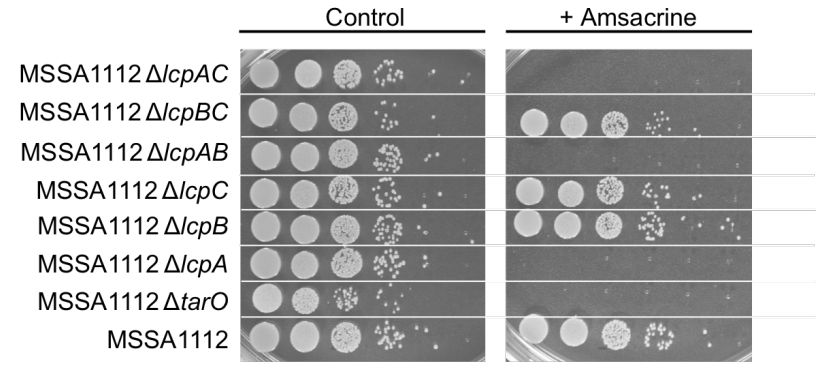

Figure 4.3 Knockouts of *lcpA* but not *lcpB* or *lcpC* are sensitive to amsacrine, suggesting LcpA is the main WTA ligase. (A) Genomic context of sequenced transposon insertion sites in control (top) and amsacrine-treated (30 µg/mL) (bottom) libraries. Graphs shown are representative of multiple replicates. (B) Number of reads of insertions in *lcpABC* from two

Figure 4.3 (Continued)

replicates of an amsacrine treated (30 μg/mL) HG003 tn-seq library. Number of reads in the control is the same for both samples because the same reference was used. A significant ten-fold decrease in insertions in *lcpA* (corrected P-value < 0.05) was observed compared to the control, but not for *lcpB* or *lcpC*. (C) Spot dilutions of WT MSSA1112 and various mutant strains on TSA containing amsacrine (10 μg/mL). All strains containing *lcpA* deletions are synthetically lethal with amsacrine treatment, suggesting these strains are lacking much if not all WTAs. Spots are dilutions of cultures from 10^{-1} to 10^{-6}.

4.4.3 Genes in the LTA pathway are synthetically lethal with D-alanylation inhibition

Two genes involved in LTA biosynthesis, *ypfP* and *ltaA*, were found to be synthetically lethal with the Dlt pathway. YpfP (UgtP) is a glycosyltransferase that transfers two sugars to the diacylglycerol (DAG) anchor.[26-27] LtaA flips the anchor extracellularly and LtaS, the processive glycerol phosphate synthase, removes glycerol from phosphatidylglycerol and incorporates it into the LTA polymer (Figure 4.4).[28] It is hypothesized that the polymer is decorated with D-alanines by the Dlt proteins as it is being produced, and bacterial two-hybrid experiments suggest that DltD and LtaS may interact.[29] The Dlt and LTA biosynthetic pathways are interconnected, and our small molecule inhibitors of D-alanylation uniquely positioned us to study this connection.

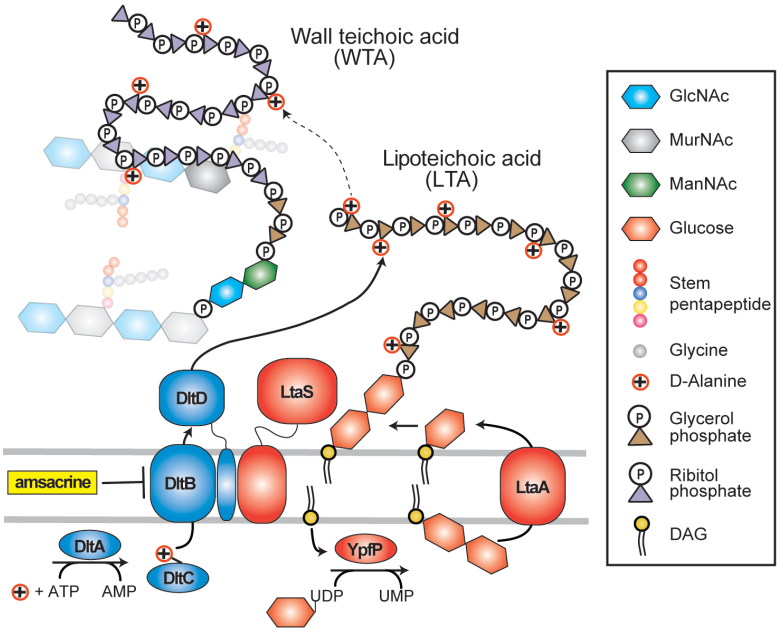

Figure 4.4 Schematic depicting the LTA and Dlt pathways, two functionally connected pathways. Lipoteichoic acids are modified with D-alanines by the Dlt pathway, which then get transferred to WTAs. Amsacrine is a DltB inhibitor, preventing D-alanine incorporation into LTAs.

To confirm the tn-seq results, the susceptibilities of genetic knockouts of *ypfP*, *ltaA* and *ltaS* to amsacrine were tested (Figure 4.5). SEJ1 tn::ypfP and tn::ltaA strains showed a synthetic lethal phenotype with amsacrine, but SEJ1 Δ*ltaS*^{4S5} did not. The latter result confirms previous studies by graduate student John Santa Maria that it is possible to delete Dlt pathway genes in the SEJ1 Δ*ltaS*^{4S5} background.[2a] However, the SEJ1 Δ*ltaS*^{4S5} strain has several suppressors, the most critical being a suppressor in *gdpP*, a gene encoding a protein important for intracellular signaling.[30] Knocking out *gdpP* results in the accumulation of cyclic-di-AMP, which acts as a secondary messenger in *S. aureus* and, among likely many downstream effects, results in a thicker cell wall.[30-31] One possible hypothesis was the presence of this suppressor protected Δ*ltaS*^{435} from

the lethal phenotype caused by amsacrine. However, double knockouts of tn::ypfP or tn::ltaA with Δ*gdpP:kan* failed to provide the complete rescue observed in the Δ*ltaS*^{4S5} strain (Figure 4.5).

SEJ1 Δ*ltaS*^{4S5} is not sensitive to amsacrine, perhaps because without lipoteichoic acids there are no polymers to attach D-alanines. Since a minimal amount of D-alanines get onto WTAs in the absence of LTAs, the SEJ1 Δ*ltaS* strain is effectively a double knockout of the LTA and Dlt pathways.[32] Deletion strains of *ypfP* or *ltaA* both still contain LTAs, except they are polymerized on a different anchor (Figure 4.6). Instead of Glc_2DAG, which is absent in the YpfP mutant or found only on the inner leaflet in the case of the LtaA mutant, LTAs are polymerized by LtaS directly on DAG and are abnormal in length.[28,33] We hypothesized that the unusual anchor or length of these abnormal LTAs is responsible for the lethality of amsacrine to the Δ*ypfP* or Δ*ltaA* strains (Figure 4.6). Interested in the importance of the LTA polymer size, we decided to determine the cause of amsacrine lethality to Δ*ypfP* backgrounds.

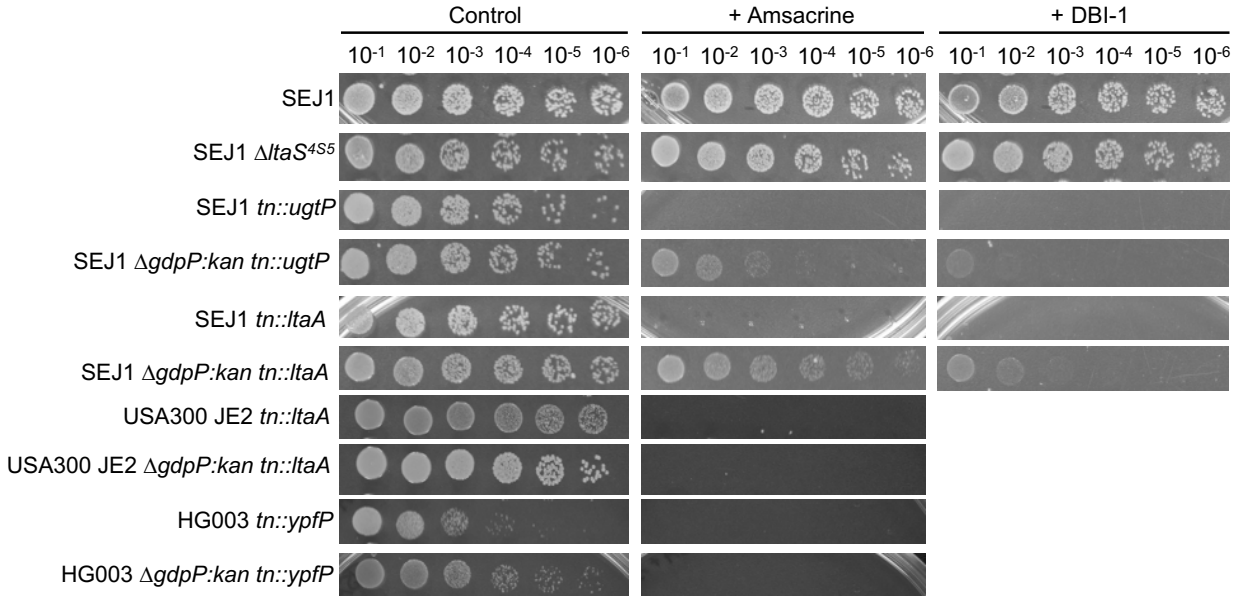

Figure 4.5 Knocking out *gdpP* is not protective against amsacrine or DBI-1 treatment in backgrounds lacking *ypfP* or *ltaA*. Spot dilutions of knockouts on control, amsacrine (10 μg/mL) and DBI-1 (1 μg/mL). SEJ1 Δ*ltaS*^{4S5} is a strain that contains a clean knockout of *ltaS* with

Figure 4.5 (Continued)

background suppressor mutations. Moving the Δ*gdpP:kan* knockout into strains containing tn::ypfP or tn::ltaA does not confer complete resistance to treatment, confirming that the background suppressor mutation in *gdpP* is not responsible for the amsacrine resistance of SEJ1 Δ*ltaS*^{4S5}.

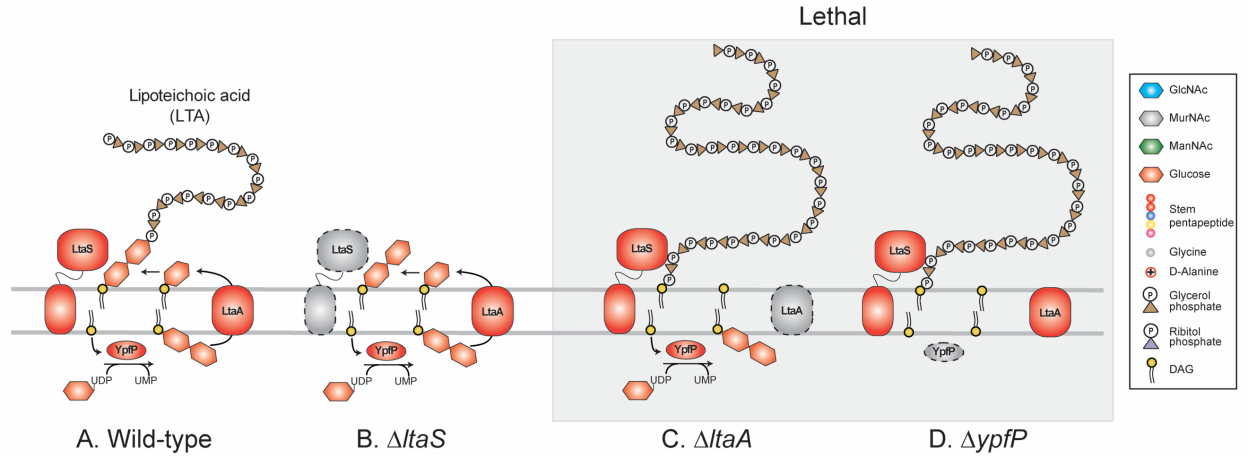

Figure 4.6 Mutant strains lacking *ltaA* or *ypfP* have abnormal LTAs that are sensitive to Dlt pathway inhibitors. Wild-type (A) or Δ*ltaS* (B) are not sensitive to D-alanylation inhibition but Δ*ltaA* (C) or Δ*ypfP* (D) are (note the LTAs lacking D-alanines). Δ*ltaA* or Δ*ypfP* have LTAs that are polymerized on diacylglycerol (DAG) directly as opposed to Glc_2DAG and appear to be aberrant in size compared to wild-type.

4.4.4 Abnormally long LTAs are toxic without D-alanylation

We raised resistant mutants in the SEJ1 tn::ypfP background to identify suppressors of amsacrine lethality and discovered mutations in *ltaS* (Table 4.4). Mutations in *ltaS* could be put into two groups: point mutations and 18 base pair in-frame insertions. To determine what these mutations do to LtaS activity, we used an *in vitro* assay to compare LTAs of mutants discovered

in the tn::ypfP background (Figure 4.7). The lipoteichoic acid profile between the wild-type and tn::ypfP mutant differ; tn::ypfP appears to make longer LTAs than wild-type. This corroborates what has been observed by others before.[28,33] The mutants were further classified into two groups: 1) mutations that restore the apparent size of LTAs to wild-type (F93L, N504K, H187K) and 2) mutations that reduce LTA production to undetectable levels (mutations L181S, L181F, Ins1, Ins2, and F94S). These mutant phenotypes suggest that lack of D-alanines on abnormally long LTAs in the tn::ypfP background is lethal, and that correcting that length or completely removing LTAs confers resistance to amsacrine. This was further confirmed by raising and testing LtaS mutants in backgrounds RN4220 Δ*ypfP* and SEJ1 Δ*ypfP:kan* (data not shown).

Table 4.4 Amsacrine resistant colonies in *S. aureus* tn::ypfP backgrounds have mutations in *ltaS*. Spontaneous mutants were raised by plating tn::ypfP strains in the presence of amsacrine, passaging in absence of inhibitor, and selecting for strains that maintained resistance to amsacrine upon second challenge. *Mutations in the SEJ1 tn::ugtP background were discovered by Dr. B. McKay Wood.

Strain	LtaS mutations
HG003 tn::ugtP	L181S
SEJ1 tn::ugtP*	S34_L35insYYVDFS (Ins1)
	L34delinsYYVDFSL (Ins2)
	F94S
	L181F
	H187K
	N504K

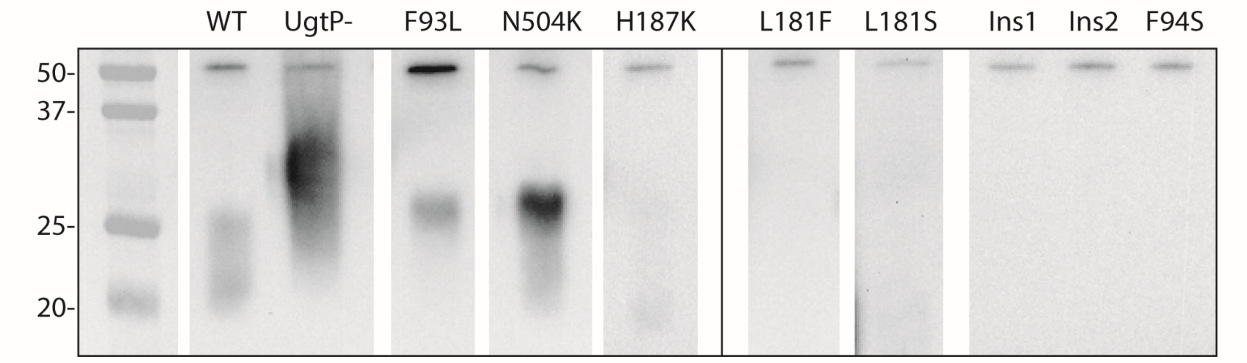

Figure 4.7 Western blots of LTAs of different tn::ypfP LtaS mutants shows changes in LTA length. Wild-type SEJ1 and SEJ1 tn::ypfP strains were grown, spun down, lysed, run on an SDS-PAGE gel and transferred to a nitrocellulose membrane. LTAs were detected using primary α-LTA and secondary α-mouse-HRP conjugate. Wild-type SEJ1 and SEJ1 tn::ypfP make visibly different sized LTAs. Mutations in LtaS appear to either correct the size to normal (first group, left panel) or reduce LTA production to undetectable levels (second group, right panel). This work was done by Dr. Christopher Vickery and was included in this thesis with his permission.

4.4.5 Distinguishing between the different functions of LtaS

The only mutations found in the tn::ypfP background were point mutants or in-frame insertions, suggesting that maintaining some functionality of LtaS is important. However, some mutants have no detectable lipoteichoic acid production (second group of mutants, Figure 4.7). These LtaS mutants may not have polymerase activity, but because the gene remains in-frame it is possible that they still hydrolyze glycerol phosphate from phosphatidylglycerol (PG). In *S. aureus*, LtaS performs two functions: 1) hydrolysis of glycerol phosphate from PG and 2) the polymerization of glycerol phosphate.[28] Previous work has shown that the extracellular LtaS domain (eLtaS) is enough to hydrolyze PG to diacylglycerol (DAG) *in vitro*.[35] Furthermore, this function is essential, as a catalytically inactivated LtaS mutant that does not hydrolyze PG failed

to complement an *ltaS* knockout.[35] Mutations in the second group occur near the N-terminus of the protein, leaving the eLtaS domain intact and perhaps decouple the hydrolase from the polymerase activity (Figure 4.8). This would allow LtaS to hydrolyze glycerolphosphate from PG to produce DAG, which spontaneously flips across the bilayer and gets recycled back into phospholipid biosynthesis.[36] Some of the pleiotropic effects observed in the absence of LtaS, such as membrane stability, could be due to the disruption in the lipid recycling process and not due to removal of the LTA polymer. To clarify the importance of these two functions, the hydrolase activity of LtaS will be assessed independently of polymerase activity in future experimentation.

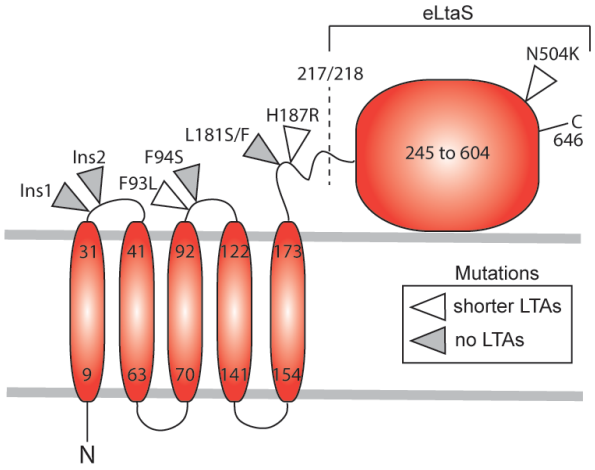

Figure 4.8 Proposed topology of LtaS with mapped mutation sites. LtaS is predicted to have five transmembrane helices, a linker region, and a large C-terminal enzymatic domain. LtaS also undergoes proteolytic cleavage at residue 217 by a signal peptidase to release an extracellular LtaS domain (eLtaS), a mechanism used to irreversibly inactivate the enzyme and prevent LTA production.[35] Many mutations that result in no visible polymerase activity (group two mutants, grey carrots) occur near the N-terminus of the protein, leaving the eLtaS domain intact and possibly still functioning as a PG hydrolase.

The discovery of the group two mutants also has broad implications for the function of LtaS. We hypothesize that the LTA polymer is dispensable (at least in a laboratory setting), but the hydrolase activity of LtaS is essential. However, more work must be done to characterize these strains. We have found that these mutants lack suppressors in *gdpP* that could explain their ability to tolerate the absence of LTA polymer, but we have yet to sequence their genomes and determine if there are other possible suppressors. In addition, work is currently ongoing to express LtaS mutants in a clean background. Then we will follow up with *in vitro* assays to measure the activities of the LtaS mutants and determine if they can hydrolyze PG. We will also need to develop a mass spectrometry method to measure DAG-linked species in the membrane. It is possible that intact LtaS is important for scaffolding purposes and not for enzymatic functions, however previous work suggests that cells expressing a catalytically inactive LtaS mutant cannot survive, making this not a likely hypothesis.[36] Studying the two enzymatic functions of LtaS and their phenotypes will be an important contribution regarding the physiology of *S. aureus* and be useful for designing phenotypic screens for the discovery of future inhibitors of this pathway.

4.5 The importance of D-alanines on LTAs

In addition to the mutations that apparently result in complete loss of LtaS polymerase activity, we have also identified mutations that reduce the length of the LTAs that are produced. Indeed, we also selected LtaS mutations in other Δ*ypfP* mutant backgrounds that result in shorter, i.e., more like wildtype, LTAs (data not shown). These findings suggest that long LTAs must be D-alanylated and that mutations that reduce LTA length or completely remove LTAs solve this problem. We have found that treating the tn::ypfP strain with D-alanylation inhibitors results in lysis after several cell divisions (data not shown). We speculate that lysis occurs when D-

alanylated LTAs become sufficiently depleted. The lytic phenotype could be due to any of several cellular dysfunctions that have been tied to defects in teichoic acids. These include: 1) delocalization of cell division machinery[28,37]; 2) disrupted cell membrane integrity or stability[29b]; and 3) dysregulation of autolysins.[33,38] Loss of D-alanines typically results in increased autolysin activity in Gram-positive bacteria.[39] The Δ*ypfP* background, which is already more susceptible to lysis than wildtype,[26-27] may simply be unable to tolerate the increased hydrolase activity resulting from D-alanylation inhibition. The pleiotropic phenotypes associated with LTAs make it a challenge to tease out the cause of synthetic lethality and work in this area is still ongoing.

4.6 Small molecule inhibitors of D-alanylation are useful probes for biological discovery

In this chapter, we discussed the use of small molecule inhibitors to discover synthetic lethal relationships and probe new biology in *S. aureus*. Small molecules serve as excellent tools to probe biology, providing temporal control over the time of pathway or enzyme inhibition. Since inhibition is usually instantaneous, there is less ability for background suppressors to develop and influence biological observation. Furthermore, in combination with gene network analyses, these two approaches are very useful for looking at a more complete picture of a pathway's importance.

We now have three small molecules from different scaffolds that inhibit the Dlt pathway: amsacrine, DBI-1 and DltI-1. The unique profile of synthetic lethality first discovered by amsacrine enabled us to screen for other D-alanylation inhibitors. We have since treated a high-density tn-seq library with each inhibitor to answer the question if different inhibitors of the same pathway have the same fingerprint. Our analysis revealed that all treatments appeared identical and five genes were synthetically lethal with Dlt pathway inhibition. Each gene from this analysis has contributed towards the study of *S. aureus* physiology. Genes of unknown function

SAOUHSC_01050 and *SAOUHSC_01025* provided useful backgrounds for raising resistant mutants and identifying the targets of amsacrine and DBI-1. The lethality of *lcpA* knockouts with D-alanylation inhibition but not *lcpB* or *lcpC* provided the context needed to establish LcpA as the main WTA ligase. Finally, the lethality of amsacrine treatment to knockouts of genes *ypfP* and *ltaA* informed us of the importance of D-alanylated LTAs and may lead to important discoveries about the essential functions of LtaS, particularly as we have been able to raise informative resistant mutants. *S. aureus* without WTAs or with abnormal LTAs require D-alanylated LTAs to survive, and understanding this requirement could provide valuable insight on the purpose of these polymers.

4.7 Methods

General methods

Unless specified, cultures were grown in tryptic soy broth (TSB) or spotted on tryptic soy broth agar (TSA). A list of strains is provided in appendix 7.

Construction of S. aureus strains by phage transduction

In general, strains were constructed by transducing marked deletions into desired backgrounds using ϕ85 transducing phage. To construct the phage lysate, from an overnight in TSB strains were diluted 1:100 and grown for ~3 hours until an early OD_{600}. 300 µL of cells were mixed with 200 µL of ϕ85 phage and allowed to sit at room temperature for 30 min. 5 mL of top agar (0.7% agar) was added along with 50 µL of 1 M $CaCl_2$. The tube was inverted and then plated on 10 mL bottom agar (1.5% agar) containing 100 µL of 1 M $CaCl_2$ and selecting antibiotic. Plates were incubated at 30ºC overnight. 10 mL of TSB was added and plates were parafilmed closed and allowed to incubate for another day at room temperature on an orbital shaker. Lysate was filter sterilized and

stored at 4ºC until use. For the transduction, 2 mL of a dense overnight culture was spun down and resuspended in 100 µL TSB. Transduction reaction was prepared as follows: 50 µL cells, 50 µL ϕ85 phage lysate, 100 µL LB + 10 mM $CaCl_2$. Reactions were incubated at 37ºC for 25 minutes and then shaken at 300 rpm at 37ºC for 15 minutes. After incubation, 100 µL of cold 0.02 M NaCitrate was added to each reaction and samples were spun down 10 minutes at 9,000 rpm. Samples were then resuspended in 100 µL cold 0.02 M sodium citrate and placed on ice for 2 hours. The full aliquot was plated on 20 mL TSA plates containing 100 µL 1 M NaCitrate plus selecting antibiotic and stored at 30ºC for 24-48 hours. Colonies were restreated twice on sodium citrate plates and then tested for transduction.

Raising spontaneous amsacrine resistant mutants and determining frequency of resistance

Backgrounds of interest (USA300 JE2 tn::1050, RN4220 Δ*ugtP*, SEJ1 tn::ugtP, HG003 tn::ugtP, SEJ1 Δ*ugtP:kan*) were grown overnight in TSB and then diluted 1:100 into fresh media. Strains were grown until an OD_{600} ~1-2 (approximately 10^8 cells/mL) and then serially diluted ten-fold. 100 µL of higher-density cultures containing 10^{6-8} cells/mL were plated on TSA plates with selecting compound (m- or o- amsacrine at 10 or 20 µg/mL, respectively). 100 µL of lower-density cultures containing 10^{1-3} cells/mL were plated on TSA control plates with no selecting compound for calculating starting cultures densities. Plates were incubated at 30ºC for 24 hours. Frequency of resistance (F.O.R.) was calculated as (colony forming units on selecting plate/number of cells plated). Colonies were picked and passaged twice on plates containing no inhibitor before being retested for amsacrine resistance. To select against *dltB* mutations, tn::1050 amsacrine resistant colonies were tested for sensitivity to amsacrine and tunicamycin (10 and 1 µg/mL, respectively). Mutants that were sensitive to combination treatment were expected to have *dltB* mutations and were not sent for whole genome sequencing.

Whole genome sequencing and alignment

Genomic DNA was extracted from eleven USA300 JE2 tn::1050 amsacrine resistant mutants and sent to Tufts University Core Facility for Genomics. There, DNA was prepped and sequenced using an Illumina MiSeq in paired-end 250 nucleotide runs. Whole genome FASTQ data was analyzed using Geneious v7.1 software, where mutant strains were aligned to the consensus sequence of the parental strain using default parameters. Single nucleotide polymorphisms (SNPs) and insertions/deletions (indels) were identified using default parameters and a minimum variant frequency of 90%.

Transposon sequencing (Tn-seq)

Transposon sequencing was performed as described previously.[2b] Briefly, a pooled transposon library ~5 x10^5 cells was grown in the presence and absence of m-amsacrine (10, 20 and 30 μg/ml), DBI-1 (2.5 and 5 μg/ml), or Dlt-1 (2.5 and 5 μg/ml) at 30°C until an OD_{600} = 1.0. Genomic DNA was prepared and sent for Illumina sequencing. Data was processed using the Tufts University Genomics Core Facility Galaxy server and mapped to S. aureus NCTC8325 using Bowtie.[43] The Mann–Whitney U test was used to identify genes with depleted reads, and genes that had more than a five-fold change in the number of reads between the untreated control and treated were considered depleted. The threshold or significance was set to $P < 0.05$. Five genes contained depleted reads between all samples.

Spot dilutions of *S. aureus* strains

S. aureus cultures were grown overnight to stationary phase and diluted 1:100 in fresh TSB and grown for several hours at 30°C. Strains were normalized to an OD_{600} = 1 and each culture was serially diluted ten-fold from 10^{-1} to 10^{-6}. Strains were then spotted on either TSA plates containing

amsacrine (10 μg/ml), or Dlt-1 (10 μg/ml) or 75% TSB agar plates containing DBI-1 (1 μg/ml). Plates were incubated at 30°C overnight and imaged after 24 hours.

Minimum inhibitory concentrations (MICs)

S. aureus strains were grown overnight in TSB and diluted 1:100 into fresh TSB in the morning. Strains were grown until an OD600 of ~1-2, and then were normalized to an OD_{600} of 1. Cultures were then diluted 1:1000 and 147 μL (approximately $1x10^5$ cells) added to each well of a 96-well plate. A two-fold dilution series of antibiotic or inhibitor was made in DMSO. Then 3 μL of antibiotic or inhibitor was added to corresponding well for a final volume of 150 μL. Plates were incubated at 30°C and OD_{600} measurements were taken after 16-18 hours. After background was accounted for, the MIC was determined at the concentration that caused less than 20% growth compared to untreated DMSO control.

4.8 References

1. Tong, A. H.; Lesage, G.; Bader, G. D.; Ding, H.; Xu, H.; Xin, X.; Young, J.; Berriz, G. F.; Brost, R. L.; Chang, M.; Chen, Y.; Cheng, X.; Chua, G.; Friesen, H.; Goldberg, D. S.; Haynes, J.; Humphries, C.; He, G.; Hussein, S.; Ke, L.; Krogan, N.; Li, Z.; Levinson, J. N.; Lu, H.; Menard, P.; Munyana, C.; Parsons, A. B.; Ryan, O.; Tonikian, R.; Roberts, T.; Sdicu, A. M.; Shapiro, J.; Sheikh, B.; Suter, B.; Wong, S. L.; Zhang, L. V.; Zhu, H.; Burd, C. G.; Munro, S.; Sander, C.; Rine, J.; Greenblatt, J.; Peter, M.; Bretscher, A.; Bell, G.; Roth, F. P.; Brown, G. W.; Andrews, B.; Bussey, H.; Boone, C. *Science.* **2004,** *303*, 808-813.

2. (a) Santa Maria, J. P., Jr.; Sadaka, A.; Moussa, S. H.; Brown, S.; Zhang, Y. J.; Rubin, E. J.; Gilmore, M. S.; Walker, S. *Proc Natl Acad Sci U S A.* **2014,** *111*, 12510-12515; (b) Pasquina, L.;

Santa Maria, J. P.; McKay Wood, B.; Moussa, S. H.; Matano, L. M.; Santiago, M.; Martin, S. E.; Lee, W.; Meredith, T. C.; Walker, S. *Nat Chem Biol.* **2016,** *12*, 40-45.

3. Campbell, J.; Singh, A. K.; Santa Maria, J. P.; Kim, Y.; Brown, S.; Swoboda, J. G.; Mylonakis, E.; Wilkinson, B. J.; Walker, S. *ACS Chem Biol.* **2011,** *6*, 106-116.

4. Hartman, J. L. t.; Garvik, B.; Hartwell, L. *Science.* **2001,** *291*, 1001-1004.

5. Shuman, H. A.; Silhavy, T. J. *Nat Rev Genet.* **2003,** *4*, 419-431.

6. Fece de la Cruz, F.; Gapp, B. V.; Nijman, S. M. *Annu Rev Pharmacol Toxicol.* **2015,** *55*, 513-531.

7. (a) van Opijnen, T.; Camilli, A. *Nat Rev Microbiol.* **2013,** *11*, 435-442; (b) Barquist, L.; Boinett, C. J.; Cain, A. K. *RNA Biol.* **2013,** *10*, 1161-1169.

8. Kleckner, N.; Roth, J.; Botstein, D. *J. Mol. Biol.* **1977,** *116*, 125-159.

9. Peschel, A.; Otto, M.; Jack, R. W.; Kalbacher, H.; Jung, G.; Gotz, F. *J. Biol. Chem.* **1999,** *274*, 8405-8410.

10. Chao, M. C.; Abel, S.; Davis, B. M.; Waldor, M. K. *Nat Rev Microbiol.* **2016,** *14*, 119-128.

11. Brochado, A. R.; Typas, A. *Curr Opin Microbiol.* **2013,** *16*, 199-206.

12. (a) Valentino, M. D.; Foulston, L.; Sadaka, A.; Kos, V. N.; Villet, R. A.; Santa Maria, J., Jr.; Lazinski, D. W.; Camilli, A.; Walker, S.; Hooper, D. C.; Gilmore, M. S. *mBio.* **2014,** *5*, e01729-01714; (b) Chaudhuri, R. R.; Allen, A. G.; Owen, P. J.; Shalom, G.; Stone, K.; Harrison, M.; Burgis, T. A.; Lockyer, M.; Garcia-Lara, J.; Foster, S. J.; Pleasance, S. J.; Peters, S. E.; Maskell, D. J.; Charles, I. G. *BMC Genomics.* **2009,** *10*, 291.

13. Hisatsune, J.; Sato'o, Y.; Yu, L.; Kutsuno, S.; Hayakawa, Y.; Sugai, M. *J. Microbiol. Methods.* **2016,** *130*, 69-72.

14. Pajunen, M. I.; Pulliainen, A. T.; Finne, J.; Savilahti, H. *Micriobiol.* **2005,** *151*, 1209-1218.

15. Bae, T.; Glass, E. M.; Schneewind, O.; Missiakas, D. *Methods Mol Biol.* **2008,** *416*, 103-116.

16. Santiago, M.; Matano, L. M.; Moussa, S. H.; Gilmore, M. S.; Walker, S.; Meredith, T. C. *BMC Genomics.* **2015,** *16*, 252.

17. Meeske, A. J.; Sham, L. T.; Kimsey, H.; Koo, B. M.; Gross, C. A.; Bernhardt, T. G.; Rudner, D. Z. *Proc Natl Acad Sci U S A.* **2015,** *112*, 6437-6442.

18. Rajagopal, M.; Martin, M. J.; Santiago, M.; Lee, W.; Kos, V. N.; Meredith, T.; Gilmore, M. S.; Walker, S. *MBio.* **2016,** *7*.

19. Santa Maria, J. P.; Sadaka, A.; Moussa, S. H.; Brown, S.; Zhang, Y. J.; Rubin, E. J.; Gilmore, M. S.; Walker, S. *Proc. Natl. Acad. Sci. U. S. A.* **2014,** *111*, 12510-12515.

20. (a) Kuroda, M.; Kuwahara-Arai, K.; Hiramatsu, K. *Biochem. Biophys. Res. Commun.* **2000,** *269*, 485-490; (b) Kuroda, M.; Kuroda, H.; Oshima, T.; Takeuchi, F.; Mori, H.; Hiramatsu, K. *Mol. Microbiol.* **2003,** *49*, 807-821.

21. Belcheva, A.; Golemi-Kotra, D. *J. Biol. Chem.* **2008,** *283*, 12354-12364.

22. Boyle-Vavra, S.; Yin, S.; Jo, D. S.; Montgomery, C. P.; Daum, R. S. *Antimicrob. Agents Chemother.* **2013,** *57*, 83-95.

23. Schaefer, K.; Matano, L. M.; Qiao, Y.; Kahne, D.; Walker, S. *Nat Chem Biol.* **2017,** *13*, 396-401.

24. (a) Dengler, V.; Meier, P. S.; Heusser, R.; Kupferschmied, P.; Fazekas, J.; Friebe, S.; Staufer, S. B.; Majcherczyk, P. A.; Moreillon, P.; Berger-Bachi, B.; McCallum, N. *FEMS Microbiol. Lett.* **2012,** *333*, 109-120; (b) Chan, Y. G.; Frankel, M. B.; Dengler, V.; Schneewind, O.; Missiakas, D. *J. Bacteriol.* **2013,** *195*, 4650-4659.

25. Over, B.; Heusser, R.; McCallum, N.; Schulthess, B.; Kupferschmied, P.; Gaiani, J. M.; Sifri, C. D.; Berger-Bachi, B.; Stutzmann Meier, P. *FEMS Microbiol. Lett.* **2011,** *320*, 142-151.

26. Percy, M. G.; Gründling, A. *Annu. Rev. Microbiol.* **2014**.

27. Grundling, A.; Schneewind, O. *J. Bacteriol.* **2007,** *189*, 2521-2530.

28. Grundling, A.; Schneewind, O. *Proc Natl Acad Sci U S A.* **2007,** *104*, 8478-8483.

29. (a) Reichmann, N. T.; Picarra Cassona, C.; Monteiro, J. M.; Bottomley, A. L.; Corrigan, R. M.; Foster, S. J.; Pinho, M. G.; Grundling, A. *Mol. Microbiol.* **2014,** *92*, 273-286; (b) Neuhaus, F. C.; Baddiley, J. *Microbiol. Mol. Biol. Rev.* **2003,** *67*, 686-723.

30. Corrigan, R. M.; Abbott, J. C.; Burhenne, H.; Kaever, V.; Grundling, A. *PLoS Pathogens.* **2011,** *7*, e1002217.

31. Schuster, C. F.; Bellows, L. E.; Tosi, T.; Campeotto, I.; Corrigan, R. M.; Freemont, P.; Grundling, A. *Sci Signal.* **2016,** *9*, ra81.

32. Haas, R.; Koch, H. U.; Fischer, W. *FEMS Microbiol. Lett.* **1984,** *21*, 27-31.

33. Fedtke, I.; Mader, D.; Kohler, T.; Moll, H.; Nicholson, G.; Biswas, R.; Henseler, K.; Gotz, F.; Zahringer, U.; Peschel, A. *Mol. Microbiol.* **2007,** *65*, 1078-1091.

34. Brown, S.; Jr, J. P.; Walker, S. *Annu. Rev. Microbiol.* **2013,** *67*, 313-336.

35. Karatsa-Dodgson, M.; Wormann, M. E.; Grundling, A. *J. Bacteriol.* **2010,** *192*, 5341-5349.

36. (a) Kuhn, S.; Slavetinsky, C. J.; Peschel, A. *Int J Med Microbiol.* **2015,** *305*, 196-202; (b) Zhang, Y. M.; Rock, C. O. *Nat Rev Microbiol.* **2008,** *6*, 222-233.

37. Atilano, M. L.; Pereira, P. M.; Yates, J.; Reed, P.; Veiga, H.; Pinho, M. G.; Filipe, S. R. *Proc Natl Acad Sci U S A.* **2010,** *107*, 18991-18996.

38. (a) Schlag, M.; Biswas, R.; Krismer, B.; Kohler, T.; Zoll, S.; Yu, W.; Schwarz, H.; Peschel, A.; Gotz, F. *Mol. Microbiol.* **2010,** *75*, 864-873; (b) Fischer, W.; Rosel, P.; Koch, H. U. *J. Bacteriol.* **1981,** *146*, 467-475.

39. (a) Steen, A.; Palumbo, E.; Deghorain, M.; Cocconcelli, P. S.; Delcour, J.; Kuipers, O. P.; Kok, J.; Buist, G.; Hols, P. *J. Bacteriol.* **2005,** *187*, 114-124; (b) Palumbo, E.; Deghorain, M.; Cocconcelli, P. S.; Kleerebezem, M.; Geyer, A.; Hartung, T.; Morath, S.; Hols, P. *J. Bacteriol.* **2006,** *188*, 3709-3715; (c) Biswas, R.; Martinez, R. E.; Gohring, N.; Schlag, M.; Josten, M.; Xia, G.; Hegler, F.; Gekeler, C.; Gleske, A. K.; Gotz, F.; Sahl, H. G.; Kappler, A.; Peschel, A. *PLoS One.* **2012,** *7*, e41415; (d) Peschel, A.; Vuong, C.; Otto, M.; Gotz, F. *Antimicrob. Agents Chemother.* **2000,** *44*, 2845-2847.

40. Calamita, H. G.; Ehringer, W. D.; Koch, A. L.; Doyle, R. J. *Proc Natl Acad Sci U S A.* **2001,** *98*, 15260-15263.

41. Biswas, R.; Voggu, L.; Simon, U. K.; Hentschel, P.; Thumm, G.; Gotz, F. *FEMS Microbiol. Lett.* **2006,** *259*, 260-268.

42. Brown, S.; Santa Maria, J. P.; Walker, S. *Annu Rev Microbiol.* **2013,** *67*, 313-336.

43. (a) Goecks, J.; Nekrutenko, A.; Taylor, J.; Galaxy, T. *Genome Biol.* **2010,** *11*, R86; (b) Blankenberg, D.; Von Kuster, G.; Coraor, N.; Ananda, G.; Lazarus, R.; Mangan, M.; Nekrutenko, A.; Taylor, J. *Curr Protoc Mol Biol.* **2010,** *Chapter 19*, Unit 19 10 11-21; (c) Giardine, B.; Riemer, C.; Hardison, R. C.; Burhans, R.; Elnitski, L.; Shah, P.; Zhang, Y.; Blankenberg, D.; Albert, I.; Taylor, J.; Miller, W.; Kent, W. J.; Nekrutenko, A. *Genome Res.* **2005,** *15*, 1451-1455; (d) Langmead, B.; Trapnell, C.; Pop, M.; Salzberg, S. L. *Genome Biol.* **2009,** *10*, R25.

Chapter 5: Pathway-directed screening is a promising approach for the discovery of new antibacterials and biological probes

A version of this chapter has been published.[1]

High throughput screening has become the primary way in which new antibacterial compounds and chemical probes are discovered.[2] Historically, high throughput assays have been divided into two types: target-based and whole cell. Although target-based assays can work, they are likely best suited for targets that have already been pharmacologically validated through previous discovery of a bioactive natural product or small molecule. For other targets, translating *in vitro* binding to biological activity may be particularly difficult, and the problem may not only be the properties of the compound, but the target itself. As noted, some targets in a pathway appear more druggable than others. Relevant to the pathways described here, several late stage wall teichoic acid inhibitors have been identified using cell-based screening approaches, and every one identified so far inhibits TarG, the transmembrane component of the ABC transporter that exports WTA precursors to the cell surface. TarG would likely not have been chosen as a target for an *in vitro* screen because it is a polytopic membrane protein for which no biochemical assay exists. What makes TarG a more "druggable" target than other proteins in the WTA pathway is unclear, but its membrane location may make it more accessible to compounds than intracellular targets are. It is also possible that TarGH is more sensitive to inhibition because WTA precursor export may be the rate-limiting step in the pathway. In any event, one lesson learned from screening for WTA inhibitors is that success is more likely if a pathway -- rather than a specific target within a pathway -- is targeted. The challenge is to design whole cell screens so that hits are strongly biased towards one, or at most a few, pathways of interest.

Here we have described two ways in which whole cell screens based on growth inhibition can be designed to identify compounds that inhibit predefined pathways. One is by exploiting suppression of bioactivity and the other is by exploiting synthetic lethality. Both strategies involve screening a wildtype and a mutant strain for growth inhibition. Time spent sorting through bioactive compounds for those with desired mechanisms is minimized by excluding all compounds that inhibit growth of both strains (Figure 5.1). This is a crucially important advantage of pathway-directed whole cell screens. For a Δ*tarO* versus wildtype growth inhibition screen, the outcome matrix results in four classes of compounds: 1) non-actives; 2) bioactive compounds having undesired mechanisms or non-specific toxicity; 3) bioactive compounds that are possible late stage wall teichoic acid inhibitors; and 4) bioactive compounds that inhibit a pathway connected through synthetic lethality to wall teichoic acids. In the 230,000 compound screen reported here, we identified approximately 2,000 compounds with biological activity due to all mechanisms, but only two primary hits were identified as new possible WTA inhibitors; another 200 were identified as inhibitors of pathways connected to WTAs. Targocil-II was one of the possible WTA inhibitors that has been confirmed. Of the 200 synthetic lethal hits, three compounds from two different scaffolds were identified as possible Dlt pathway inhibitors through cherry pick testing against a diagnostic panel of strains. One of these hits, named DBI-1, has been identified as a DltB inhibitor. The second scaffold of Dlt pathway inhibitors, DltI-1 and DltI-2, have not been followed up on yet but are likely also on-pathway based on the following lines of evidence: they have the expected growth inhibition profile against the diagnostic panel of strains and DltI-1 was shown to inhibit D-alanylation of lipoteichoic acids in a cell-based biochemical assay. The success of this approach indicates that, when possible, screen design should be pathway based.

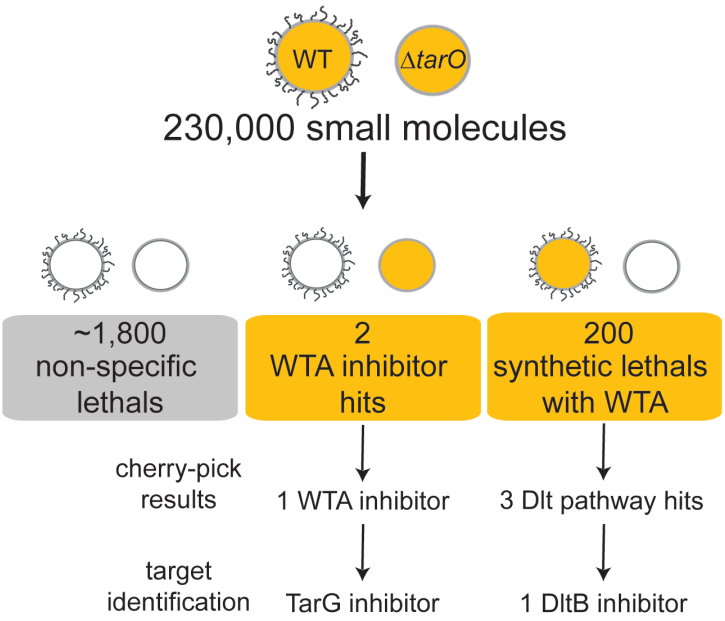

Figure 5.1. Summary of results from a pathway-directed screen of 230,000 small molecules. Approximately 2,000 compounds had some biological activity. Most of these compounds inhibited growth of both wildtype and Δ*tarO S. aureus* and were not considered further. We identified two possible WTA inhibitors, of which one has been confirmed as a new TarG inhibitor and will henceforth be called targocil-II. We identified 200 synthetic lethal compounds and designed a cherry-pick screening panel to sort these compounds into Dlt pathway inhibitors and other types of inhibitors. Of three possible Dlt pathway inhibitors, one has been confirmed as a new Dlt pathway inhibitor.

From our pathway-directed phenotypic screens we have identified multiple inhibitors for the WTA and Dlt pathways. Having inhibitors from more than one scaffold with different chemical properties is extremely beneficial and we are already making use of them. The discovery of a new class of TarGH inhibitors that are much more soluble than the previous generation means we can use this class for experiments we couldn't before, such as: 1) *in vitro* biochemical assays; 2) co-

crystallization with TarGH; and 3) evaluation of pharmacological targeting of WTA pathway *in vivo*. Targocil-II promises to teach us more about TarGH and the WTA pathway, and could be instrumental in the design of inhibitors of other ABC transporters. Likewise, with the discovery of more than one inhibitor for the Dlt pathway, we can now explore interesting *S. aureus* biology. From treating a high-saturated transposon library, we identified the synthetic lethal network of the D-alanylation pathway. Using synthetic lethal relationships and multiple compounds as probes, we: 1) discovered the targets of these inhibitors; 2) provided the genetic context needed to identify the main WTA ligase as LcpA; and 3) raised resistant mutants that gave us insight on genes of unknown function and interesting biology behind the essentiality of LtaS. Amsacrine's eukaryotic toxicity prevented our ability to evaluate the therapeutic potential behind Dlt pathway inhibition *in vivo*, but we have new possibilities with these two new classes. Work is currently underway to determine the therapeutic promise of these new inhibitors.

Can these screening results – the identification of biologically active compounds with on-target activity in a primary screen or at the cherry-pick stage of hit validation – be duplicated for other cases? We are confident that the answer is yes. Advances in genetic and genomic technologies have made it possible to rapidly characterize genetic suppressors of lethal blocks in cellular pathways as well as synthetic lethal interactions between pathways, which in turn enables the design of simple cell-based screens based on an informed understanding of possible outcomes. Reducing the time spent following up on compounds that cannot be developed as therapeutics or have no applications as biological probes is crucial to leveraging the power of high throughput screening. By integrating a sophisticated understanding of biological pathways with simple screening readouts such as differential growth, we have shown that it is possible to rapidly identify multiple biologically active compounds with cellular activity against desired targets.

5.1 References

1. Matano, L. M.; Morris, H. G.; Wood, B. M.; Meredith, T. C.; Walker, S. *Bioorg. Med. Chem.* **2016,** *24*, 6307-6314.

2. (a) Macarron, R.; Banks, M. N.; Bojanic, D.; Burns, D. J.; Cirovic, D. A.; Garyantes, T.; Green, D. V. S.; Hertzberg, R. P.; Janzen, W. P.; Paslay, J. W. *Nat. Rev. Drug Discovery.* **2011,** *10*, 188-195; (b) Castoreno, A. B.; Eggert, U. S. *ACS Chem. Biol.* **2010**.

Appendices

Appendix 1: Matlab code for analyzing high-throughput sequencing data

```
%% Importing and appending excel file to existing file
filename = 'screeninganalysis10_23.mat';

source_dir = 'C:\Users\lmm313\Documents\Harvard\Walker\Screening\Screening matlab\excel files from
Jen';
dest_dir = 'C:\Users\lmm313\Documents\Harvard\Walker\Screening\Screening matlab\excel files formated';
source_files = dir(fullfile(source_dir, '*.xlsx'));
C = length(source_files);

%% Combining data from imported files
G = {C};
num = cell(G{1,1},1);
txt = cell(G{1,1},1);
raw = cell(G{1,1},1);

for i = 1:27
  [num{i},txt{i},raw{i}] = xlsread(fullfile(source_dir, source_files(i).name));
   extractcell = raw{i};
   extractcell8 = extractcell(2:end,1:8);
   extractcelltest = extractcell8;
   mean5 = cell2mat(extractcell8(:,5));
   mean7 = cell2mat(extractcell8(:,7));
   if (i > 1)
       if mean(mean5) > mean(mean7)
           extractcell8 = extractcelltest;
       else
           extractcell8(:,5:6) = extractcelltest(:,7:8);
           extractcell8(:,7:8) = extractcelltest(:,5:6);
       end
   rawdata = vertcat(extractcelltotal, extractcell8);
   elseif i == 1
        if mean(mean5) > mean(mean7)
           extractcell8 = extractcelltest;
       else
           extractcell8(:,5:6) = extractcelltest(:,7:8);
           extractcell8(:,7:8) = extractcelltest(:,5:6);
        end
   extractcelltotal = extractcell8;
   rawdata = extractcelltotal;
   end
   extractcelltotal = rawdata;
  %xlswrite(fullfile(dest_dir, source_files(i).name));
end
%% Removing NaN
%problem is cellfun is looking for a scalar and not a cell. So fh takes
%care of that by coupling isnan and all together. How that works I'm not
%exactly sure but it works
fh = @(x) all(isnan(x(:)));
rawdata(cellfun(fh, rawdata)) = {' '};

%% Removing dark media before removing pos and neg controls - so dark media controls get removed too.
%Dark media – day where cells were grown in darker TSB than usual. This was prevented in the future by
sterile filtering TSB media to avoid variability. Due to the difference in background, these wells were
analyzed separately and then the same Z score was applied as a cut off for hits.
load('Darkwellsindex.mat');

% make an index of the raw data with combined first two columns
   for  jj=1:size(rawdata,1)
    rawdataindex2{jj,1} = [num2str(rawdata{jj,1}),num2str(rawdata{jj,2})]; %for each row, combine the
two columns into 1
   end

%Make an index of the row number of the location of each element in the raw
%dataindex
for j = 1:size(Darkwellsindex,1)
    [truefalsedark2(j),indexdark2(j,1)] = ismember(Darkwellsindex(j),rawdataindex2);
end

%% Move dark data to new matrix, remove from total raw data
```

```
%The dark data was from a day where the media was darker. This was avoided in the future by switching
to sterile-filtered TSB. To evaluate this data, the data from the dark media was analyzed separately
and the same Z-score cutoff was used as the other media days.

indexdark1 = indexdark2(:,1);
dataonlydark = rawdata(indexdark1,:);
rawdatanodark = rawdata;
rawdatanodark(indexdark1,:) = [];
dataonly = rawdatanodark;

%% Removing controls and excludes
Negcontrols = dataonly(strcmp(dataonly(:,3), 'N'), :);
Negcontrolsdark = dataonlydark(strcmp(dataonlydark(:,3), 'N'), :);
Negcontrolstotal = vertcat(Negcontrols,Negcontrolsdark);

Poscontrols = dataonly(strcmp(dataonly(:,3), 'P'), :);
Poscontrolsdark = dataonlydark(strcmp(dataonlydark(:,3), 'P'), :);
Poscontrolstotal = vertcat(Poscontrols,Poscontrolsdark);
datacontroltotalall = vertcat(Negcontrolstotal,Poscontrolstotal);

rawdataD = dataonly(strcmp(dataonly(:,3), 'D'), :);
rawdataDdark = dataonlydark(strcmp(dataonlydark(:,3), 'D'), :);

rawdataX = dataonly(strcmp(dataonly(:,3), 'X'), :);
rawdataXdark = dataonlydark(strcmp(dataonlydark(:,3), 'X'), :);

rawdataE = dataonly(strcmp(dataonly(:,3), 'E'), :);
rawdataEdark = dataonlydark(strcmp(dataonlydark(:,3), 'E'), :);
rawdataEtotal = vertcat(rawdataE,rawdataEdark);

rawdataYes = dataonly(strcmp(dataonly(:,4), 'Yes'), :);
rawdataYesdark = dataonlydark(strcmp(dataonlydark(:,4), 'Yes'), :);
rawdataXYes = rawdataX(strcmp(rawdataX(:,4), 'Yes'),:);
rawdataXYesdark = rawdataXdark(strcmp(rawdataXdark(:,4), 'Yes'),:);
rawdataXYestotal = vertcat(rawdataXYes, rawdataXYesdark);
rawdataXnoYes = rawdataX;
rawdataXnoYesdark = rawdataXdark;
rawdataXnoYes(strcmp(rawdataXnoYes(:,4), 'Yes'),:) = [];
rawdataXnoYesdark(strcmp(rawdataXnoYesdark(:,4), 'Yes'),:) = [];
dataonlytotal = rawdataXnoYes;
dataonlydarktotal = rawdataXnoYesdark;
%% check to make sure all wells are accounted for - final row number of datatotal should be the same as
dataonly
datatotal = vertcat(Negcontrols,Poscontrols,rawdataE,rawdataX,rawdataD);
save(filename);
%% Convert cell to matrix to perform operations
rawdata1181 = cell2mat(dataonlytotal(:,5:6));
rawdata1181dark = cell2mat(dataonlydarktotal(:,5:6));
rawdata1183 = cell2mat(dataonlytotal(:,7:8));
rawdata1183dark = cell2mat(dataonlydarktotal(:,7:8));

%% Data analysis
%Data analysis of newly added data sets
[mean1181] = mean(rawdata1181,2);
[mean1181dark] = mean(rawdata1181dark,2);
[std1181] = std(rawdata1181,0,2);
[std1181dark] = std(rawdata1181dark,0,2);
[mean1183] = mean(rawdata1183,2);
[mean1183dark] = mean(rawdata1183dark,2);
[std1183] = std(rawdata1183,0,2);
[std1183dark] = std(rawdata1183dark,0,2);
%Combine above data
[stdmeandata] = horzcat(mean1181, mean1183, std1181, std1183);
[stdmeandatadark] = horzcat(mean1181dark, mean1183dark, std1181dark, std1183dark);
%paste appropriate collumns into a cell for filtering:
indexstdmeandata = [dataonlytotal, num2cell(stdmeandata)]; %well/plate, type, exclude,
1181_A,1181_B,1183_A,1183_B,Mean1181,mean1183,std1181,std1183
indexstdmeandatadark = [dataonlydarktotal, num2cell(stdmeandatadark)];

%% separating data versus wells for analysis for controls
datacontroltotal = vertcat(Negcontrols, Poscontrols); %datacontrols3265, datacontrols3295);
datacontroldark = vertcat(Negcontrolsdark,Poscontrolsdark);
rawdatacontrols = cell2mat(datacontroltotal(:,5:8));
rawdatacontrolsdark = cell2mat(datacontroldark(:,5:8));
screeningwellscontrols = datacontroltotal(:,1);
screeningwellscontrolsdark = datacontroldark(:,1);
%Control data analysis
[meancontrols1181] = mean(rawdatacontrols(:,1:2),2);
```

```
[meancontrols1181dark] = mean(rawdatacontrolsdark(:,1:2),2);
[stdcontrols1181] = std(rawdatacontrols(:,1:2),0,2);
[stdcontrols1181dark] = std(rawdatacontrolsdark(:,1:2),0,2);
[meancontrols1183] = mean(rawdatacontrols(:,3:4),2);
[meancontrols1183dark] = mean(rawdatacontrolsdark(:,3:4),2);
[stdcontrols1183] = std(rawdatacontrols(:,3:4),0,2);
[stdcontrols1183dark] = std(rawdatacontrolsdark(:,3:4),0,2);
%% Combine above data with the plate/well numbers for filtering
[stdmeancontrols] = horzcat(meancontrols1181, meancontrols1183, stdcontrols1181, stdcontrols1183);
[stdmeancontrolsdark] = horzcat(meancontrols1181dark, meancontrols1183dark, stdcontrols1181dark,
stdcontrols1183dark);
indexstdmeancontrols = [datacontroltotal, num2cell(stdmeancontrols)];
indexstdmeancontrolsdark = [datacontroldark, num2cell(stdmeancontrolsdark)];

%% Filter out samples with a std greater than 0.25
Filteredindexdata = indexstdmeandata([indexstdmeandata{:,11}] < 0.25 & [indexstdmeandata{:,12}] <
0.25,:); %Both WT and tarO samples std <0.25
Filteredindexdatadark = indexstdmeandatadark([indexstdmeandatadark{:,11}] < 0.25 &
[indexstdmeandatadark{:,12}] < 0.25,:);
Filteredindexcontrols = indexstdmeancontrols([indexstdmeancontrols{:,11}] < 0.25 &
[indexstdmeancontrols{:,12}] < 0.25,:);
Filteredindexcontrolsdark = indexstdmeancontrolsdark([indexstdmeancontrolsdark{:,11}] < 0.25 &
[indexstdmeancontrolsdark{:,12}] < 0.25,:);
%Make master lists
Filteredindexdata8_12 = Filteredindexdata;
Filteredindexdatadark8_12 = Filteredindexdatadark;
masterlistindex8_12 = Filteredindexdata8_12;
masterlistindex8_12dark = Filteredindexdatadark8_12;
Filteredindexcontrols8_12 = Filteredindexcontrols;
Filteredindexcontrolsdark8_12 = Filteredindexcontrolsdark;
masterlistindexcontrols8_12 = Filteredindexcontrols8_12;
masterlistindexcontrolsdark8_12 = Filteredindexcontrolsdark8_12;

%% Set aside std > 0.25 for annotation
HighStdindexdata = indexstdmeandata([indexstdmeandata{:,11}] >= 0.25 | [indexstdmeandata{:,12}] >=
0.25,:); %Both WT and tarO samples std <0.25
HighStdindexdatadark = indexstdmeandatadark([indexstdmeandatadark{:,11}] >= 0.25 |
[indexstdmeandatadark{:,12}] >= 0.25,:); %Both WT and tarO samples std <0.25
HighStdindexcontrols = indexstdmeancontrols([indexstdmeancontrols{:,11}] >= 0.25 |
[indexstdmeancontrols{:,12}] >= 0.25,:);
HighStdindexcontrolsdark = indexstdmeancontrolsdark([indexstdmeancontrolsdark{:,11}] >= 0.25 |
[indexstdmeancontrolsdark{:,12}] >= 0.25,:);
HighStdindexcontrolstotal = vertcat(HighStdindexcontrols,HighStdindexcontrolsdark);
HighStdindexdatatotal = vertcat(HighStdindexdata,HighStdindexdatadark);
%% Ploting points
%Plot controls to get line of best fit
Xcontrols = cell2mat(masterlistindexcontrols8_12(:, 9)); %convert to matrices so I can perform
operations
Ycontrols = cell2mat(masterlistindexcontrols8_12(:, 10));

%Plot X&Y controls
close all;
figure;
hold on;
scatter(Xcontrols,Ycontrols);
p = polyfit(Xcontrols, Ycontrols,1);
r = p(1).* Xcontrols + p(2);
plot(Xcontrols, r,'-','linewidth', 2);
hold off;
m = p(1,1);
bfit = p(1,2);

%%
Xcontrolsdark = cell2mat(masterlistindexcontrolsdark8_12(:,9));
Ycontrolsdark = cell2mat(masterlistindexcontrolsdark8_12(:,10));
%Plot X&Y controls
close all;
figure;
hold on;
scatter(Xcontrolsdark,Ycontrolsdark);
pdark = polyfit(Xcontrolsdark, Ycontrolsdark,1);
rdark = pdark(1).* Xcontrolsdark + pdark(2);
plot(Xcontrolsdark, rdark,'-','linewidth', 2);
hold off;
mdark = pdark(1,1);
bfitdark = pdark(1,2);

%% Find X and Y intercepts of line perpendicular to line of best fit going
```

```
%through point
%line y = mx + b

%convert X and Y data to matrices
Xdata = cell2mat(masterlistindex8_12(:,9));
Xdatadark = cell2mat(masterlistindex8_12dark(:,9));
Ydata = cell2mat(masterlistindex8_12(:,10));
Ydatadark = cell2mat(masterlistindex8_12dark(:,10));

%Calculate line through point
bvalues = Ydata + (1/m).*Xdata;
bvaluesdark = Ydatadark + (1/mdark).*Xdatadark;
Xintercepts = (bvalues - bfit)./(m+(1/m));
Xinterceptsdark = (bvaluesdark - bfitdark)./(mdark + (1/mdark));
Yintercepts = m.*Xintercepts + bfit;
Yinterceptsdark = mdark.*Xinterceptsdark + bfitdark;

%Distance between two points
distances = sqrt((Xintercepts-Xdata).^2 + (Yintercepts - Ydata).^2);
distancesdark = sqrt((Xinterceptsdark-Xdatadark).^2 + (Yinterceptsdark - Ydatadark).^2);

%% Correct distances based on above or below the line
[a,b] = size(Ydata);
[c,d] = size(Ydatadark);

distancecorrect = a:1; %this number needs to be changed with the addition of more compounds otherwise
the distance numbers will be wrong
for n = 1:a
    if Ydata(n,1) < Yintercepts(n,1); %if the Y coordinate is less than the calculated Y intercept,
distance remains +
        distancecorrect(n,1) = distances(n,1);
    else
        distancecorrect(n,1) = -1.*distances(n,1);
    end
end

distancecorrectdark = c:1; %this number needs to be changed with the addition of more compounds
otherwise the distance numbers will be wrong
for nn = 1:c
    if Ydatadark(nn,1) < Yinterceptsdark(nn,1); %if the Y coordinate is less than the calculated Y
intercept, distance remains +
        distancecorrectdark(nn,1) = distancesdark(nn,1);
    else
        distancecorrectdark(nn,1) = -1.*distancesdark(nn,1);
    end
end
%% Plot points, controls and line without Zscores
close all;
figure;
hold on;
scatter(Xdata, Ydata,'b');
scatter(Xcontrols,Ycontrols,'c');
plot(Xcontrols, r,'-k');
hold off;
%close all;

%% Plot points, controls and line without Zscores dark
close all;
figure;
hold on;
scatter(Xdatadark, Ydatadark,'b');
scatter(Xcontrolsdark,Ycontrolsdark,'c');
plot(Xcontrolsdark, rdark,'-k');
hold off;
%close all;

%% Determining lethals
%%Determining lethal compounds cut off
Filteredmean1181 = cell2mat(masterlistindex8_12(:,9));
Filteredmean1181dark = cell2mat(masterlistindex8_12dark(:,9));
Filteredmean1183 = cell2mat(masterlistindex8_12(:,10));
Filteredmean1183dark = cell2mat(masterlistindex8_12dark(:,10));
AvOD1181 = mean(Filteredmean1181);
AvOD1181dark = mean(Filteredmean1181dark);
AvOD1183 = mean(Filteredmean1183);
AvOD1183dark = mean(Filteredmean1183dark);
%%
```

```
A_1181 = 0.2*AvOD1181;
A_1181dark = 0.2*AvOD1181dark;
A_1183 = 0.2*AvOD1183;
A_1183dark = 0.2*AvOD1183dark;

%% Plot lethals
Lethals20 = masterlistindex8_12([masterlistindex8_12{:,9}] < A_1181 & [masterlistindex8_12{:,10}] <
A_1183,:);
Lethals20dark = masterlistindex8_12dark([masterlistindex8_12dark{:,9}] < A_1181dark &
[masterlistindex8_12dark{:,10}] < A_1183dark,:);

close all;
figure;
hold on;
x81 = [A_1181,A_1181];
y81 = [0,1];
x83 = [0,1.2];
y83 = [A_1183,A_1183];
LethalsX = cell2mat(Lethals20(:,9));
LethalsY = cell2mat(Lethals20(:,10));
scatter(Xdata, Ydata,'b');
scatter(LethalsX,LethalsY,'k');
title('Cell Wall Small Molecule Screen Lethals');
xlabel('S. aureus Newman WT OD600');
ylabel('S. aureus Newman tarO OD600');
plot(x81,y81,'k',x83,y83,'k');
legend('All Compounds', 'Lethals');
saveas(gcf,'Lethals20_8_17.png')
hold off;

%% Plot dark lethals
close all;
figure;
hold on;
x81dark = [A_1181dark,A_1181dark];
y81dark = [0,1];
x83dark = [0,1.2];
y83dark = [A_1183dark,A_1183dark];
LethalsXdark = cell2mat(Lethals20dark(:,9));
LethalsYdark = cell2mat(Lethals20dark(:,10));
scatter(Xdatadark,Ydatadark,'b');
scatter(LethalsXdark,LethalsYdark,'k');
title('Lethals Dark Media');
xlabel('S. aureus Newman WT OD600');
ylabel('S. aureus Newman \DeltatarO OD600');
plot(x81dark,y81dark,'k',x83dark,y83dark,'k');
legend('All Compounds', 'Lethals');
hold off;
%% Summing up all Lethals for regular and dark
Lethalstotal20 = vertcat(Lethals20,Lethals20dark);
filenamelethals = 'Lethals20';
xlswrite(filenamelethals,Lethalstotal20);


%% Finding Zscore and generating a list of top scores negative and positive
stddistance = std(distancecorrect);
stddistancedark = std(distancecorrectdark);
Zscore = distancecorrect./stddistance;
Zscoredark = distancecorrectdark./stddistancedark;

%Put in Zscore column into Filteredindexdata so we can filter and find hits
Zscoreindexdata = [masterlistindex8_12, num2cell(Zscore), num2cell(distancecorrect)];
Zscoreindexdatadark = [masterlistindex8_12dark, num2cell(Zscoredark), num2cell(distancecorrectdark)];
Zscoreindexdatacomment = Zscoreindexdata;
Zscoreindexdatacomment(:,11) = {' '};
Zscoreindexdatadarkcomment = Zscoreindexdatadark;
Zscoreindexdatadarkcomment(:,11) = {'Higher absorbance due to darker media'};
Zscoreindexdatatotal = vertcat(Zscoreindexdata,Zscoreindexdatadark);
Zscoreindexdatatotalcomment = vertcat(Zscoreindexdatacomment,Zscoreindexdatadarkcomment);

%% Zscore back calculate to confirm
%Z3_5 = 3.5;
%Distance3_5 = Z3_5./stddistance;
%Zscorepoint3_5 = Zscoreindexdata([Zscoreindexdata{:,13}] == 3.5,:);
%ZscorehitsTarOsort2 = sortrows(ZscorehitsTarOlethal,-13);
```

```
%% Filter based on Zscore and sort the rows high to low
ZscorehitsTarO = Zscoreindexdata([Zscoreindexdata{:,13}] >= 3.5,:); %Zscore greater than 5
ZscorehitsTarOdark = Zscoreindexdatadark([Zscoreindexdatadark{:,13}] >= 3.5,:);
ZscorehitsTarOlethal = ZscorehitsTarO([ZscorehitsTarO{:,10}] <= 2*A_1183,:); %remove hits with high
tarO OD
ZscorehitsTarOlethaldark = ZscorehitsTarOdark([ZscorehitsTarOdark{:,10}] <= 2*A_1183,:); %remove hits
with high tarO OD
ZscorehitsTarOsort = sortrows(ZscorehitsTarOlethal,-13); %- sign will sort high to low
ZscorehitsTarOsortdark = sortrows(ZscorehitsTarOlethaldark,-13);

%ZscoreODlow = ZscorehitsTarOsort_3_5([ZscorehitsTarOsort_3_5{:,3}] <= 0.1,:);
ZscorehitsWT = Zscoreindexdata([Zscoreindexdata{:,13}] <= -3.5,:); %Zscore less than 3.5
ZscorehitsWTdark = Zscoreindexdatadark([Zscoreindexdatadark{:,13}] <= -3.5,:); %Zscore less than 5
ZscorehitsWTlethal = ZscorehitsWT([ZscorehitsWT{:,9}] <= 1.5*A_1181,:); %remove hits with high WT OD
ZscorehitsWTlethaldark = ZscorehitsWTdark([ZscorehitsTarOdark{:,9}] <= 1.5*A_1181,:);
ZscorehitsWTsort = sortrows(ZscorehitsWTlethal,13); %no negative sign, will sort lowest first

%% Combine Hits from dark, save
filename3 = 'ZscorehitsTarO8_17_final';
ZscorehitsTarOtotal = sortrows(vertcat(ZscorehitsTarOsort,ZscorehitsTarOsortdark));
xlswrite(filename3,ZscorehitsTarOtotal);

filename5 = 'ZscorehitsWT_8_17_final';
ZscorehitsWTtotal = sortrows(ZscorehitsWTsort); %Checked – there are no hits in dark media, so I did
not need to combine the two.
xlswrite(filename5,ZscorehitsWTtotal);

%% Save work
%filename = 'screeninganalysis';
%save(filename);
save(strrep(date,'-','_')); %saves matlab file with current date
%% Save cherrypicks lethal and otherwise in a new file
filename6 = 'cherrypicksfinal8_17';
save(filename6, 'Lethalstotal20', 'ZscorehitsTarOtotal', 'ZscorehitsWTtotal');
```

Appendix 2: Cherry-picked hits from pathway-directed high-throughput screen at ICCB-L

Table A2.1 Cherry-picked hits from screens 1181/1183. Hits were classified based on strong (S), weak (W) and medium (M) based off Z score. Screens were numbered 1181 (for the wild-type Newman *S. aureus* strain) and 1183 (for the Newman Δ*tarO* strain). "Lethal for 1181 and 1183" means killing of both strains, "hit for 1183" means only killing of the Δ*tarO* strain, and "hit for 1181" means only killing of the wild-type strain.

Stock ID	Well	Positive	Cherry Pick	Comments
Plate_0533	E13	S	C	Lethal for 1181 and 1183
Plate_0534	C05	S	C	Lethal for 1181 and 1183
Plate_0534	C17	S	C	Lethal for 1181 and 1183
Plate_0535	C11	S	C	Hit for 1183
Plate_0535	D21	S	C	Lethal for 1181 and 1183
Plate_0539	I04	W	C	Hit for 1183
Plate_0539	L14	W	C	Hit for 1183
Plate_0540	P12	S	C	Lethal for 1181 and 1183
Plate_0540	P16	S	C	Lethal for 1181 and 1183
Plate_0590	I14	S	C	Lethal for 1181 and 1183
Plate_0601	D10	S	C	Lethal for 1181 and 1183
Plate_0608	F15	W	C	Hit for 1183
Plate_0608	N09	S	C	Lethal for 1181 and 1183
Plate_0614	F14	W	C	Hit for 1183
Plate_0614	J14	M	C	Hit for 1183
Plate_0614	P18	S	C	Lethal for 1181 and 1183
Plate_0616	J12	S	C	Lethal for 1181 and 1183
Plate_0617	N18	S	C	Lethal for 1181 and 1183
Plate_0618	D11	S	C	Hit for 1183
Plate_0619	H17	W	C	Hit for 1183
Plate_0620	F11	S	C	Lethal for 1181 and 1183
Plate_0620	K12	S	C	Lethal for 1181 and 1183
Plate_0640	B17	M	C	Hit for 1183
Plate_0641	I05	S	C	Lethal for 1181 and 1183
Plate_0642	D18	S	C	Lethal for 1181 and 1183
Plate_0642	E13	S	C	Lethal for 1181 and 1183
Plate_0642	G13	S	C	Lethal for 1181 and 1183
Plate_0642	I13	S	C	Lethal for 1181 and 1183
Plate_0642	K13	S	C	Lethal for 1181 and 1183

Plate_0642	P12	S	C	Lethal for 1181 and 1183
Plate_0645	C19	S	C	Lethal for 1181 and 1183
Plate_0646	B11	M	C	Hit for 1183
Plate_0652	D17	S	C	Hit for 1183
Plate_0652	F17	S	C	Hit for 1183
Plate_0652	G19	S	C	Lethal for 1181 and 1183
Plate_0652	J15	S	C	Hit for 1183
Plate_0652	N13	S	C	Hit for 1183
Plate_0653	H13	S	C	Lethal for 1181 and 1183
Plate_0653	L22	S	C	Lethal for 1181 and 1183
Plate_0657	A20	M	C	Hit for 1183
Plate_0657	E09	S	C	Lethal for 1181 and 1183
Plate_0657	J04	S	C	Lethal for 1181 and 1183
Plate_0664	D11	M	C	Hit for 1183
Plate_0666	H08	W	C	Hit for 1183
Plate_0667	B06	S	C	Lethal for 1181 and 1183
Plate_0667	D10	S	C	Lethal for 1181 and 1183
Plate_0667	F22	S	C	Lethal for 1181 and 1183
Plate_0668	B18	S	C	Lethal for 1181 and 1183
Plate_1364	I10	M	C	Hit for 1183
Plate_1364	N13	S	C	Lethal for 1181 and 1183
Plate_1366	K17	M	C	Hit for 1183
Plate_1367	J11	S	C	Lethal for 1181 and 1183
Plate_1367	P22	S	C	Lethal for 1181 and 1183
Plate_1394	D13	M	C	Hit for 1183
Plate_1397	L19	S	C	Lethal for 1181 and 1183
Plate_1398	E03	S	C	Lethal for 1181 and 1183
Plate_1400	G12	S	C	Lethal for 1181 and 1183
Plate_1407	N22	W	C	Hit for 1183
Plate_1408	G01	S	C	Hit for 1183
Plate_1408	L13	S	C	Lethal for 1181 and 1183
Plate_1410	E04	M	C	Hit for 1183
Plate_1413	C19	S	C	Lethal for 1181 and 1183
Plate_1413	D15	S	C	Lethal for 1181 and 1183
Plate_1413	F10	S	C	Lethal for 1181 and 1183
Plate_1414	C08	S	C	Lethal for 1181 and 1183
Plate_1414	E09	W	C	Hit for 1183
Plate_1415	L16	S	C	Lethal for 1181 and 1183
Plate_1417	F02	S	C	Lethal for 1181 and 1183
Plate_1421	C14	S	C	Lethal for 1181 and 1183
Plate_1421	E15	S	C	Hit for 1183

Plate_1421	F17	S	C	Lethal for 1181 and 1183
Plate_1421	I14	S	C	Lethal for 1181 and 1183
Plate_1421	K14	S	C	Lethal for 1181 and 1183
Plate_1423	D16	S	C	Lethal for 1181 and 1183
Plate_1425	D21	S	C	Lethal for 1181 and 1183
Plate_1426	F20	S	C	Lethal for 1181 and 1183
Plate_1427	L08	S	C	Lethal for 1181 and 1183
Plate_1429	L04	S	C	Lethal for 1181 and 1183
Plate_1430	I17	S	C	Lethal for 1181 and 1183
Plate_1432	M09	S	C	Lethal for 1181 and 1183
Plate_1434	I16	S	C	Lethal for 1181 and 1183
Plate_1434	J12	S	C	Lethal for 1181 and 1183
Plate_1434	K16	S	C	Lethal for 1181 and 1183
Plate_1435	K05	S	C	Lethal for 1181 and 1183
Plate_1437	G19	M	C	Hit for 1181
Plate_1439	C09	S	C	Lethal for 1181 and 1183
Plate_1439	G19	S	C	Lethal for 1181 and 1183
Plate_1441	G08	S	C	Lethal for 1181 and 1183
Plate_1441	L01	S	C	Lethal for 1181 and 1183
Plate_1443	J12	S	C	Lethal for 1181 and 1183
Plate_1443	K19	S	C	Lethal for 1181 and 1183
Plate_1444	E05	S	C	Lethal for 1181 and 1183
Plate_1446	J21	S	C	Lethal for 1181 and 1183
Plate_1446	L01	S	C	Lethal for 1181 and 1183
Plate_1446	N16	S	C	Lethal for 1181 and 1183
Plate_1447	A19	S	C	Lethal for 1181 and 1183
Plate_1448	K13	S	C	Lethal for 1181 and 1183
Plate_1449	H08	S	C	Lethal for 1181 and 1183
Plate_1449	J18	S	C	Lethal for 1181 and 1183
Plate_1450	H21	S	C	Lethal for 1181 and 1183
Plate_1459	M11	S	C	Lethal for 1181 and 1183
Plate_1459	P05	W	C	Hit for 1183
Plate_1473	J15	S	C	Lethal for 1181 and 1183
Plate_1473	O05	S	C	Lethal for 1181 and 1183
Plate_1474	F07	S	C	Lethal for 1181 and 1183
Plate_1474	F10	S	C	Lethal for 1181 and 1183
Plate_1474	N10	S	C	Lethal for 1181 and 1183
Plate_1474	N11	S	C	Lethal for 1181 and 1183
Plate_1475	B09	S	C	Lethal for 1181 and 1183
Plate_1475	O05	M	C	Hit for 1183
Plate_1476	A18	M	C	Hit for 1183

Plate_1476	N10	S	C	Lethal for 1181 and 1183
Plate_1476	P09	S	C	Lethal for 1181 and 1183
Plate_1476	P10	S	C	Hit for 1181
Plate_1477	M05	S	C	Lethal for 1181 and 1183
Plate_1477	O18	S	C	Lethal for 1181 and 1183
Plate_1479	G14	S	C	Lethal for 1181 and 1183
Plate_1479	J11	S	C	Hit for 1183
Plate_1480	E12	S	C	Lethal for 1181 and 1183
Plate_1481	N11	S	C	Lethal for 1181 and 1183
Plate_1482	A07	S	C	Lethal for 1181 and 1183
Plate_1482	E19	S	C	Lethal for 1181 and 1183
Plate_1482	K02	W	C	Hit for 1183
Plate_1483	D20	S	C	Lethal for 1181 and 1183
Plate_1484	E16	S	C	Lethal for 1181 and 1183
Plate_1484	I08	S	C	Lethal for 1181 and 1183
Plate_1484	J19	M	C	Hit for 1183
Plate_1484	O12	S	C	Lethal for 1181 and 1183
Plate_1484	P04	S	C	Lethal for 1181 and 1183
Plate_1485	C11	S	C	Lethal for 1181 and 1183
Plate_1485	C22	S	C	Lethal for 1181 and 1183
Plate_1486	B13	S	C	Lethal for 1181 and 1183
Plate_1486	H11	M	C	Hit for 1183
Plate_1486	L11	W	C	Hit for 1183
Plate_1486	P02	S	C	Hit for 1183
Plate_1487	J21	W	C	Hit for 1183
Plate_1489	B15	S	C	Lethal for 1181 and 1183
Plate_1490	H19	S	C	Lethal for 1181 and 1183
Plate_1490	I12	S	C	Lethal for 1181 and 1183
Plate_1492	P06	S	C	Lethal for 1181 and 1183
Plate_1493	A08	S	C	Hit for 1183
Plate_1493	B19	S	C	Lethal for 1181 and 1183
Plate_1493	C06	S	C	Lethal for 1181 and 1183
Plate_1493	D11	S	C	Lethal for 1181 and 1183
Plate_1493	F10	S	C	Lethal for 1181 and 1183
Plate_1494	I18	S	C	Lethal for 1181 and 1183
Plate_1494	K18	S	C	Lethal for 1181 and 1183
Plate_1495	H12	S	C	Hit for 1183
Plate_1496	C11	S	C	Lethal for 1181 and 1183
Plate_1496	I18	M	C	Hit for 1183
Plate_1505	F10	S	C	Hit for 1183
Plate_1509	B21	S	C	Lethal for 1181 and 1183

Plate_1509	F07	S	C	Lethal for 1181 and 1183
Plate_1510	I08	S	C	Lethal for 1181 and 1183
Plate_1511	L15	S	C	Lethal for 1181 and 1183
Plate_1511	M21	S	C	Lethal for 1181 and 1183
Plate_1512	F04	S	C	Hit for 1183
Plate_1513	N01	W	C	Hit for 1183
Plate_1514	B01	S	C	Hit for 1181
Plate_1514	M10	S	C	Lethal for 1181 and 1183
Plate_1515	D07	S	C	Lethal for 1181 and 1183
Plate_1515	N16	S	C	Lethal for 1181 and 1183
Plate_1517	K09	S	C	Lethal for 1181 and 1183
Plate_1517	L18	S	C	Lethal for 1181 and 1183
Plate_1519	O05	S	C	Lethal for 1181 and 1183
Plate_1520	J17	S	C	Lethal for 1181 and 1183
Plate_1520	P12	S	C	Lethal for 1181 and 1183
Plate_1521	B11	S	C	Lethal for 1181 and 1183
Plate_1521	C09	S	C	Lethal for 1181 and 1183
Plate_1521	F03	S	C	Lethal for 1181 and 1183
Plate_1521	O06	S	C	Lethal for 1181 and 1183
Plate_1522	A12	M	C	Hit for 1183
Plate_1522	B06	S	C	Lethal for 1181 and 1183
Plate_1522	C16	S	C	Lethal for 1181 and 1183
Plate_1522	H06	S	C	Lethal for 1181 and 1183
Plate_1522	H19	S	C	Lethal for 1181 and 1183
Plate_1522	J06	S	C	Lethal for 1181 and 1183
Plate_1522	L14	S	C	Lethal for 1181 and 1183
Plate_1523	C18	S	C	Lethal for 1181 and 1183
Plate_1523	J13	S	C	Lethal for 1181 and 1183
Plate_1523	P02	S	C	Lethal for 1181 and 1183
Plate_1524	A21	S	C	Lethal for 1181 and 1183
Plate_1524	M08	S	C	Lethal for 1181 and 1183
Plate_1525	M08	S	C	Lethal for 1181 and 1183
Plate_1526	C08	S	C	Lethal for 1181 and 1183
Plate_1526	M14	S	C	Lethal for 1181 and 1183
Plate_1527	C16	S	C	Lethal for 1181 and 1183
Plate_1527	F09	S	C	Lethal for 1181 and 1183
Plate_1527	M05	S	C	Lethal for 1181 and 1183
Plate_1527	M15	S	C	Lethal for 1181 and 1183
Plate_1528	F20	S	C	Lethal for 1181 and 1183
Plate_1528	J16	S	C	Lethal for 1181 and 1183
Plate_1528	M04	S	C	Lethal for 1181 and 1183

Plate_1528	M10	S	C	Lethal for 1181 and 1183
Plate_1528	N02	S	C	Lethal for 1181 and 1183
Plate_1528	O04	S	C	Lethal for 1181 and 1183
Plate_1529	A14	S	C	Lethal for 1181 and 1183
Plate_1529	A20	S	C	Lethal for 1181 and 1183
Plate_1529	C12	S	C	Lethal for 1181 and 1183
Plate_1529	C17	S	C	Lethal for 1181 and 1183
Plate_1529	I03	S	C	Lethal for 1181 and 1183
Plate_1529	O14	S	C	Lethal for 1181 and 1183
Plate_1530	C20	S	C	Lethal for 1181 and 1183
Plate_1530	D09	S	C	Lethal for 1181 and 1183
Plate_1530	F09	S	C	Lethal for 1181 and 1183
Plate_1530	F16	S	C	Lethal for 1181 and 1183
Plate_1530	H22	S	C	Lethal for 1181 and 1183
Plate_1530	N13	S	C	Lethal for 1181 and 1183
Plate_1531	B09	S	C	Lethal for 1181 and 1183
Plate_1531	I02	S	C	Lethal for 1181 and 1183
Plate_1531	I08	S	C	Lethal for 1181 and 1183
Plate_1532	B03	S	C	Lethal for 1181 and 1183
Plate_1532	D18	S	C	Lethal for 1181 and 1183
Plate_1532	D19	S	C	Lethal for 1181 and 1183
Plate_1532	L07	S	C	Lethal for 1181 and 1183
Plate_1532	N07	S	C	Lethal for 1181 and 1183
Plate_1533	D19	S	C	Lethal for 1181 and 1183
Plate_1533	G08	S	C	Lethal for 1181 and 1183
Plate_1534	A16	W	C	Hit for 1183
Plate_1535	K09	S	C	Hit for 1183
Plate_1536	P09	S	C	Lethal for 1181 and 1183
Plate_1537	A04	S	C	Lethal for 1181 and 1183
Plate_1537	A11	S	C	Lethal for 1181 and 1183
Plate_1537	C11	S	C	Lethal for 1181 and 1183
Plate_1537	D18	M	C	Hit for 1183
Plate_1537	O17	S	C	Lethal for 1181 and 1183
Plate_1538	F15	S	C	Lethal for 1181 and 1183
Plate_1538	J15	M	C	Hit for 1183
Plate_1538	O19	S	C	Lethal for 1181 and 1183
Plate_1539	F08	S	C	Lethal for 1181 and 1183
Plate_1539	I03	M	C	Hit for 1183
Plate_1539	J20	S	C	Lethal for 1181 and 1183
Plate_1539	K04	S	C	Lethal for 1181 and 1183
Plate_1539	M05	S	C	Lethal for 1181 and 1183

Plate_1540	B20	S	C	Lethal for 1181 and 1183
Plate_1540	I04	S	C	Lethal for 1181 and 1183
Plate_1543	J06	S	C	Lethal for 1181 and 1183
Plate_1543	J21	S	C	Lethal for 1181 and 1183
Plate_1543	L02	S	C	Lethal for 1181 and 1183
Plate_1544	A03	S	C	Lethal for 1181 and 1183
Plate_1544	F05	S	C	Lethal for 1181 and 1183
Plate_1544	J07	M	C	Hit for 1183
Plate_1545	H17	S	C	Lethal for 1181 and 1183
Plate_1546	B18	S	C	Lethal for 1181 and 1183
Plate_1546	H16	S	C	Lethal for 1181 and 1183
Plate_1548	D20	S	C	Lethal for 1181 and 1183
Plate_1548	F05	S	C	Lethal for 1181 and 1183
Plate_1548	M18	S	C	Lethal for 1181 and 1183
Plate_1549	B16	S	C	Lethal for 1181 and 1183
Plate_1549	C13	S	C	Lethal for 1181 and 1183
Plate_1549	N22	S	C	Lethal for 1181 and 1183
Plate_1550	K16	S	C	Lethal for 1181 and 1183
Plate_1551	E06	W	C	Hit for 1183
Plate_1551	F14	S	C	Lethal for 1181 and 1183
Plate_1552	D01	S	C	Lethal for 1181 and 1183
Plate_1552	D13	S	C	Lethal for 1181 and 1183
Plate_1552	O17	S	C	Lethal for 1181 and 1183
Plate_1553	P13	S	C	Lethal for 1181 and 1183
Plate_1554	I07	S	C	Lethal for 1181 and 1183
Plate_1556	A09	M	C	Hit for 1183
Plate_1557	G09	S	C	Lethal for 1181 and 1183
Plate_1558	E05	S	C	Lethal for 1181 and 1183
Plate_1607	F05	S	C	Lethal for 1181 and 1183
Plate_1610	J15	S	C	Lethal for 1181 and 1183
Plate_1612	C20	S	C	Lethal for 1181 and 1183
Plate_1612	M07	W	C	Hit for 1183
Plate_1613	E05	S	C	Lethal for 1181 and 1183
Plate_1613	F06	S	C	Lethal for 1181 and 1183
Plate_1615	A13	S	C	Lethal for 1181 and 1183
Plate_1615	E19	W	C	Hit for 1183
Plate_1616	B09	S	C	Lethal for 1181 and 1183
Plate_1616	M11	M	C	Hit for 1183
Plate_1618	A11	M	C	Hit for 1183
Plate_1618	K12	M	C	Hit for 1183
Plate_1620	O01	S	C	Lethal for 1181 and 1183

Plate_1632	E08	M	C	Hit for 1183
Plate_1634	E03	W	C	Hit for 1183
Plate_1634	H15	S	C	Lethal for 1181 and 1183
Plate_1638	H05	S	C	Lethal for 1181 and 1183
Plate_1639	B02	S	C	Lethal for 1181 and 1183
Plate_1639	P09	S	C	Lethal for 1181 and 1183
Plate_1642	I02	M	C	Hit for 1183
Plate_1646	J15	S	C	Hit for 1183
Plate_1647	P06	M	C	Hit for 1183
Plate_1649	O18	W	C	Hit for 1181
Plate_1649	O19	S	C	Lethal for 1181 and 1183
Plate_1650	C01	S	C	Lethal for 1181 and 1183
Plate_1650	K01	S	C	Lethal for 1181 and 1183
Plate_1650	M01	S	C	Lethal for 1181 and 1183
Plate_1652	N01	S	C	Hit for 1181
Plate_1653	K10	S	C	Lethal for 1181 and 1183
Plate_1653	M06	S	C	Lethal for 1181 and 1183
Plate_1653	O05	S	C	Lethal for 1181 and 1183
Plate_1653	P18	S	C	Lethal for 1181 and 1183
Plate_1654	F05	S	C	Lethal for 1181 and 1183
Plate_1654	M12	S	C	Lethal for 1181 and 1183
Plate_1656	C16	S	C	Lethal for 1181 and 1183
Plate_1656	M16	S	C	Lethal for 1181 and 1183
Plate_1657	E10	S	C	Hit for 1181
Plate_1657	I10	S	C	Lethal for 1181 and 1183
Plate_1658	G05	S	C	Lethal for 1181 and 1183
Plate_1658	I10	S	C	Lethal for 1181 and 1183
Plate_1659	B03	S	C	Lethal for 1181 and 1183
Plate_1659	B20	S	C	Lethal for 1181 and 1183
Plate_1659	L20	S	C	Lethal for 1181 and 1183
Plate_1659	N09	S	C	Lethal for 1181 and 1183
Plate_1662	F10	S	C	Lethal for 1181 and 1183
Plate_1665	B04	S	C	Lethal for 1181 and 1183
Plate_1665	E05	S	C	Lethal for 1181 and 1183
Plate_1665	I12	S	C	Lethal for 1181 and 1183
Plate_1665	N03	S	C	Lethal for 1181 and 1183
Plate_1668	B20	S	C	Lethal for 1181 and 1183
Plate_1668	I07	S	C	Lethal for 1181 and 1183
Plate_1668	L12	S	C	Hit for 1183
Plate_1668	P05	S	C	Lethal for 1181 and 1183
Plate_1668	P08	S	C	Lethal for 1181 and 1183

Plate_1668	P11	S	C	Lethal for 1181 and 1183
Plate_1669	A14	S	C	Lethal for 1181 and 1183
Plate_1669	E13	S	C	Lethal for 1181 and 1183
Plate_1669	H21	S	C	Lethal for 1181 and 1183
Plate_1669	K04	S	C	Lethal for 1181 and 1183
Plate_1669	K15	S	C	Lethal for 1181 and 1183
Plate_1669	K17	S	C	Lethal for 1181 and 1183
Plate_1669	M22	S	C	Lethal for 1181 and 1183
Plate_1716	E05	S	C	Lethal for 1181 and 1183
Plate_1722	F05	S	C	Lethal for 1181 and 1183
Plate_1726	K21	S	C	Lethal for 1181 and 1183
Plate_1730	M02	S	C	Lethal for 1181 and 1183
Plate_1731	K21	S	C	Lethal for 1181 and 1183
Plate_1734	I08	S	C	Lethal for 1181 and 1183
Plate_1734	K03	S	C	Lethal for 1181 and 1183
Plate_1737	F22	S	C	Lethal for 1181 and 1183
Plate_1740	D04	M	C	Hit for 1183
Plate_1740	D15	S	C	Lethal for 1181 and 1183
Plate_1740	P19	S	C	Lethal for 1181 and 1183
Plate_1741	K08	S	C	Lethal for 1181 and 1183
Plate_1743	A16	S	C	Lethal for 1181 and 1183
Plate_1744	G03	S	C	Lethal for 1181 and 1183
Plate_1744	G04	S	C	Lethal for 1181 and 1183
Plate_1745	H06	S	C	Lethal for 1181 and 1183
Plate_1745	N07	S	C	Lethal for 1181 and 1183
Plate_1747	N19	S	C	Lethal for 1181 and 1183
Plate_1749	B11	S	C	Lethal for 1181 and 1183
Plate_1749	D21	S	C	Lethal for 1181 and 1183
Plate_1750	N21	S	C	Lethal for 1181 and 1183
Plate_1751	N03	S	C	Lethal for 1181 and 1183
Plate_1753	O14	S	C	Lethal for 1181 and 1183
Plate_1755	P21	S	C	Lethal for 1181 and 1183
Plate_1756	H03	M	C	Hit for 1183
Plate_1756	N20	S	C	Lethal for 1181 and 1183
Plate_1757	A05	S	C	Lethal for 1181 and 1183
Plate_1757	D22	S	C	Hit for 1183
Plate_1759	H15	S	C	Lethal for 1181 and 1183
Plate_1760	D03	S	C	Lethal for 1181 and 1183
Plate_1760	D15	S	C	Lethal for 1181 and 1183
Plate_1761	E12	M	C	Hit for 1183
Plate_1762	I07	W	C	Hit for 1183

Plate_1762	O13	S	C	Lethal for 1181 and 1183
Plate_1764	C10	W	C	Hit for 1183
Plate_1766	M04	W	C	Hit for 1183
Plate_1766	N08	M	C	Hit for 1181
Plate_1767	J04	M	C	Hit for 1183
Plate_1768	D16	S	C	Lethal for 1181 and 1183
Plate_1768	M11	S	C	Lethal for 1181 and 1183
Plate_1768	O22	S	C	Lethal for 1181 and 1183
Plate_1769	D14	S	C	Lethal for 1181 and 1183
Plate_1769	E04	S	C	Lethal for 1181 and 1183
Plate_1769	J21	W	C	Hit for 1183
Plate_1769	K06	S	C	Lethal for 1181 and 1183
Plate_1769	M04	S	C	Lethal for 1181 and 1183
Plate_1770	C06	S	C	Lethal for 1181 and 1183
Plate_1770	D09	M	C	Hit for 1183
Plate_1771	L18	S	C	Lethal for 1181 and 1183
Plate_1772	B02	M	C	Hit for 1183
Plate_1772	G04	S	C	Lethal for 1181 and 1183
Plate_1772	L20	S	C	Lethal for 1181 and 1183
Plate_1779	K19	S	C	Lethal for 1181 and 1183
Plate_1781	I03	W	C	Hit for 1183
Plate_1781	N10	S	C	Lethal for 1181 and 1183
Plate_1782	F16	S	C	Lethal for 1181 and 1183
Plate_1782	I15	S	C	Hit for 1183
Plate_1782	L12	S	C	Lethal for 1181 and 1183
Plate_1783	K16	S	C	Lethal for 1181 and 1183
Plate_1783	L11	S	C	Lethal for 1181 and 1183
Plate_1784	G17	S	C	Lethal for 1181 and 1183
Plate_1784	J09	S	C	Lethal for 1181 and 1183
Plate_1785	K07	S	C	Lethal for 1181 and 1183
Plate_1786	G12	S	C	Lethal for 1181 and 1183
Plate_1786	O16	W	C	Hit for 1183
Plate_1787	E20	S	C	Lethal for 1181 and 1183
Plate_1790	E11	S	C	Lethal for 1181 and 1183
Plate_1790	M20	S	C	Lethal for 1181 and 1183
Plate_1795	E01	S	C	Lethal for 1181 and 1183
Plate_1796	A03	W	C	Hit for 1183
Plate_1796	B12	W	C	Hit for 1183
Plate_1796	G20	S	C	Lethal for 1181 and 1183
Plate_1796	H07	S	C	Lethal for 1181 and 1183
Plate_1796	N07	S	C	Lethal for 1181 and 1183

Plate_1797	F07	S	C	Lethal for 1181 and 1183
Plate_1797	J01	S	C	Lethal for 1181 and 1183
Plate_1798	A19	S	C	Lethal for 1181 and 1183
Plate_1798	N21	S	C	Lethal for 1181 and 1183
Plate_1799	H03	S	C	Lethal for 1181 and 1183
Plate_1799	N11	M	C	Hit for 1183
Plate_1800	I02	W	C	Hit for 1183
Plate_1800	N12	S	C	Lethal for 1181 and 1183
Plate_1801	F02	S	C	Lethal for 1181 and 1183
Plate_1801	F22	M	C	Hit for 1183
Plate_1802	B05	S	C	Lethal for 1181 and 1183
Plate_1802	C05	S	C	Lethal for 1181 and 1183
Plate_1802	G05	S	C	Lethal for 1181 and 1183
Plate_1802	P08	S	C	Lethal for 1181 and 1183
Plate_1804	M01	S	C	Lethal for 1181 and 1183
Plate_1806	I09	S	C	Hit for 1183
Plate_1807	K13	S	C	Lethal for 1181 and 1183
Plate_1807	M11	W	C	Hit for 1183
Plate_1807	M13	S	C	Lethal for 1181 and 1183
Plate_1808	I17	S	C	Hit for 1183
Plate_1808	K08	M	C	Hit for 1183
Plate_1808	M05	S	C	Lethal for 1181 and 1183
Plate_1808	N08	S	C	Lethal for 1181 and 1183
Plate_1808	N10	S	C	Lethal for 1181 and 1183
Plate_1809	M05	S	C	Lethal for 1181 and 1183
Plate_1810	A18	S	C	Lethal for 1181 and 1183
Plate_1810	C18	S	C	Lethal for 1181 and 1183
Plate_1810	E16	S	C	Lethal for 1181 and 1183
Plate_1810	I02	S	C	Lethal for 1181 and 1183
Plate_1810	K02	S	C	Lethal for 1181 and 1183
Plate_1810	O16	S	C	Lethal for 1181 and 1183
Plate_1811	A19	W	C	Hit for 1181
Plate_1811	P10	S	C	Lethal for 1181 and 1183
Plate_1812	O19	M	C	Hit for 1183
Plate_1813	J06	S	C	Lethal for 1181 and 1183
Plate_1814	C22	S	C	Lethal for 1181 and 1183
Plate_1816	C21	S	C	Lethal for 1181 and 1183
Plate_1816	E21	S	C	Lethal for 1181 and 1183
Plate_1816	G21	S	C	Lethal for 1181 and 1183
Plate_1816	K19	S	C	Lethal for 1181 and 1183
Plate_1816	M19	S	C	Lethal for 1181 and 1183

Plate_1816	O19	S	C	Lethal for 1181 and 1183
Plate_1817	M15	S	C	Lethal for 1181 and 1183
Plate_1817	M17	S	C	Lethal for 1181 and 1183
Plate_1819	I08	S	C	Lethal for 1181 and 1183
Plate_1819	M06	S	C	Lethal for 1181 and 1183
Plate_1822	K01	S	C	Lethal for 1181 and 1183
Plate_1823	B12	S	C	Lethal for 1181 and 1183
Plate_1823	N10	S	C	Lethal for 1181 and 1183
Plate_1824	A11	S	C	Lethal for 1181 and 1183
Plate_1824	O02	W	C	Hit for 1183
Plate_1826	O07	S	C	Lethal for 1181 and 1183
Plate_1827	A15	S	C	Lethal for 1181 and 1183
Plate_1827	C11	S	C	Lethal for 1181 and 1183
Plate_1827	C15	S	C	Lethal for 1181 and 1183
Plate_1827	E21	S	C	Lethal for 1181 and 1183
Plate_1827	K17	S	C	Lethal for 1181 and 1183
Plate_1828	D01	M	C	Hit for 1183
Plate_1831	I17	S	C	Lethal for 1181 and 1183
Plate_1831	M19	S	C	Lethal for 1181 and 1183
Plate_1831	O19	S	C	Lethal for 1181 and 1183
Plate_1833	A11	S	C	Lethal for 1181 and 1183
Plate_1833	I17	S	C	Lethal for 1181 and 1183
Plate_1835	F03	W	C	Hit for 1181
Plate_1836	J07	S	C	Lethal for 1181 and 1183
Plate_1836	L22	S	C	Lethal for 1181 and 1183
Plate_1836	P22	S	C	Lethal for 1181 and 1183
Plate_1837	M15	W	C	Hit for 1183
Plate_1837	O17	S	C	Hit for 1183
Plate_1838	D22	S	C	Lethal for 1181 and 1183
Plate_1838	E10	S	C	Lethal for 1181 and 1183
Plate_1838	I09	S	C	Lethal for 1181 and 1183
Plate_1838	J20	S	C	Lethal for 1181 and 1183
Plate_1838	M10	S	C	Lethal for 1181 and 1183
Plate_1841	C20	S	C	Lethal for 1181 and 1183
Plate_1842	A04	S	C	Lethal for 1181 and 1183
Plate_1842	A06	S	C	Lethal for 1181 and 1183
Plate_1842	C18	S	C	Lethal for 1181 and 1183
Plate_1842	E06	W	C	Hit for 1183
Plate_1842	E16	S	C	Lethal for 1181 and 1183
Plate_1842	F07	M	C	Hit for 1183
Plate_1842	G18	S	C	Lethal for 1181 and 1183

Plate_1842	K22	W	C	Hit for 1183
Plate_1842	M13	S	C	Lethal for 1181 and 1183
Plate_1842	M19	S	C	Lethal for 1181 and 1183
Plate_1842	N07	M	C	Hit for 1183
Plate_1843	A19	S	C	Lethal for 1181 and 1183
Plate_1843	C19	S	C	Hit for 1183
Plate_1843	I21	S	C	Lethal for 1181 and 1183
Plate_1843	M17	S	C	Lethal for 1181 and 1183
Plate_1843	N08	S	C	Lethal for 1181 and 1183
Plate_1843	P06	S	C	Lethal for 1181 and 1183
Plate_1844	D05	S	C	Lethal for 1181 and 1183
Plate_1844	H03	S	C	Lethal for 1181 and 1183
Plate_1844	L03	M	C	Hit for 1183
Plate_1844	N05	S	C	Lethal for 1181 and 1183
Plate_1845	M07	S	C	Lethal for 1181 and 1183
Plate_1845	O01	S	C	Lethal for 1181 and 1183
Plate_1845	O07	S	C	Lethal for 1181 and 1183
Plate_1846	A16	S	C	Lethal for 1181 and 1183
Plate_1846	M14	S	C	Lethal for 1181 and 1183
Plate_1847	L02	M	C	Hit for 1183
Plate_1847	P02	W	C	Hit for 1183
Plate_1848	I06	M	C	Hit for 1183
Plate_1848	M06	S	C	Lethal for 1181 and 1183
Plate_1849	B03	S	C	Lethal for 1181 and 1183
Plate_1849	H21	S	C	Lethal for 1181 and 1183
Plate_1850	B16	S	C	Lethal for 1181 and 1183
Plate_1850	D14	S	C	Lethal for 1181 and 1183
Plate_1850	D16	S	C	Lethal for 1181 and 1183
Plate_1851	A12	S	C	Lethal for 1181 and 1183
Plate_1851	O10	S	C	Lethal for 1181 and 1183
Plate_1852	B16	S	C	Lethal for 1181 and 1183
Plate_1854	A03	S	C	Lethal for 1181 and 1183
Plate_1854	C03	S	C	Lethal for 1181 and 1183
Plate_1854	D14	M	C	Hit for 1183
Plate_1854	G03	S	C	Lethal for 1181 and 1183
Plate_1854	I03	S	C	Lethal for 1181 and 1183
Plate_1854	K03	S	C	Lethal for 1181 and 1183
Plate_1854	M05	S	C	Lethal for 1181 and 1183
Plate_1854	O03	S	C	Lethal for 1181 and 1183
Plate_1854	P12	S	C	Lethal for 1181 and 1183
Plate_1854	P14	S	C	Lethal for 1181 and 1183

Plate_1855	C03	W	C	Hit for 1183
Plate_1855	E03	M	C	Hit for 1183
Plate_1855	K03	M	C	Hit for 1183
Plate_1855	M17	S	C	Lethal for 1181 and 1183
Plate_1856	A21	S	C	Lethal for 1181 and 1183
Plate_1856	M17	W	C	Hit for 1181
Plate_1857	O09	W	C	Hit for 1183
Plate_1859	B09	S	C	Lethal for 1181 and 1183
Plate_1859	F20	S	C	Lethal for 1181 and 1183
Plate_1862	L08	S	C	Lethal for 1181 and 1183
Plate_1863	D11	W	C	Hit for 1183
Plate_1863	E08	S	C	Hit for 1183
Plate_1863	L11	S	C	Lethal for 1181 and 1183
Plate_1869	C06	S	C	Lethal for 1181 and 1183
Plate_1869	D11	W	C	Hit for 1183
Plate_1869	D13	S	C	Lethal for 1181 and 1183
Plate_1869	F15	S	C	Lethal for 1181 and 1183
Plate_1869	K08	S	C	Lethal for 1181 and 1183
Plate_1869	M08	S	C	Lethal for 1181 and 1183
Plate_1869	P13	S	C	Lethal for 1181 and 1183
Plate_1873	E12	W	C	Hit for 1183
Plate_1874	E22	W	C	Hit for 1183
Plate_1875	A17	S	C	Lethal for 1181 and 1183
Plate_1875	C17	S	C	Lethal for 1181 and 1183
Plate_1878	A06	S	C	Lethal for 1181 and 1183
Plate_1878	B05	S	C	Lethal for 1181 and 1183
Plate_1878	E21	S	C	Lethal for 1181 and 1183
Plate_1878	I02	S	C	Lethal for 1181 and 1183
Plate_1878	I08	S	C	Lethal for 1181 and 1183
Plate_1878	M04	S	C	Lethal for 1181 and 1183
Plate_1880	F05	M	C	Hit for 1183
Plate_1882	D04	S	C	Lethal for 1181 and 1183
Plate_1882	F21	S	C	Lethal for 1181 and 1183
Plate_1882	J04	M	C	Hit for 1183
Plate_1882	L04	S	C	Hit for 1183
Plate_1882	M09	S	C	Hit for 1183
Plate_1882	P02	S	C	Lethal for 1181 and 1183
Plate_1882	P04	S	C	Lethal for 1181 and 1183
Plate_1882	P08	S	C	Lethal for 1181 and 1183
Plate_1882	P10	M	C	Hit for 1183
Plate_1890	L09	W	C	Hit for 1183

Plate_1890	O13	W	C	Hit for 1183
Plate_1893	I19	S	C	Hit for 1183
Plate_1894	G16	S	C	Lethal for 1181 and 1183
Plate_1895	H22	M	C	Hit for 1183
Plate_1895	J22	M	C	Hit for 1183
Plate_1897	C20	W	C	Hit for 1183
Plate_1900	A08	S	C	Lethal for 1181 and 1183
Plate_1900	C08	S	C	Lethal for 1181 and 1183
Plate_1900	E08	S	C	Lethal for 1181 and 1183
Plate_1900	G06	S	C	Lethal for 1181 and 1183
Plate_1900	G08	S	C	Lethal for 1181 and 1183
Plate_1900	I08	S	C	Lethal for 1181 and 1183
Plate_1900	K06	S	C	Lethal for 1181 and 1183
Plate_1900	O06	S	C	Lethal for 1181 and 1183
Plate_1902	G22	S	C	Lethal for 1181 and 1183
Plate_1906	D21	M	C	Hit for 1183
Plate_1908	D19	S	C	Lethal for 1181 and 1183
Plate_1909	B14	M	C	Hit for 1183
Plate_1910	B13	S	C	Lethal for 1181 and 1183
Plate_1910	F13	S	C	Lethal for 1181 and 1183
Plate_1910	N11	S	C	Lethal for 1181 and 1183
Plate_1912	A19	S	C	Lethal for 1181 and 1183
Plate_1912	L13	M	C	Hit for 1183
Plate_1912	M17	M	C	Hit for 1183
Plate_1912	M22	S	C	Hit for 1183
Plate_1913	E16	S	C	Lethal for 1181 and 1183
Plate_1913	L02	S	C	Lethal for 1181 and 1183
Plate_1916	A02	S	C	Lethal for 1181 and 1183
Plate_1916	E02	S	C	Lethal for 1181 and 1183
Plate_1916	G02	S	C	Lethal for 1181 and 1183
Plate_1916	H22	S	C	Lethal for 1181 and 1183
Plate_1916	K21	S	C	Lethal for 1181 and 1183
Plate_1916	L04	S	C	Lethal for 1181 and 1183
Plate_1916	M21	S	C	Lethal for 1181 and 1183
Plate_1917	E10	S	C	Lethal for 1181 and 1183
Plate_1918	B15	S	C	Lethal for 1181 and 1183
Plate_1919	H21	M	C	Hit for 1183
Plate_2043	A18	S	C	Lethal for 1181 and 1183
Plate_2043	B07	W	C	Hit for 1183
Plate_2043	B09	S	C	Lethal for 1181 and 1183
Plate_2043	K01	S	C	Lethal for 1181 and 1183

Plate_2043	O17	S	C	Lethal for 1181 and 1183
Plate_3153	M08	S	C	Lethal for 1181 and 1183
Plate_3153	M14	S	C	Lethal for 1181 and 1183
Plate_3265	A17	S	C	Lethal for 1181 and 1183
Plate_3265	E15	S	C	Lethal for 1181 and 1183
Plate_3265	E19	S	C	Lethal for 1181 and 1183
Plate_3295	C23	S	C	Lethal for 1181 and 1183
Plate_3295	C24	S	C	Lethal for 1181 and 1183
Plate_3295	D23	S	C	Lethal for 1181 and 1183
Plate_3426	G11	S	C	Lethal for 1181 and 1183
Plate_3426	K05	S	C	Lethal for 1181 and 1183
Plate_3428	K17	S	C	Lethal for 1181 and 1183
Plate_3428	K21	S	C	Lethal for 1181 and 1183
Plate_3429	E06	S	C	Lethal for 1181 and 1183
Plate_3430	C21	M	C	Hit for 1183
Plate_3430	K19	M	C	Hit for 1183
Plate_3432	D02	S	C	Lethal for 1181 and 1183
Plate_3432	E10	S	C	Lethal for 1181 and 1183
Plate_3432	F02	S	C	Lethal for 1181 and 1183
Plate_3432	N08	S	C	Lethal for 1181 and 1183
Plate_3432	P08	S	C	Lethal for 1181 and 1183
Plate_3434	N04	S	C	Lethal for 1181 and 1183
Plate_3435	E09	S	C	Hit for 1183
Plate_3437	F04	W	C	Hit for 1183
Plate_3437	N19	M	C	Hit for 1183
Plate_3437	P19	M	C	Hit for 1183
Plate_3438	J10	M	C	Hit for 1183
Plate_3440	F07	S	C	Lethal for 1181 and 1183
Plate_3440	H05	S	C	Lethal for 1181 and 1183
Plate_3440	L03	S	C	Lethal for 1181 and 1183
Plate_3441	E01	W	C	Hit for 1183
Plate_3441	E13	S	C	Lethal for 1181 and 1183
Plate_3442	L07	S	C	Lethal for 1181 and 1183
Plate_3444	F02	S	C	Lethal for 1181 and 1183
Plate_3444	P02	S	C	Lethal for 1181 and 1183
Plate_3447	I11	S	C	Lethal for 1181 and 1183
Plate_3449	F15	S	C	Lethal for 1181 and 1183
Plate_3449	H15	S	C	Lethal for 1181 and 1183
Plate_3450	J11	W	C	Hit for 1183
Plate_3451	A02	S	C	Lethal for 1181 and 1183
Plate_3451	E21	S	C	Lethal for 1181 and 1183

Plate_3451	G21	S	C	Lethal for 1181 and 1183
Plate_3451	K21	S	C	Lethal for 1181 and 1183
Plate_3451	O02	S	C	Lethal for 1181 and 1183
Plate_3453	F18	S	C	Lethal for 1181 and 1183
Plate_3453	H18	S	C	Lethal for 1181 and 1183
Plate_3453	J10	S	C	Lethal for 1181 and 1183
Plate_3453	J18	S	C	Lethal for 1181 and 1183
Plate_3453	K04	S	C	Lethal for 1181 and 1183
Plate_3453	L16	S	C	Lethal for 1181 and 1183
Plate_3453	P16	S	C	Lethal for 1181 and 1183
Plate_3454	J12	S	C	Lethal for 1181 and 1183
Plate_3454	K06	S	C	Lethal for 1181 and 1183
Plate_3455	B06	S	C	Lethal for 1181 and 1183
Plate_3455	G22	S	C	Lethal for 1181 and 1183
Plate_3455	M18	S	C	Lethal for 1181 and 1183
Plate_3455	O22	S	C	Lethal for 1181 and 1183
Plate_3458	B08	S	C	Lethal for 1181 and 1183
Plate_3458	F08	S	C	Lethal for 1181 and 1183
Plate_3458	J12	S	C	Lethal for 1181 and 1183
Plate_3458	L04	S	C	Lethal for 1181 and 1183
Plate_3459	F08	S	C	Lethal for 1181 and 1183
Plate_3459	N10	S	C	Lethal for 1181 and 1183
Plate_3461	F13	S	C	Hit for 1183
Plate_3461	H13	M	C	Hit for 1183
Plate_3462	D03	M	C	Hit for 1183
Plate_3462	H15	S	C	Lethal for 1181 and 1183
Plate_3462	K18	S	C	Hit for 1183
Plate_3463	G15	S	C	Hit for 1183
Plate_3463	K09	S	C	Lethal for 1181 and 1183
Plate_3463	K15	M	C	Hit for 1183
Plate_3463	M09	S	C	Lethal for 1181 and 1183
Plate_3463	M13	W	C	Hit for 1183
Plate_3464	B17	S	C	Lethal for 1181 and 1183
Plate_3464	L21	S	C	Lethal for 1181 and 1183
Plate_3464	N15	S	C	Lethal for 1181 and 1183
Plate_3464	N21	S	C	Lethal for 1181 and 1183
Plate_3464	P13	S	C	Lethal for 1181 and 1183
Plate_3465	K01	S	C	Lethal for 1181 and 1183
Plate_3465	K10	W	C	Hit for 1183
Plate_3465	M10	M	C	Hit for 1183
Plate_3466	F01	S	C	Lethal for 1181 and 1183

Plate_3466	G21	M	C	Hit for 1183
Plate_3466	G22	M	C	Hit for 1183
Plate_3466	K22	M	C	Hit for 1183
Plate_3466	M10	W	C	Hit for 1183
Plate_3466	M22	S	C	Lethal for 1181 and 1183
Plate_3467	C11	S	C	Lethal for 1181 and 1183
Plate_3467	E18	W	C	Hit for 1183
Plate_3467	G18	M	C	Hit for 1183
Plate_3468	F18	S	C	Lethal for 1181 and 1183
Plate_3468	M12	M	C	Hit for 1183
Plate_3468	M15	S	C	Lethal for 1181 and 1183
Plate_3474	E02	S	C	Lethal for 1181 and 1183
Plate_3474	G02	S	C	Lethal for 1181 and 1183
Plate_3474	N12	W	C	Hit for 1183
Plate_3477	D16	S	C	Lethal for 1181 and 1183
Plate_3478	A11	S	C	Lethal for 1181 and 1183
Plate_3478	C13	S	C	Lethal for 1181 and 1183
Plate_3478	K09	S	C	Lethal for 1181 and 1183
Plate_3478	L21	S	C	Hit for 1183
Plate_3478	O13	S	C	Lethal for 1181 and 1183
Plate_3479	F04	S	C	Lethal for 1181 and 1183
Plate_3479	K16	S	C	Lethal for 1181 and 1183
Plate_3479	N21	S	C	Lethal for 1181 and 1183
Plate_3480	I01	M	C	Hit for 1183
Plate_3481	A05	S	C	Lethal for 1181 and 1183
Plate_3482	K04	S	C	Lethal for 1181 and 1183
Plate_3482	O02	S	C	Lethal for 1181 and 1183
Plate_3484	B04	S	C	Lethal for 1181 and 1183
Plate_3484	B19	S	C	Lethal for 1181 and 1183
Plate_3484	B21	S	C	Lethal for 1181 and 1183
Plate_3484	D04	S	C	Lethal for 1181 and 1183
Plate_3484	D17	S	C	Lethal for 1181 and 1183
Plate_3484	D19	S	C	Lethal for 1181 and 1183
Plate_3484	D21	S	C	Lethal for 1181 and 1183
Plate_3484	F04	S	C	Lethal for 1181 and 1183
Plate_3484	F19	S	C	Lethal for 1181 and 1183
Plate_3484	H02	S	C	Lethal for 1181 and 1183
Plate_3484	H04	S	C	Lethal for 1181 and 1183
Plate_3484	H17	S	C	Lethal for 1181 and 1183
Plate_3484	H19	S	C	Lethal for 1181 and 1183
Plate_3484	H21	S	C	Lethal for 1181 and 1183

Plate_3484	J02	S	C	Lethal for 1181 and 1183
Plate_3484	J17	S	C	Lethal for 1181 and 1183
Plate_3484	J19	S	C	Lethal for 1181 and 1183
Plate_3484	J21	S	C	Lethal for 1181 and 1183
Plate_3484	L02	S	C	Lethal for 1181 and 1183
Plate_3484	L21	S	C	Lethal for 1181 and 1183
Plate_3484	N02	S	C	Lethal for 1181 and 1183
Plate_3484	N17	S	C	Lethal for 1181 and 1183
Plate_3484	N21	S	C	Lethal for 1181 and 1183
Plate_3484	P02	S	C	Lethal for 1181 and 1183
Plate_3484	P19	S	C	Lethal for 1181 and 1183
Plate_3487	I11	S	C	Lethal for 1181 and 1183
Plate_3489	F15	S	C	Lethal for 1181 and 1183
Plate_3489	H15	S	C	Lethal for 1181 and 1183
Plate_3490	J11	W	C	Hit for 1183
Plate_3491	A02	S	C	Lethal for 1181 and 1183
Plate_3491	E21	S	C	Lethal for 1181 and 1183
Plate_3491	G21	S	C	Lethal for 1181 and 1183
Plate_3491	K21	S	C	Lethal for 1181 and 1183
Plate_3491	O02	S	C	Lethal for 1181 and 1183
Plate_3493	F18	S	C	Lethal for 1181 and 1183
Plate_3493	H18	S	C	Lethal for 1181 and 1183
Plate_3493	J10	S	C	Lethal for 1181 and 1183
Plate_3493	J18	S	C	Lethal for 1181 and 1183
Plate_3493	K04	S	C	Lethal for 1181 and 1183
Plate_3493	L16	S	C	Lethal for 1181 and 1183
Plate_3493	P16	S	C	Lethal for 1181 and 1183
Plate_3494	J12	S	C	Lethal for 1181 and 1183
Plate_3494	K06	S	C	Lethal for 1181 and 1183
Plate_3495	B06	S	C	Lethal for 1181 and 1183
Plate_3495	G22	S	C	Lethal for 1181 and 1183
Plate_3495	M18	S	C	Lethal for 1181 and 1183
Plate_3495	O22	S	C	Lethal for 1181 and 1183
Plate_3498	B08	S	C	Lethal for 1181 and 1183
Plate_3498	F08	S	C	Lethal for 1181 and 1183
Plate_3498	J12	S	C	Lethal for 1181 and 1183
Plate_3498	L04	S	C	Lethal for 1181 and 1183
Plate_3499	F08	S	C	Lethal for 1181 and 1183
Plate_3499	N10	S	C	Lethal for 1181 and 1183
Plate_3501	F13	S	C	Hit for 1183
Plate_3501	H13	M	C	Hit for 1183

Plate_3502	D03	M	C	Hit for 1183
Plate_3502	H15	S	C	Lethal for 1181 and 1183
Plate_3502	K18	S	C	Hit for 1183
Plate_3503	G15	S	C	Hit for 1183
Plate_3503	K09	S	C	Lethal for 1181 and 1183
Plate_3503	K15	M	C	Hit for 1183
Plate_3503	M09	S	C	Lethal for 1181 and 1183
Plate_3503	M13	W	C	Hit for 1183
Plate_3504	B17	S	C	Lethal for 1181 and 1183
Plate_3504	L21	S	C	Lethal for 1181 and 1183
Plate_3504	N15	S	C	Lethal for 1181 and 1183
Plate_3504	N21	S	C	Lethal for 1181 and 1183
Plate_3504	P13	S	C	Lethal for 1181 and 1183
Plate_3505	K01	S	C	Lethal for 1181 and 1183
Plate_3505	K10	W	C	Hit for 1183
Plate_3505	M10	M	C	Hit for 1183
Plate_3506	E04	S	C	Lethal for 1181 and 1183
Plate_3506	E13	M	C	Hit for 1183
Plate_3506	G02	S	C	Lethal for 1181 and 1183
Plate_3506	G03	W	C	Hit for 1183
Plate_3506	G04	S	C	Lethal for 1181 and 1183
Plate_3506	G19	S	C	Lethal for 1181 and 1183
Plate_3506	I19	S	C	Lethal for 1181 and 1183
Plate_3506	K11	S	C	Lethal for 1181 and 1183
Plate_3506	K19	S	C	Lethal for 1181 and 1183
Plate_3506	O02	S	C	Lethal for 1181 and 1183
Plate_3506	O04	S	C	Lethal for 1181 and 1183
Plate_3506	O19	S	C	Lethal for 1181 and 1183
Plate_3510	N03	S	C	Lethal for 1181 and 1183
Plate_3511	C08	M	C	Hit for 1183
Plate_3511	E08	S	C	Hit for 1183
Plate_3511	E10	M	C	Hit for 1183
Plate_3511	G15	S	C	Lethal for 1181 and 1183
Plate_3511	H06	S	C	Hit for 1183
Plate_3511	I10	S	C	Hit for 1183
Plate_3511	I15	S	C	Lethal for 1181 and 1183
Plate_3511	K15	S	C	Lethal for 1181 and 1183
Plate_3511	L06	S	C	Hit for 1183
Plate_3511	O12	M	C	Hit for 1183
Plate_3511	O15	S	C	Lethal for 1181 and 1183
Plate_3511	O17	M	C	Hit for 1183

Plate_3512	C08	S	C	Hit for 1183
Plate_3512	D18	W	C	Hit for 1183
Plate_3512	L22	S	C	Hit for 1183
Plate_3512	N18	S	C	Lethal for 1181 and 1183
Plate_3512	O10	S	C	Lethal for 1181 and 1183
Plate_3512	O19	S	C	Lethal for 1181 and 1183
Plate_3512	P16	S	C	Lethal for 1181 and 1183
Plate_3515	A15	S	C	Lethal for 1181 and 1183
Plate_3515	C15	S	C	Lethal for 1181 and 1183
Plate_3515	E15	S	C	Lethal for 1181 and 1183
Plate_3515	G03	S	C	Lethal for 1181 and 1183
Plate_3515	G15	S	C	Lethal for 1181 and 1183
Plate_3515	I15	S	C	Lethal for 1181 and 1183
Plate_3515	K13	S	C	Lethal for 1181 and 1183
Plate_3515	K15	S	C	Lethal for 1181 and 1183
Plate_3515	M15	S	C	Lethal for 1181 and 1183
Plate_3516	D10	S	C	Lethal for 1181 and 1183
Plate_3516	E12	S	C	Lethal for 1181 and 1183
Plate_3516	F05	S	C	Lethal for 1181 and 1183
Plate_3516	M06	S	C	Lethal for 1181 and 1183
Plate_3516	P10	S	C	Lethal for 1181 and 1183
Plate_3517	M04	S	C	Lethal for 1181 and 1183
Plate_3519	C21	M	C	Hit for 1183
Plate_3519	N07	S	C	Lethal for 1181 and 1183
Plate_3520	B22	S	C	Lethal for 1181 and 1183
Plate_3521	J03	M	C	Hit for 1183
Plate_3522	E06	W	C	Hit for 1183
Plate_3523	M11	S	C	Lethal for 1181 and 1183
Plate_3524	O04	S	C	Lethal for 1181 and 1183
Plate_3548	D19	S	C	Lethal for 1181 and 1183
Plate_3548	F07	S	C	Hit for 1183
Plate_3552	B13	W	C	Hit for 1183
Plate_3552	D13	W	C	Hit for 1183
Plate_3552	D20	S	C	Lethal for 1181 and 1183
Plate_3552	J04	S	C	Lethal for 1181 and 1183
Plate_3553	A21	W	C	Hit for 1183
Plate_3554	A17	S	C	Lethal for 1181 and 1183
Plate_3554	B08	S	C	Lethal for 1181 and 1183
Plate_3554	B16	M	C	Hit for 1183
Plate_3554	H22	S	C	Lethal for 1181 and 1183
Plate_3554	J16	S	C	Lethal for 1181 and 1183

Plate_3554	L14	S	C	Lethal for 1181 and 1183
Plate_3554	L18	S	C	Lethal for 1181 and 1183
Plate_3555	A09	S	C	Lethal for 1181 and 1183
Plate_3555	E05	M	C	Hit for 1183
Plate_3555	E15	S	C	Lethal for 1181 and 1183
Plate_3555	G11	S	C	Lethal for 1181 and 1183
Plate_3555	I03	S	C	Lethal for 1181 and 1183
Plate_3555	I07	S	C	Lethal for 1181 and 1183
Plate_3555	K03	W	C	Hit for 1183
Plate_3555	K09	S	C	Hit for 1183
Plate_3555	M09	W	C	Hit for 1183
Plate_3555	O07	S	C	Lethal for 1181 and 1183
Plate_3556	B16	S	C	Lethal for 1181 and 1183
Plate_3556	B19	S	C	Lethal for 1181 and 1183
Plate_3556	D04	S	C	Lethal for 1181 and 1183
Plate_3556	E06	M	C	Hit for 1183
Plate_3556	I10	M	C	Hit for 1183
Plate_3556	J10	S	C	Lethal for 1181 and 1183
Plate_3556	J15	S	C	Lethal for 1181 and 1183
Plate_3556	J19	S	C	Lethal for 1181 and 1183
Plate_3556	L17	S	C	Lethal for 1181 and 1183
Plate_3556	L18	S	C	Lethal for 1181 and 1183
Plate_3556	L22	M	C	Hit for 1183
Plate_3556	M06	M	C	Hit for 1183
Plate_3556	N18	S	C	Lethal for 1181 and 1183
Plate_3556	N22	S	C	Hit for 1183
Plate_3556	P04	S	C	Lethal for 1181 and 1183
Plate_3556	P16	S	C	Lethal for 1181 and 1183
Plate_3556	P18	S	C	Lethal for 1181 and 1183
Plate_3557	C03	S	C	Hit for 1183
Plate_3557	C05	S	C	Hit for 1183
Plate_3557	C11	M	C	Hit for 1183
Plate_3557	K01	S	C	Hit for 1183
Plate_3557	O09	W	C	Hit for 1183
Plate_3558	B21	S	C	Lethal for 1181 and 1183
Plate_3558	J19	S	C	Lethal for 1181 and 1183
Plate_3558	N19	S	C	Lethal for 1181 and 1183
Plate_3559	C20	M	C	Hit for 1183
Plate_3560	P14	S	C	Lethal for 1181 and 1183
Plate_3564	K06	M	C	Hit for 1183
Plate_3566	I02	S	C	Lethal for 1181 and 1183

Appendix 3: Additional analogs of targocil-II tested

Analogs were purchased and grouped based off whether they had different substituents on the left arm (carboxylic acid side) or the right arm (halogenated benzene) of the molecule.

Table A3.1 MICs for targocil-II left arm analogs with modifications to the carboxylic acid.

Reported MIC values of "0.5-5" indicate that the value fell between 0.5 to 5 μg/mL.

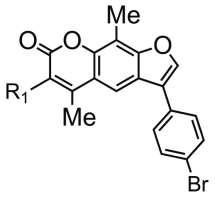

Analog	R_1	MIC	Analog	R_1	MIC
1	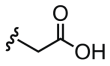	1	31	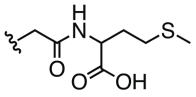	0.125
19	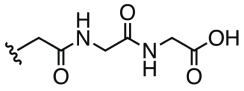	0.5			
20	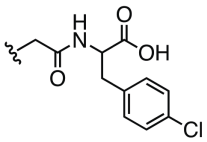	0.5-5	32	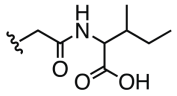	0.125
21	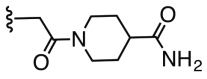	0.125	33	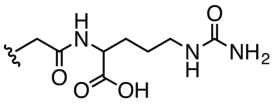	0.125
22	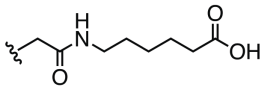	0.125	34	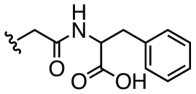	0.5
23	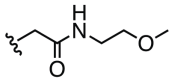	0.5-5	35	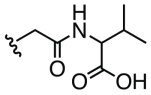	0.125
26	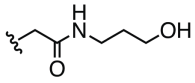	0.5-5	36	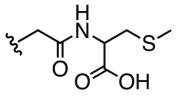	0.125
27	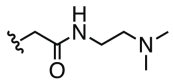	0.125	38	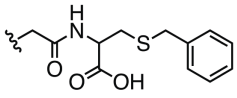	0.5
28	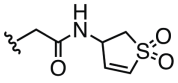	>10			
30	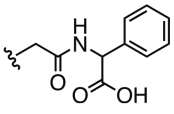	0.0625	39	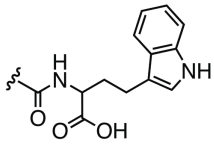	0.5-5

Table A3.2 MICs of targocil-II right arm analogs. Reported MIC values of "0.5-5" indicate that the value fell between 0.5 to 5 μg/mL.

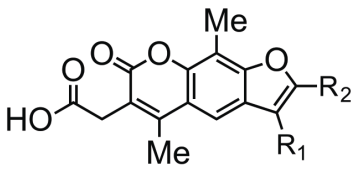

Analog	R_1	R_2	MIC
1	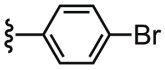	-H	1
41	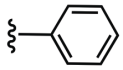	$-CH_3$	0.5-5
42	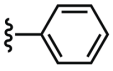	-H	0.5-5
43	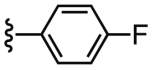	-H	0.5-5
44	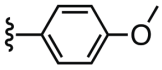	-H	0.5-5
25	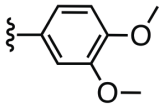	-H	0.5-5
46	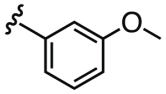	-H	0.5-5
45	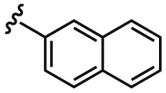	-H	0.125
47	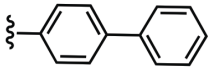	-H	0.25
48	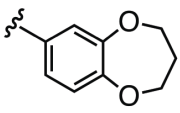	-H	0.5-5

Appendix 4: Additional analogs of DBI-1 tested

Analogs were purchased and grouped based off whether they had different substituents on the left arm (dimethoxybenzene side) or the right arm (cinnamic acid side) of the molecule.

Table A4.1 MICs for DBI-1 analogs with modifications to the left arm and thiazole of the molecule. Moving or removing the methoxy substituents kills activity.

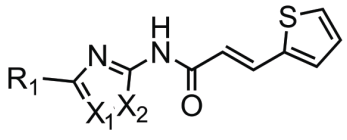

Analog	R_1	X_1	X_2	MIC
DBI-1	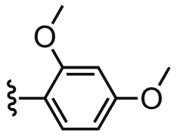	-CH	-S	0.5
DBI-19	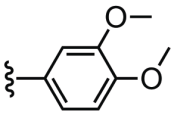	-CH	-S	>32
DBI-20	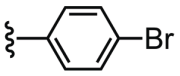	-CH	-S	>32
DBI-21	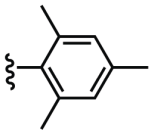	-CH	-S	>32
DBI-22	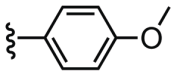	-CH	-S	>32
DBI-23	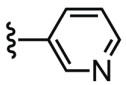	-CH	-S	>32
DBI-24	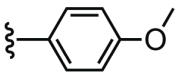	-NH	-N	>32
DBI-25	-H	-CH	-S	>32

Table A4.2 MICs for DBI-1 analogs with modifications to the right arm of the molecule.

DBI-11 and DBI-12 MICs were not determined due to solubility issues.

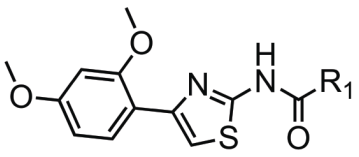

Analog	R_1	MIC	Analog	R_1	MIC
DBI-1	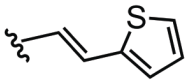	0.5	DBI-13	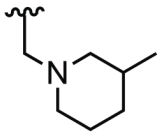	>32
DBI-7	-H	>32			
DBI-8	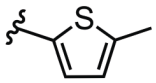	>32	DBI-14	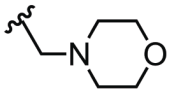	>32
DBI-9	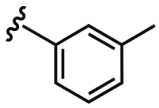	>32	DBI-15	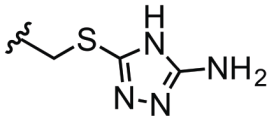	>32
DBI-10	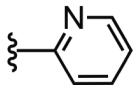	>32	DBI-16	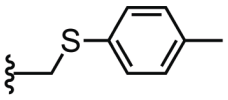	>32
DBI-11	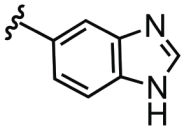	n.d.	DBI-17	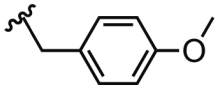	>32
DBI-12	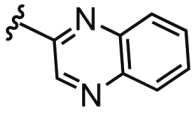	n.d.	DBI-18	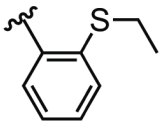	>32

Appendix 5: NMR of DBI-1

Figure A5.1 400 MHz 1H NMR spectrum of DBI-1 (10 mg/mL) in deuterated DMSO.

Spectrum is referenced to the DMSO shift at 2.5 ppm.

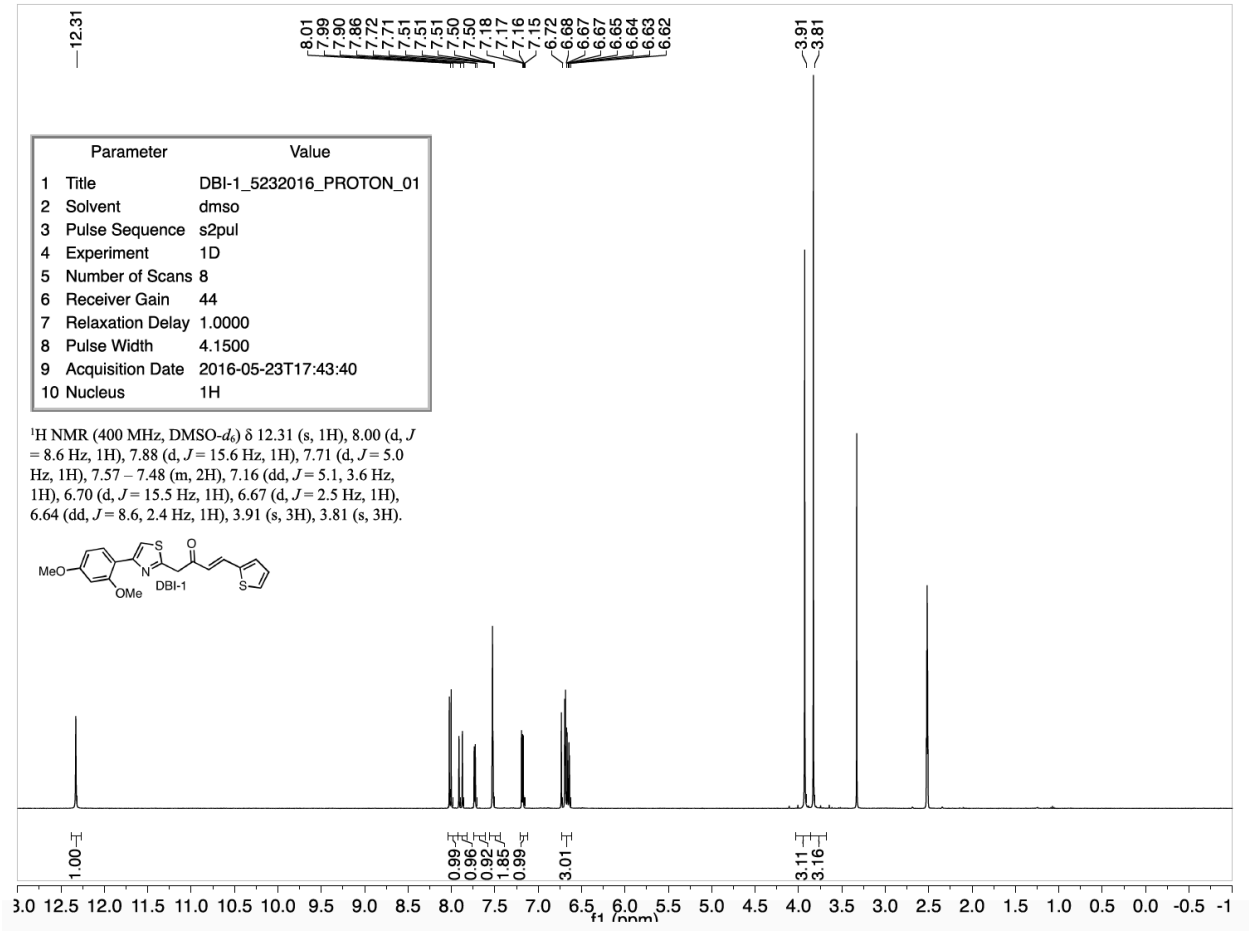

Appendix 6: Additional tn-seq tables

Table A6.1 Tn-seq sample names, treatment, library reads and TA sites hit for all treatments referenced in this work.

Sample	Inhibitor	Treatment (ug/mL)	Reads (total)	TA sites hit
LM1	No treatment	N/A	3936229	173478
LM2	Amsacrine	10	3890256	182522
LM3 "20-1"	Amsacrine	20	4038306	171772
LM4 "20-2"	Amsacrine	20	4371542	177622
LM5 "20-3"	Amsacrine	20	2862690	164624
LM6 "30-1"	Amsacrine	30	4031910	176569
LM7 "30-2"	Amsacrine	30	3136746	146091
LM8 "30-3"	Amsacrine	30	2607178	148562
LM101	No treatment	N/A	10004691	184124
LM102	DBI-1	5	10589449	199273
LM103	DltI-1	5	9003678	181544
LM105	DBI-1	2.5	5387162	177754
LM105	DltI-1	2.5	7880206	181590

Table A6.2 Tn-seq results for HG003 transposon library treated with DBI-1 (2.5 µg/mL).

List of genes with fold-change in transposon insertions <0.25 for DBI-1 treatment 2.5 µg/mL, p-value <0.05.

Locus Tag	Gene	P-value	Corrected p-value	Fold-change
SAOUHSC_00718	Hypothetical protein	3.39E-05	0.013	0.14
SAOUHSC_01050	Hypothetical protein	5.82E-09	4.02E-06	0.13
SAOUHSC_01361	*lcpA*	1.64E-03	0.17	0.11
SAOUHSC_02793	*pgcA*	1.74E-09	1.61E-06	0.11
SAOUHSC_01025	Hypothetical protein	7.73E-19	2.14E-15	0.05
SAOUHSC_00953	*ugtP*	2.79E-07	1.54E-04	0.04
SAOUHSC_00952	*ltaA*	9.85E-17	1.36E-13	0.03

Table A6.3 Tn-seq results for HG003 transposon library treated with DltI-1 (2.5 µg/mL).

List of genes with fold-change in transposon insertions <0.25 for DltI-1 treatment 2.5 µg/mL, p-value <0.05.

Locus Tag	Gene	P-value	Corrected p-value	Fold-change
SAOUHSC_01050	Hypothetical protein	9.20E-06	5.09E-03	0.22
SAOUHSC_02793	*pgcA*	2.71E-06	1.88E-03	0.16
SAOUHSC_01361	*lcpA*	5.74E-03	0.5	0.15
SAOUHSC_00718	Hypothetical protein	2.53E-06	1.88E-03	0.11
SAOUHSC_00953	*ugtP*	1.14E-03	0.39360	0.10
SAOUHSC_01025	Hypothetical protein	3.41E-14	9.43E-11	0.08
SAOUHSC_00952	*ltaA*	1.35E-13	1.87E-10	0.05

Table A6.4 Tn-seq results for HG003 transposon library treated with DBI-1 (5 µg/mL). List of genes with fold-change in transposon insertions <0.5 for DBI-1 treatment 5 µg/mL, p-value <0.05.

Locus Tag	Gene	P-value	Corrected p-value	Fold-change
SAOUHSC_01050	Hypothetical protein	9.68E-03	0.48	0.46
SAOUHSC_01361	*lcpA*	9.78E-02	0.48	0.40
SAOUHSC_02793	*pgcA*	3.70E-03	0.48	0.34
SAOUHSC_01025	Hypothetical protein	3.41E-05	0.03	0.28
SAOUHSC_00953	*ugtP*	2.00E-02	0.48	0.20
SAOUHSC_00952	*ltaA*	2.34E-05	0.03	0.19

Table A6.5 Tn-seq results for HG003 transposon library treated with DltI-1 (5 µg/mL). List of genes with fold-change in transposon insertions <0.3 for DltI-1 treatment 5 µg/mL, p-value <0.05.

Locus Tag	Gene	P-value	Corrected p-value	Fold-change
SAOUHSC_02801	*gtaB*	1.75E-01	0.5	0.26
SAOUHSC_01361	*lcpA*	2.04E-02	0.5	0.25
SAOUHSC_00718	Hypothetical protein	5.34E-05	2.96E-02	0.15
SAOUHSC_02793	*pgcA*	1.85E-07	1.71E-04	0.14
SAOUHSC_01025	Hypothetical protein	6.88E-11	9.52E-08	0.14
SAOUHSC_00953	*ugtP*	4.38E-06	3.03E-03	0.06
SAOUHSC_00952	*ltaA*	1.11E-13	3.06E-10	0.05

Table A6.6 Tn-seq results for HG003 transposon library treated with amsacrine (10 µg/mL). List of genes with fold-change in transposon insertions <0.25 compared to control for amsacrine treatment 10 µg/mL, p-value <0.05

Locus Tag	Gene	P-value	Corrected p-value	Fold-change
SAOUHSC_02801	*gtaB*	8.26E-03	0.5	0.23
SAOUHSC_01050	Hypothetical protein	1.89E-07	1.05E-04	0.22
SAOUHSC_01361	*lcpA*	2.85E-03	0.5	0.12
SAOUHSC_00953	*ugtP*	4.28E-05	1.98E-02	0.11
SAOUHSC_01025	Hypothetical protein	4.63E-14	1.29E-10	0.08
SAOUHSC_00952	*ltaA*	2.67E-13	3.71E-10	0.07
SAOUHSC_00718	Hypothetical protein	7.38E-09	6.83E-06	0.07

Table A6.7 Tn-seq results for HG003 transposon library treated with amsacrine (20 µg/mL). Representative list of genes with fold-change in transposon insertions <0.25 for amsacrine treatment 20 µg/mL, p-value <0.05.

Locus Tag	Gene	P-value	Corrected p-value	Fold-change
SAOUHSC_01050	Hypothetical protein	1.76E-08	9.76E-06	0.22
SAOUHSC_02793	*pgcA*	4.33E-06	1.83E-03	0.21
SAOUHSC_00953	*ugtP*	5.10E-03	0.5	0.18
SAOUHSC_01025	Hypothetical protein	1.48E-15	4.10E-12	0.07
SAOUHSC_01361	*lcpA*	2.62E-04	0.07	0.07
SAOUHSC_00952	*ltaA*	2.30E-13	3.20E-10	0.06
SAOUHSC_00718	Hypothetical protein	5.35E-10	4.44E-07	0.05

Table A6.8 Tn-seq results for HG003 transposon library treated with amsacrine (30 µg/mL). Representative list of genes with fold-change in transposon insertions <0.25 for amsacrine treatment 30 ug/mL, p-value <0.05. Increased number of hits relative to Table A.6.6 and A.6.7 due to off-target activity of amsacrine at higher concentrations.

Locus Tag	Gene	P-value	Corrected p-value	Fold-change
SAOUHSC_01971	Hypothetical protein	1.58E-07	1.03E-05	0.24
SAOUHSC_01462	Hypothetical protein	4.57E-03	4.33E-02	0.22
SAOUHSC_01797	*pgcA*	3.71E-17	3.43E-14	0.20
SAOUHSC_01908	Hypothetical protein	1.42E-05	3.45E-04	0.19
SAOUHSC_01827	Hypothetical protein	1.21E-10	2.23E-08	0.17
SAOUHSC_00959	Hypothetical protein	1.03E-09	1.36E-07	0.17
SAOUHSC_01050	Hypothetical protein	3.13E-11	6.68E-09	0.14
SAOUHSC_01034	Hypothetical protein	3.81E-07	1.96E-05	0.10
SAOUHSC_01361	*lcpA*	1.53E-06	6.09E-05	0.09
SAOUHSC_01194	Hypothetical protein	1.02E-14	4.72E-12	0.07
SAOUHSC_02793	*pgcA*	5.75E-15	3.19E-12	0.07
SAOUHSC_01025	Hypothetical protein	3.03E-19	4.21E-16	0.05
SAOUHSC_00953	*ugtP*	9.53E-10	1.32E-07	0.05
SAOUHSC_01875	*leuS*	1.51E-09	1.91E-07	0.05
SAOUHSC_01781	Hypothetical protein	3.61E-16	2.51E-13	0.04
SAOUHSC_00952	*ltaA*	1.44E-20	4.00E-17	0.03
SAOUHSC_00718	Hypothetical protein	6.74E-14	2.45E-11	0.02

Appendix 7: Strains used in this work

Table A7.1 Strain table

Strain	Relevant features	Source or reference
S. aureus Newman	Clinical isolate	ATCC25904
S. aureus Newman Δ*tarO*	Unmarked deletion	1
S. aureus MW2	Clincal isolate	Dr. David Hooper
S. aureus USA300 JE2	Derived from USA300 LAC	2
S. aureus 1784A	Clincal isolate	3
S. aureus USA100	Clincal isolate	Dr. David Hooper
S. aureus RN4220	Lab strain	4
LM071	*S. aureus* Newman *tarG* L195F	This study
LM072	*S. aureus* Newman *tarG* W196L	This study
LM073	*S. aureus* Newman tarG W196C	This study
LM074	*S. aureus* Newman *tarG* V54L	This study
LM075	*S. aureus* Newman *tarG* F55L	This study
B. Subtilis PY79	Prototrophic derivative of B. subtilis 168	5
KS002	PY79 Δ*tagGHBs ::cat amyE::Phyperspank tarGHSa spc*	5
ARH102	*E. coli* KRX with pCDFDuet: TarG, TarH-His_6	From Anthony Hesser
ARH135	*E. coli* KRX with pCDFDuet: TarG, TarH-His_6 (E169Q)	From Anthony Hesser
ARH153	*E. coli* KRX with pTP63-P_{atc}: TarH-His_6, TarG	From Anthony Hesser
ARH154	*E. coli* KRX with pTP63-P_{atc}: TarH-His_6, TarG (W196L)	From Anthony Hesser
ARH159	*S. aureus* RN4220 pTP63-P_{atc}-TarH-His_6, TarG	From Anthony Hesser
ARH160	*S. aureus* RN4220 pTP63-P_{atc}-TarH-His_6, TarG W196L	From Anthony Hesser
ARH172	*E. coli* KRX with pCDFDuet: FLAG-TarG, TarH-His_6	From Anthony Hesser
S. aureus SEJ1 Δ*ltaS*	4S5: SEJ1Δ$ltaS_S$ suppressor strain	6
S. aureus USA300 JE2 tn::1050	Transposon insertion in *SAOUHSC_01050*	2
S. aureus RN4220 Δ*ypfP*	Δ*ypfP*::*ermR*	7
LP401	*S. aureus* USA300 JE2 tn::1050 DltB S175T	7
LP402	*S. aureus* USA300 JE2 tn::1050 DltB A219D	7
LP405	*S. aureus* USA300 JE2 tn::1050 DltB F255L	7
LM010	*S. aureus* USA300 JE2 tn::1050 DltB A355E	This study
LM049	*S. aureus* USA300 JE2 tn::1050 DltC V44L	This study
LM059	*S. aureus* RN4220 Δ*ugtP:kan*	From Dr. Wonsik Lee
LM090	*S. aureus* SEJ1 Δ*ugtP:kan*	This study

Table A7.1 (Continued)

LM091	*S. aureus* SEJ1 4S5 Δ*ugtP:kan* Δ*ltaS*	This study
LM101	ugtP (unmarked) LtaS N383K	This study
LM102	ugtP (unmarked) LtaS DdelinsDFYYVD	This study
LM103	ugtP (unmarked) LtaS S256I	This study
LM104	ugtP (unmarked) LtaS Q338*	This study
LM105	ugtP:kan LtaS DdelinsDFYYVD	This study
LM106	ugtP:kan LtaS N383K	This study
LM107	ugtP (unmarked) LtaS G317D	This study
LM108	ugtP:kan LtaS G478V	This study
LM111	ugtP:kan LtaS DdelinsDFYYVD	This study
LM114	ugtP:kan LtaS Q212H	This study
LM116	ugtP (unmarked) LtaS Y133*	This study
LM117	ugtP (unmarked) LtaS F93L	This study
LM119	ugtP:kan LtaS R183H	This study
LM101	ugtP (unmarked) LtaS N383K	This study
LM134	*S. aureus* RN4220 Δ*ugtP* (umarked)	From Dr. Wonsik Lee
LM135	*S. aureus* RN4220 Δ*ugtP* Δ*gdpP:kan*	This study
LM136	*S. aureus* RN4220 Δ*ugtP* Δ*gdpP:kan* Δ*ltaS:erm*	This study
LM137	*S. aureus* SEJ1 tn::ugtP	This study
LM138	*S. aureus* SEJ1 4S5 tn::ugtP Δ*ltaS*	This study
LM139	*S. aureus* HG003 tn::ugtP Δ*gdpP:kan*	This study
LM140	*S. aureus* SEJ1 tn::ltaA	This study
LM141	*S. aureus* HG003 tn::ugtP	This study
LM142	*S. aureus* SEJ1 tn::ltaA Δ*gdpP:kan*	This study
LM143	*S. aureus* USA300 JE2 tn::ltaA	This study
LM144	*S. aureus* USA300 JE2 tn::ltaA Δ*gdpP:kan*	This study
LM145	*S. aureus* HG003 tn::ugtP LtaS L181S	This study
LM146	*S. aureus* USA300 JE2 tn::1050 VraT P174S	This study
LM147	*S. aureus* USA300 JE2 tn::1050 VraS D26Y	This study
LM148	*S. aureus* USA300 JE2 tn::1050 VraS G64V	This study
LM149	*S. aureus* USA300 JE2 tn::1050 VraS R6*	This study
LM150	*S. aureus* USA300 JE2 tn::1050 VraS T125N	This study
LM151	*S. aureus* USA300 JE2 tn::1050 VraS Q288K	This study
LM152	*S. aureus* USA300 JE2 tn::1050 VraS W77C	This study
LM154	*S. aureus* USA300 JE2 tn::1050 VraS L50*	This study
LM155	*S. aureus* USA300 JE2 tn::1050 VraS S175T	This study
LM156	*S. aureus* USA300 JE2 tn::1050 VraS T129N	This study

A7.1 References for strain table

1. Grundling, A.; Schneewind, O. *J. Bacteriol.* **2006,** *188*, 2463-2472.

2. Fey, P. D.; Endres, J. L.; Yajjala, V. K.; Widhelm, T. J.; Boissy, R. J.; Bose, J. L.; Bayles, K. W. *mBio.* **2013,** *4*, 12.

3. Swoboda, J. G.; Meredith, T. C.; Campbell, J.; Brown, S.; Suzuki, T.; Bollenbach, T.; Malhowski, A. J.; Kishony, R.; Gilmore, M. S.; Walker, S. *ACS Chem. Biol.* **2009,** *4*, 875-883.

4. Kreiswirth, B. N.; Lofdahl, S.; Betley, M. J.; O'Reilly, M.; Schlievert, P. M.; Bergdoll, M. S.; Novick, R. P. *Nature.* **1983,** *305*, 709-712.

5. Schirner, K.; Stone, L. K.; Walker, S. *ACS Chem. Biol.* **2011,** *6*, 407-412.

6. Corrigan, R. M.; Abbott, J. C.; Burhenne, H.; Kaever, V.; Grundling, A. *PLoS Pathogens.* **2011,** *7*, e1002217.

7. Pasquina, L.; Santa Maria, J. P.; McKay Wood, B.; Moussa, S. H.; Matano, L. M.; Santiago, M.; Martin, S. E.; Lee, W.; Meredith, T. C.; Walker, S. *Nat Chem Biol.* **2016,** *12*, 40-45.

Appendix 8: Appendix materials

A8.1 Purchased analogs of targocil-II

Targocil-II analog compounds **19**-**39** were purchased from Aurora Fine Chemicals. In order, their catalog numbers are: K00.232.529 (**19**), K00.233.459 (**20**), K00.233.761 (**21**), K00.234.828 (**22**), K00.328.750 (**23**), K00.328.831 (**24**), K02.218.159 (**25**), K02.267.523 (**26**), K02.267.785 (**27**), K02.269.262 (**28**), K02.269.662 (**29**), K04.009.971 (**30**), K04.010.131 (**31**), K04.010.211 (**32**), K04.010.499 (**33**), K04.010.558 (**34**), K04.010.563 (**35**), K04.010.840 (**36**), K04.030.867 (**37**), K04.166.055 (**38**), and K04.166.142 (**39**). Targocil-II analog compounds **40**-**48** were purchased from ChemDiv. In order, their catalog numbers are: D143-0309 (**40**), D143-0312 (**41**), D143-0313 (**42**), D143-0315 (**43**), D143-0318 (**44**), D143-0320 (**45**), D143-0321 (**46**), D143-0322 (**47**), and Y040-9252 (**48**).

A8.2 Purchased analogs of DBI-1

DBI analogs purchased from enamine are: Z29465418 (**7**), Z29465458 (**8**), Z29465671 (**9**), Z29465430 (**10**), Z2241102090 (**11**), Z73299706 (**12**), Z137702006 (**13**), Z137786892 (**14**), Z18355844 (**15**), Z27852472 (**22**), Z29459294 (**23**), Z119635942 (**24**), Z28173819 (**25**). Compounds purchased from Life Chemicals are: F2537-0094 (**16**), F2976-0102 (**17**), F2646-0109 (**18**), F0440-0146 (**19**), F0440-0137 (**20**), and F0440-0144 (**21**).